PLASTIC FLOW IN THE METAL ROLLING PROCESS

by

F. ELLIS B. Sc.(Eng.)

A Thesis submitted for the degree of Doctor of Philosopy in the University of London

and

The Diploma of Imperial College.

April, 1961.

Abstract.

A technique of incorporating a network, or grid, of lines on an interior plane of a copper specimen by pressure welding is described. The properties of such a weld suitable for examining deformation processes taking place under conditions of plane strain are examined and optimum conditions for a satisfactory weld established.

A method of analysing an initially square grid, which has been distorted by the deformation of the specimen, to which the grid is attached, is developed and expressions obtained for the direction and magnitude of the principal strain increments. The expressions are most conveniently presented in the form of graphs covering a suitable range of the parameters involved. Application of the flow rule enables the maximum shear stress directions to be obtained and hence the slip line field.

The technique and method outlined are applicable to any metal forming process which takes place under conditions of plane strain but in this investigation they have been used to examine the problem of cold rolling of strip.

A critical examination of a number of basic assumptions made in theories of rolling is carried out. In particular, assumptions about the variation of the coefficient of friction over the arc of contact and the variation of stress over a vertical section of the material in the roll gap are compared with the experimental results.

The design and operation of a quick release mechanism to enable a satisfactory roll gap impression to be obtained is described.

Measurements of deformed roll profile are found to agree reasonably closely with the predictions of Hitchcock's roll flattening formula.

It is concluded that assumptions made about the nature of the process in theories of cold rolling do, in fact, represent in a very satisfactory manner the actual behaviour of metal in the cold rolling process.

ACKNOWLEDGEMENTS.

Thanks are due to Professor Hugh Ford D.Sc(Eng.), Ph.d. for much helpful discussion and encouragement throughout this investigation.

The work was started during the tenure of a Clayton Fellowship and thanks are due to the Clayton and Manville Fellowship Committee of the Institution of Mechanical Engineers.

CONTENTS.

		Page.
1.	Introduction.	1
2.	Nature of the Strip Rolling Process.	5
3.	Theory of the Rolling Process.	
3.1.	Assumptions made in Theories of Rolling.	8
3.2.	Derivation of Differential Equation of Equilibrium in the Roll Gap.	9
3.3.	Theory due to Siebel.	13
3.4.	Theory due to Von Karman.	15
3.5.	Orowan's Theory.	16
3.6.	Comment on Theories of Rolling.	20
4.	Survey of Experimental Work.	21
4.1.	Qualitative Experiments.	21
4.2.	Discussion of Qualitative Experiments.	25
4.3.	Quantitative Experiments.	28
4.4.	Coefficient of Friction Measurements.	30
4.5.	Determination of Yield Stress.	33
5.	Discussion of Theories of Rolling.	36
6.	Measurement of Stress in Roll Gap.	41
6.1.	Introduction.	41
6.2.	Plasticity Theory.	41
6.3.	Outline of Technique Used.	48
6.4.	Production of Grid.	49
6.5.	Specimen Requirements.	51
6.6.	Preparation of Specimens.	55
6.7.	Obtaining the Roll Gap Pattern.	60

		Page.
6.8.	Quick Release Mechanism.	61
6.9.	Operation and Performance of the Quick Release Mechanism.	65
6.10.	Measurement of Roll Force and Roll Torque.	66
6.11.	Rolling of Specimens.	68
7.	Analysis of Deformed Network.	69
7.1.	Introduction.	69
7.2.	Measuring Equipment.	71
7.3.	Method of Measurement.	72
7.4.	Method of Analysis.	73
8.	Results.	80
8.1.	The Rolling Schedule.	80
8.2.	The Deformation Pattern.	82
8.3.	The Elastic-Plastic Boundary.	85
8.4.	Obtaining a/b and θ .	87
8.5.	Details of Calculations for One Specimen.	90
8.6.	Determination of Yield Stress.	93
8.7.	Investigation of Redundant Shear.	95
8.8.	The Roll Pressure Distribution.	96
8.9.	The Deformed Roll Profile.	103
8.10.	Discussion of Results.	105
References		110
Appendix I	Derivation of Formula giving direction and magnitude of principal strains.	115
Appendix II	Modifications to formula derived in Appendix I	120

		Page
Appendix III	Two Dimensional Strain Tests.	126
Appendix IV	Roll Force and Roll Torque Calculations.	129

LIST OF FIGURES

Fig.		Page
1.	Spread in Rolling.	133
2.	Material in Roll Gap.	133
3.	Section Through Roll Gap.	134
4.	Siebel's Friction Hill.	135
5.	Pattern of Deformation Across Width. (after Metz).	136
6.	Pattern of Deformation Across Width. (after Weiss).	136
7.	Greatest Gripping Angle.	137
8.	Photograph of Circular Grid.	138
9.	Photograph of Distorted Circular Grid.	138
10.	Milling Machine set up for Engraving Grid.	139
11.	Photograph of Square Grid.	140
12.	Welding Jig.	141
13.	Heating and Cooling Rate Curves.	142
14.	Position of Tensile Test Specimens.	143
15.	General View of Rolling Mill.	144
16.	General View of Rolling Mill.	145
17.	Principle of Quick Release Blocks.	146
18.	Quick Release Element.	147
19.	Complete Quick Release Mechanism.	147
20.	Drawing of Quick Release Assembly.	148
21.	Roll Gap Impression.	149
22.	Roll Gap Profile.	150

Fig.		Page.
23.	Calibration Graph for Load Cell.	151
24.	Calibration Graph for Torque Meters.	152
25.	Roll Force and Torque v. Reduction.	153
26.	Deformation of Square Grid.	154
27.	O.M.T. Toolmaker's Microscope.	155
28.	Deformation of Circular Element.	156
29.	Graph of Principal Strain Direction (Large range).	157
30(a)	Graph of Principal Strain Direction. (Small range).	158
30(b)	Graph of Principal Strain Direction. (Small range).	159
31.	Graph of Magnitude of Principal Strains. (Large range).	160
32.	Graph of Magnitude of Principal Strains (Small range).	161
33.	Modified Graph of Principal Strain Direction. (Large range).	162
34(a)	Modified Graph of Principal Strain Direction. (Small range).	163
34(b)	Modified Graph of Principal Strain Direction. (Small range).	164
35.	Incremental Deformation of Element.	165
36.	Angular Changes in Element in Roll Gap.	165
37.	General Quadrilateral Distortion.	166
38.	Photographs of Rolled Specimens.	167

Fig.		Page.
39.	Pattern of Deformation.	168
40.	Distorted Grid and Slip Line Field Specimen A.	169
41.	Distorted Grid and Slip Line Field. Specimen B.	170
42.	Distorted Grid and Slip Line Field. Specimen C.	171
43.	Elastic-Plastic Boundary	172
44.	Variation of ψ through Roll Gap. Speciman A.	173
45.	Variation of ψ through Roll Gap. Speciman B.	174
46.	Variation of ψ through Roll Gap. Specimen C.	175
47.	Variation of 2a through Roll Gap Specimen A.	176
48.	Variation of 2a through Roll Gap. Specimen B.	177
49.	Variation of 2a through Roll Gap. Specimen C.	178
50.	Variation of 2b through Roll Gap. Specimen A.	179
51.	Variation of 2b through Roll Gap Specimen B.	180
52.	Variation of 2b through Roll Gap. Specimen C.	181

Fig.		Page.
53.	Variation of ϕ through Roll Gap Specimen A.	182
54.	Variation of ϕ through Roll Gap Specimen B.	183
55.	Variation of ϕ through Roll Gap Specimen C.	184
56.	Sign Convention for Angular Measurements.	185
57.	Yield Stress v% reduction curve.	186
58.	Yield Stress v Hardness curve.	187
59.	Determination of Stress along Entry Slip line.	188
60.	Calculation of Coefficient of Friction.	189
61.	Stress Conditions in Region of Neutral Zone.	190
62.	Roll Pressure Distribution. Specimen A.	191
63.	Roll Pressure Distribution. Specimen B.	192
64.	Roll Pressure Distribution. Specimen C.	193
65.	Deformed Roll Profile. Specimen A.	194
66.	Deformed Roll Profile. Specimen B.	195
67.	Deformed Roll Profile. Specimen C.	196
68.	Figure for Derivation of Strain Formulae	App I 197
69.	Two-Dimensional Strain Tests.	App III 198

LIST OF TABLES

Table.		Page.
I	Tensile Strength of Welded Joints.	59
II(a)	Calculation of α for One Value of $(a'/b')^2$	199
II(b)	Values of α for Range of $(a'/b')^2$	200
III(a)	Calculation of r/a' for One Value of $(a'/b')^2$	201
III(b)	Values of r/a' for Range of $(a'/b')^2$	202
IV	Values of A and B in Modified Formula for α	203
V(a)	Values of Θ for Given Error.	204
V(b)	Values of Θ and α for 1% Error.	205
VI	Co-ordinate Readings of Nodal Points Specimen A.	206
VII	Co-ordinate Readings of Nodal Points Specimen B.	207
VIII	Co-ordinate Readings of Nodal Points Specimen C.	208
IX	Values of ψ for Two Streamlines Specimen A	209
X	Values of 2a for Two Streamlines Specimen A.	210
XI	Values of 2b and ϕ for Two Streamlines Specimen A.	211

Table.		Page.
XII	Detailed Calculations for One Streamline. Specimen A	212
XIII	Hardness Survey of Rolled Specimen	213

1. INTRODUCTION.

The rolling of metals is of great technological importance and like so many other engineering processes the art was well advanced long before attempts were made to apply science to the problem.

Leonardo da Vinci, in his notebooks, has a sketch depicting his ideas for a mill for rolling metals but there is no evidence that such a machine was ever built. There are however records that rolls were used as a stage in the production of coins as early as the middle of the 16th century. The working of iron was practiced in Sweden from very early days and Singer in "The History of Technology" quotes a description of a Swedish mill for rolling plates. The period is the beginning of the 18th century.

Until the invention of the steam engine, rolling mills were usually driven by water power and were of very limited capacity. After the introduction of steam, as a source of power, mills increased rapidly in capacity and speed as did the number of installations. Rolling at this stage was still more of an art than a science and it was not until the 1920's that the foundations of a real understanding of the rolling process were laid, notably by Siebel and his co-workers. Nearly all the theoretical analysis which has been carried out has been confined to the rolling

of flat sheet or strip. The rolling of structural sections presents a much more complex problem and at present understanding has not advanced much beyond the empirical stage.

For this reason, all that follows will be understood to refer to flat sheet or strip rolling only, a subject which has engaged the attention of many workers.

Theories have been formulated by various investigators, notably Siebel (1), Karman(2) and Orowan (3), in an attempt to explain the process in terms of the fundamental mechanism of deformation of metals.

A feature common to all the theories proposed, is the prediction of the distribution of the pressure between the roll face and the material in the roll gap. The force required to maintain the rolls at the correct distance apart is then obtained by a summation of the pressure distribution through the zone of contact between roll and material.

The roll force can be measured to a high degree of accuracy (4) and therefore comparison can be made between the theoretical and experimental values.

The theoretical analysis, as will be seen later, is dependent on a number of assumptions. Some

of these assumptions concern the deformation process and others the value of certain of the physical constants which are very difficult to measure directly under the conditions found in the roll gap, e.g., the coefficient of friction between the roll and material.

There is no doubt that, in the past, agreement between theoretical and experiment has been obtained by using spurious values of the coefficient of friction.

Attempts have been made by Siebel and Lueg (5) Smith et al (6) to measure the distributions of pressure by means of a load measuring pin fitted into the face of the roll. Qualitative agreement as to the form of the pressure distribution has been obtained by this means.

Examination of the theories of rolling reveals that in all cases an assumption is made about the variation of stress through the thickness of the material.

The present investigation describes an experimental method whereby the stress distribution through the thickness of the material can be obtained and also the normal and tangential stresses between roll and material through the arc of contact.

The technique, which was evolved in a attempt to study the mechanism of deformation during the cold rolling of metal strip, can however be applied to a large class of technologically important metal forming processes which involve large plastic deformations under

conditions of plane strain.

2. NATURE OF THE STRIP ROLLING PROCESS

Before considering details of the more important theories of rolling some of the physical concepts which are common to most of them will be described.

The material to be rolled enters the roll gap and the frictional forces between rolls and material act to draw the material between the rolls and appear on the opposite side, reduced in thickness, having suffered a plastic deformation as it passes through the roll gap.

It is a matter of observation that for flat strip with a width/thickness ratio greater than about 10, the lateral spread which takes place during the passage through the roll gap is very small. The reason is indicated in Fig. 1. which represents a plan view of a strip being rolled.

The deforming material in the area of contact is restricted from flow in a direction parallel to the roll axes by the constraint exerted by the elastic material to the left of the entry point and to the right of the exit point. The condition of constancy of volume (7) in plastic deformation therefore requires that the flow of the deforming material shall take place in the direction of rolling.

The problem thus becomes a two dimensional

one and, except for narrow regions at the edges, the condition in the rolled material is one of plane strain.

Fig. 2. indicates a section through the roll gap and, as has been seen, will therefore be a plane of flow.

The material enters with a thickness h_1 and a velocity v_1, and leaves with a reduced thickness h_2 and increased velocity v_2.

Constancy of volume requires that the volume passing any one section shall be the same.

Therefore, per unit width of material

$$v_1 . h_1 = v_2 . h_2$$

The speed of the roll surface is ωR. If the component of v_1, tangential to the roll face is equal to ωR then V_2 will be greater than ωR. Conversely if $V_2 = \omega R$ then the component of V_1 tangential to the roll face will be less than ωR. Equilibrium considerations, as will be seen later, indicate that the strip and roll face must have a common velocity at a point somewhere between entry and exit. Such a point N in Fig. 3. is known as the neutral point. From A to N there is a relative velocity between roll face and strip, the peripheral speed of the roll being everywhere greater than that of the strip. Between N and B the relative velocity is reversed and the strip has a greater velocity, at all points, than the periphery of the roll. For this phenomenon to take place the

product of the normal roll pressure at any point and the coefficient of friction must not exceed the yield shear stress of the material otherwise the material "sticks" to the roll face. Orowan (3) has suggested that this takes place in "hot" rolling where the coefficient of friction is much higher than that obtained in cold rolling.

Support for the view that there is in fact relative movement between rolls and material in cold rolling is provided by Capus and Cockroft (8). They have pointed out that, if this relative movement does take place, the small unavoidable asperities on the roll surface will produce scratches on the surface of the material in contact with the roll. The relative movement in the rolling direction combined with the small amount of lateral spread near the edges of the strip, give rise to scratches having a characteristic "fish-hook" shape.

At a suitable magnification these are clearly visible on the surface of rolled material.

3. THEORY OF THE ROLLING PROCESS.

INTRODUCTION.

One of the earliest contributions to an understanding of the rolling process is a theory due to Siebel (1) often known as the theory of the friction hill.

The accumulative effect of the pressure on the friction hill, neglected by Siebel, was taken into account by von Karman (2), The most recent contribution has been made by Orowan (3). The fundamental work done by these three workers has formed a basis on which others have built.

In particular the work of von Karman (2) has been used by Ekelund (11), Tselikov (12), Trinks (13) and Nadai (14), and the work of Orowan by Bland and Ford (15) and Sims (16), who have modified the original theories by introducing various simplifying assumptions to reduce the amount of mathematical computation involved.

3.1. ASSUMPTIONS MADE IN THEORIES OF ROLLING.

Certain physical assumptions are common to all theories. The more important of these are that :-

(a) There is no flow in a direction parallel to the roll axes, i.e. the problem is a two-dimensional one - plane strain.

(b) Plane vertical sections remain plane, i.e. homogeneous compression.

(c) Elastic deformation of the material being rolled is negligible in comparison with the plastic deformations which take place.

(d) The material is originally isotropic and remains so during the deformation.

(e) The material 'slips' relative to the roll surface, except at the neutral point, for cold rolling.

(f) The coefficient of friction between material and roll face is constant through the arc of contact.

With the exception of Orowan's general theory, the theories of rolling which have been proposed take as their starting point, for the calculation of roll face pressure, consideration of the equilibrium of an element contained between two adjacent parallel vertical planes in the roll gap. The next section will therefore be devoted to deriving the basic differential equation governing the equilibrium of such an element.

3.2. DERIVATION OF DIFFERENTIAL EQUATION OF EQUILIBRIUM IN THE ROLL GAP.

A typical cross-section through rolls and strip is shown in Fig. 3.

The material, of initial thickness h_1, contacts the roll at the entry point A and leaves at the exit point B with a thickness h_2. The neutral point is at N.

Consider unit width of strip and a vertical element of thickness dx at a distance x from the exit plane. The height of this element is h. The radial pressure at the point X on the roll surface is P_{rr}, therefore the radial force is $P_{rr} \frac{dx}{\cos\phi}$.

The tangential force F due to the relative motion between strip and roll at this point is

$$F = \mu p_{rr} \frac{dx}{\cos\phi} \qquad (1)$$

The component of the radial force outwards, i.e. in the x - positive direction is

$$p_{rr}.dx.\tan\phi$$

and the component of F inwards is

$$\mu.p_{rr}\,dx$$

The horizontal forces acting on the section are considered to be uniformly distributed to give rise to a stress p_{xx}.

For equilibrium of the shaded element.

$$2p_{rr}\frac{dx}{\cos\phi}.\sin\phi - 2\mu p_{rr}\frac{dx}{\cos\phi}.\cos\phi + p_{xx}h - (p_{xx}+dp_{xx})(h+dh) = 0$$

or $$2p_{rr}dx.\tan\phi - 2\mu.p_{rr}.dx - d(hp_{xx}) = 0 \qquad (2)$$

Now $$p\,dx = p_{rr}\frac{dx}{\cos\phi}\cdot\cos\phi = p_{rr}\,dx$$

$$\therefore \quad p = p_{rr} \tag{3}$$

and $$p(\tan\phi - \mu)\,dx = d\left(\frac{h p_{xx}}{2}\right) \tag{4}$$

If X lies between N and B the equation becomes

$$p(\tan\phi + \mu)\,dx = d\left(\frac{h p_{xx}}{2}\right) \tag{5}$$

Combining (4) and (5)

$$p(\tan\phi \mp \mu)\,dx = d\left(\frac{h p_{xx}}{2}\right) \tag{6}$$

From the geometry of the element, Fig.3.

$$\frac{dh}{2dx} = \tan\phi$$

substituting, (6) becomes

$$\frac{1}{2}\cdot p\frac{dh}{dx} \mp \mu p = \frac{d\left(\frac{h p_{xx}}{2}\right)}{dx} \tag{7}$$

A relation between p and p_{xx} is obtained by considering the conditions governing yielding. Two criteria which have been proposed to describe, with some success, the behaviour of a ductile material are those due to Tresca (17) and V. Mises (18). (See section

6.2).

Under conditions of plane strain if the principal stresses are p_1 and p_2 both criteria reduce to the form that at yield

$$p_1 - p_2 = k_1$$

k_1 being a constant and related to the yield stress in simple tension k.

In the case of the Tresca criterion $k_1 = k$ and in the von Mises case $k_1 = \frac{2}{\sqrt{3}} k$

If the total vertical force on the section xx is p'dx, then

$$p'dx = pdx \pm F \sin\phi$$

$$= pdx \pm \mu p \tan\phi dx$$

or $$p' = p(1 \pm \mu \tan\phi) \qquad (8)$$

If p' and pxx are considered as principal stresses

$$p' - p_{xx} = k_1$$

$$\therefore \quad p(1 \pm \mu \tan\phi) - p_{xx} = k_1 \qquad (9)$$

Equations (4) and (9) can be combined to give an equation in which p and x are the two variables since h can be expressed in terms of x and the exit

thickness h_2.

3.3. THEORY DUE TO SIEBEL (1)

In this theory, as is usual, the yield criterion (9) is written as

$$p - p_{xx} = k_1 \qquad (10)$$

k_1 being taken as constant.

The assumption made being that $\mu \tan\phi$ can be neglected in comparison with 1. This is probably justified for cold rolling where the coefficient of friction μ is low and the angle of contact ϕ small.

An expression for the horizontal force H at any section is then obtained from equation (6)

For $$H = hp_{xx}$$

$$\therefore \quad 2p(\tan\phi \mp \mu)dx = dH$$

It is further assumed that $\tan\phi \sim \phi$ and that p is constant and equal to the yield stress k. Then

$$H = \int 2k(\phi \mp \mu)dx + C$$

C is a constant of integration.

It is of course necessary to express ϕ in terms of x and to use the appropriate sign in the expression depending on the position of x with respect to x_n and the entry and exit point.

Then, using the yield criterion (10) the normal pressure

$$p = k_1 + p_{xx}$$

but $$p_{xx} = \frac{H}{h}$$

the pressure p at any point is

$$p = k_1 + \frac{H}{h}$$

It will be seen that the quantity to be found, p, is first assumed to be constant to enable the variation of the horizontal force H through the gap to be calculated. The variation in p is then taken to be the increase necessary to cause yielding in the presence of the horizontal force H.

The tatal roll force is then the summation of $k_1 + \frac{H}{h}$ over the arc of contact. The pressure distribution is illustrated graphically in Fig.4.

It will be seen that the assuptions made in this theory are such as to produce a peak value which is too low since the accumulative effect on the pressure

of the build up due to friction is neglected. It has been shown, however, by Ford, Ellis and Bland (19) that values of roll force and torque given by this theory compare very well with more exact theories even when tensions are applied to the strip.

3. 4. THEORY OF VON KARMAN.

Von Karman's theory (2) takes into account the accumulative effect of the build up of the roll pressure due to friction and was the first theory to do so.

By considering the equilibrium of an element as has been done in section 3.1. von Karman arrives at the differential equation equivalent to (6) i.e.

$$d\left(\frac{h p_{xx}}{2}\right) = p(\tan\phi \mp \mu)\,dx$$

A relation between p_{xx} and p is then obtained through the yield criterion. In this theory also the vertical component of the tangential friction force F Fig. 3. is neglected.

The solution involves a tedious numerical integration procedure to obtain the roll force.

The yield stress for the material is assumed to remain constant throughout the arc of contact.

A number of theories have been based on von Karman's work. Among the more interesting are those of Trinks (13), Tselikov (12) and Nadai (14). Trinks made the assumption that the arc of contact is parabolic and

was thus able to carry out the integration more easily. He then calculated values of roll pressure for a range of the parameters involved and presented the results in the form of a series of curves enabling a solution to be obtained very rapidly: Tselikov made a number of approximations additional to those made by von Karman to enable the equations to be integrated directly, although the resulting equations are cumbersome to use. Nadai used the von Karman equation in a form which allowed the effect on the roll pressure of differing assumptions about the frictional conditions in the roll gap to be investigated.

3. 5. OROWAN'S THEORY

Orowan (3) has put forward two theories

(a) "The Homogeneous Graphical Method" in which the assumptions of homogeneous compression and slipping friction are made.

(b)"The General Theory" in which the assumptions of homogeneous compression and slipping friction are not made.

In theory (a) the analysis follows very closely that of von Karman (2) but the vertical component of the frictional force is not neglected.

Theory (a). Orowan's solution is obtained by combining equations (6) and (9). From (9)

$$p = \frac{k_1 + p_{xx}}{1 \pm \mu \tan \phi}$$

Substituting this value into (6) gives

$$\frac{d(hp_{xx})}{dx} = 2(k_1 + p_{xx})\frac{(\tan\phi \mp \mu)}{1 \pm \mu\tan\phi}$$

Which on putting $\alpha = \tan^{-1}\mu$

becomes

$$\frac{d(hp_{xx})}{dx} = 2(k_1 + p_{xx}).\tan(\phi \mp \alpha)$$

Orowan indicates how this equation may be solved by using graphical integration and points out that variations in yield stress as the material passes through the roll gap can quite easily be fed into the computations.

Theory (b)

In this theory, which is applicable to both cold and hot rolling, account is taken of the fact that when the coefficient of friction is high (of the order of •3 to •4) as in hot rolling, the product of the normal pressure and the coefficient of friction may exceed the yield stress of the material. This is clearly impossible and under such circumstances the surface material 'sticks' to the rolls. The tangential force in this case remains at a constant value equal to the yield shear stress of the rolled material.

Orowan pointed out that the assumption of a uniform distribution of the horizontal stress over a vertical section within the roll gap made by earlier theories was not necessarily true. What was required to enable a solution to the differential equation of equilibrium to be obtained was an expression giving the variation in horizontal stress over the section.

Orowan makes use of the fact that for the plane problem it is possible to find a stress distribution without reference to the deformations and uses a solution due to Nadai (10) for the stress distribution in a plastic mass compressed between rough inclined plattens. Nadai's solution is an extension of a result due to Prandtl (9) for the case when the plattens are parallel. The material is assumed to 'stick' to the plattens and the flow is toward the apex of the wedge. Lee (20) has shown that the form of the solution is still valid when the material flows away from the apex. The solution can therefore be applied both between exit and neutral point and between neutral point and entry. The results are directly applicable to the rolling case where the coefficient of friction is high and the material sticks to the rolls.

For the case of slipping friction an artifice is adopted. The shear stress distribution given by Prandtl's solution varies linearly across the section having its greatest value at the surface. A fictitious wedge is considered with an apex angle of ϕ^*

such that for an angle ϕ ($\phi^* > \phi$) the shear stress is equal to the product of the direct pressure and the coefficient of friction.

This procedure is open to objection as it assumes that the mode of deformation with slipping friction is the same as when the material 'sticks'. Reference to the solution for plane compression between flat plattens with slipping friction and the solution for rough plattens given by Alexander (21) shows the difference in deformation in the two cases.

It has also been shown by Hill (22) that solutions to problems in plane strain which neglect the velocity pattern are incomplete solutions. On this ground the solutions used by Orowan are open to criticism.

Orowan's work has been a starting point for other investigators.

Cook and Larke (23) have taken Orowan's original equations and by rearrangement have produced a form more convenient for carrying out calculations. The saving of time is considerable when compared with the original method of computation. Even so the amount of work involved in calculating a pass is formidable and, although the time involved in carrying out the calculation is not important for fundamental work, it is desirable to have a method which involves a small amount of computation when the calculation of a large

number of passes has to be carried out.

By making a number of simplifying assumptions Bland and Ford (15) have modified the equation which forms the starting point of Orowan's Homogeneous graphical method in such a way that cold rolling calculations, both with and without tensions, can very easily and quickly be carried out. That the simplifying assumptions made do not adversely affect accuracy of the calculations over a wide range of rolling conditions can be seen by referring to the results given in a paper by Ford, Ellis and Bland (19).

Sims(16) making somewhat similar assumptions to those made by Bland and Ford for cold rolling has modified and applied Orowan's equation to the case of hot rolling.

3. 6. COMMENT ON THEORIES OF ROLLING.

The theories of rolling described in the foregoing sections are seen to depend on a number of physical assumptions and mathematical approximations.

The significance and justification for these assumptions and approximations can only be assessed by an appeal to experiment and the next section will therefore be devoted to a critical survey of experiments on rolling. The behaviour of the material as revealed in such experiments will then be used as a basis for the discussion of theories of rolling.

4. SURVEY OF EXPERIMENTAL WORK.

INTRODUCTION.

Experimental methods that have been employed to investigate various aspects of the rolling problem may be divided into two broad categories. In the first category are the very numerous experiments which have been directed towards obtaining a qualitative idea of the pattern of flow occuring in a metal as it passes between the rolls. In the second category are placed those experiments in which an attempt has been made to obtain accurate quantitive measurements of such things as pressure distribution in the roll gap, roll force, roll torque and energy, and to determine the appropriate values of yield stress and coefficient of friction to be used in theories of rolling.

4. 1. QUALITATIVE EXPERIMENTS.

As has been mentioned, experiments of a qualitative nature which have been carried out by various investigators are extremely numerous and varied in character. In what follows only a few representative investigations will be considered as indicating the type of experiment and typical techniques which have been used to carry them out.

One of the earliest investigations into the plastic flow of metals during rolling was carried out by Hollenburg (24) in 1883. A series of holes were drilled through the thickness of a wrought- iron bar and then

plugged with close fitting wrought-iron plugs. The bar was rolled hot and the mill stopped with the bar between the rolls. The rolls were then lifted and the bar withdrawn. After cooling, the bar was sectioned longitudinally through the plugs. The deformation of the plugs then gave an indication of the flow that had taken place.

By substituting screws for the plain plugs Metz (25) was able to obtain an indication of the amount of compression at various points through the thickness by the altered pitch of the screw. The distortion of the axis indicating the direction of flow. The material, low carbon steel, was hot rolled. Metz obtained information on surface flow by machining a network of grooves on the four surfaces of a rectangular bars. The grooves were extremely coarse and must have had a considerable influence on conditions in the roll gap.

Examination of flow in a plane perpendicular to the direction of rolling was made by inserting screwed plugs in pairs, one above the other, with their axes parallel to the roll axes. After rolling, the bars were sectioned through the screws. The result is shown in Fig. 5. which is a diagram, drawn approximately to scale, from a photograph appearing in the paper by Metz for a reduction of approximately 50%. It will be observed that the flow of metal near the outer edges is

peculiar to this zone and is not characteristic of the flow in the bulk of the bar.

Unckel (26) investigated the flow pattern occurring in the hot rolling of aluminium.

A block of aluminium was cut in half longitudinally and the cut faces machined. One face was drilled with a series of small holes to form a network and the holes fitted with pegs of an alloy of aluminium and copper which would show up clearly on etching. A square network of grooves was machined on the mating face and fitted with strips of aluminium-copper alloy. The two halves, with the prepared faces in contact were fastened together by means of dowels. A network of grooves was also machined on the upper and lower faces of the block.

The composite block was then rolled down from a thickness of 40 m.m. to 30 m.m. in one pass. The block was then cut into two lengths and the one length reduced to 10 m.m. in three passes. After rolling, the block was photographed and then parted on the original interface for an examination of the deformed network of holes and grooves.

A photograph of the composite bar, reproduced in the paper, reveals that parting of the interface had taken place during rolling and therefore a condition of plane strain along the interface had not been obtained.

Weiss (27) described hot rolling tests on aluminium bars and flow lines are given for a cross-section. The form of distortion is indicated in Fig. 6.

No information is given in the paper as to how this pattern was obtained but the form of distortion indicated follows closely that given by Metz (25) using screwed plugs.

Cold rolling tests on copper bars were also carried out by Weiss (28) in which copper rods were inserted in holes drilled in the bars parallel to the axes of the rolls. The bars were rolled and circular section of the rods became elliptical. The orientation of the axes of the ellipses enabled the distribution of strain to be examined. It appears, however, that for some of the holes the material has fractured both in front and behind the plug.

Siebel and Osenburg (29) investigated the effect of roll roughness on flow by a series of tests on copper strip ruled with a rectangular network of lines on the surface. The method adopted was to stop the mill when half the length of the strip had been rolled and then withdraw the strip for examination. The main conclusions these workers have drawn from their results is that spread with rough rolls is greater than with smooth. Longitudinal lines remain sensibly parallel but lines parallel to the roll axes are bent to produce a shallow curve concave to the direction of

rolling. The effect however is slight.

The flow pattern in cold rolling was studied by Siebel and Huhne (30) using the technique of cutting the test pieces longitudinally and scribing a square network on one of the cut faces. The two halves were kept in contact during the passage through the rolls by providing guides on the entry side of the rolls.

A somewhat different type of test was carried out by Orowan (3). In this case the flow was examined by the use of laminated plasticene models. Green (31) has considered the use of plasticene models to study plastic flow in metals and has shown that with suitable precautions such models simulate the flow behaviour of a non work hardening metal very closely. He found that plasticenes of different colours tend to have differing physical properties and hence that caution should be exercised in using laminated models to study plastic flow.

4. 2. DISCUSSION OF QUALITATIVE EXPERIMENTS.

Nearly all the experiments on metal rolling described are open to the serious objection that the method adopted for examining the flow pattern would itself alter the conditions to such an extent that the flow pattern would be modified. With the experiments of Hollenburg, Metz, and Weiss the homogeneity of the material would be markedly affected by the insertion of

the plugs. The plugs used in Unckels experiments would violate the requirement of homogeneity to an even greater extent since they were of a different composition to the bulk of the test specimens although any effect would probably be minimised by the small diameter of the plugs used.

Surface grooves as used by Metz, Unckel, and Siebel and Osenburg would alter the frictional conditions between roll and material and as has been indicated in considering theories of rolling the value of the coefficient of friction has a pronounced effect on roll pressure distribution and hence on the flow pattern. The results obtained by these workers must therefore be treated with some caution. The validity of investigations of Unckel, and Siebel and Huhne into the flow pattern occuring within the material as opposed to the flow pattern on the surface depend on the success with which plane strain conditions were achieved. It is obvious from the photographs reproduced in Unckel's paper that the use of dowels to keep the two halves of the specimen in contact was not completely successful.

The method used by Siebel and Huhne of having guides at entry to the rolls is somewhat inadequate and the condition during their experiments must have departed very considerably from that of plane strain on the plane being examined.

In the experiments of Orowan the laminated plasticene models were rolled between wooden rollers and the coefficient of friction between rolls and the material was of the order of unity. This condition would simulate hot rolling where the material "sticks" to the rollface but could not be used to indicate the flow pattern that would be obtained in cold rolling.

In all experiments where the material is stopped while between the rolls, and then the rolls lifted to obtain a picture of the deformation in the roll gap, it is probable that the deformation pattern was modified by the creep which must have taken place.

Consideration of the experiments designed to examine the flow pattern in rolling reveals, however, a wide measure of agreement on the principal features of the deformation which takes place. Subject to the qualifications which have just been discussed these can be summarized as follows.

(a) Planes in the material parallel to the direction of rolling and normal to the roll axes remain parallel after rolling.

(b) Planes initially parallel to a plane through the roll axes become distorted and concave to the direction of rolling.

(c) The flow pattern near the edges of the rolled material differs appreciably from that in the bulk of the material.

4. 3. QUANTITATIVE EXPERIMENTS.

Quantitative tests have been designed to check theoretical predictions by measuring such things as roll force, roll torque and pressure distribution in the roll gap.

The measurement of roll force has been carried out by attaching some form of extensometer such as an electric resistance strain gauge to the mill housing and measuring the elastic deformation produced in the housing by the roll force. A disadvantage of this method is the difficulty of calibration and a more usual method is by the use of a load cell between screw-down and bearing chock. The design construction and use of such load cells has been described in various papers (4), (32).

A given roll force can be produced by widely differing pressure distributions and for this reason measurements of roll force alone are not conclusive. When experimental results for a wide range of rolling conditions, both with and without tensions, agree closely with the results predicted by theory, (see e.g. (19)) it is reasonable to assume that the theoretical roll pressure distribution must be quite close to the true distribution.

It is desirable, however, to have a check on the actual roll pressure distribution but owing to the formidable experimental difficulties involved, very

little data is available. One of the first published investigations was by Siebel and Lueg (5) and similar experiments have been carried out by Smith, Scott and Sylwestrowicz (6). A description of apparatus designed to measure the roll pressure distribution has been described by Macgregor and Palme (33), but no results have been published using their apparatus. Similar experiments have been reported by Russian workers.

In each case the principle of measurement was the same. A load measuring pin was let into the surface of the roll and was attached to a dynamometer. Siebel and Lueg used a piezo-electric element for the force measurement while Smith et al. used a photo-elastic dynamometer. The load measuring device used by Macgregor and Palme consisted of a weigh-bar fitted with electric resistance strain gauges.

The roll pressure distribution as given by Orowan's theory is in close agreement with the experimental results although one marked difference is the rounded peak of the pressure curve found in experimental results. Most theories of rolling suggest that the peak should be sharp.

The pressure measured by a pin let into the roll surface is very greatly affected by the amount of pin projection as was shown by the result of some tests carried out by Smith (6). Since the stiffness

of the dynamometer and roll invariably differ, the amount of pin projection varies as it passes through the roll gap. For this reason the results of Siebel and Lueg and Smith et al are both subject to a correction of an unknown amount.

4. 4. COEFFICIENT OF FRICTION MEASUREMENTS.

Before a theory of rolling can be applied a suitable value for the coefficient of friction for the particular conditions assumed must be obtained. An experimental determination of the coefficient under the conditions found in the roll gap presents great difficulties and most measurements are of an indirect nature.

As described in Section 2. the material leaves the rolls at a greater velocity than the roll surface. The relative magnitude of this difference, which is known as the forward slip, is fixed by the position of the neutral point which in turn is a function of the value of the coefficient of friction. Measurements of forward slip have been used by Pomp and Lueg (34) to determine the coefficient of friction.

Another method involves making a measurement of the maximum angle at which the material will be just drawn into the roll gap.

The material to be rolled is brought up to the rolls and kept in contact while the rolls are raised. At a certain setting the material is drawn

into the rolls and appears at exit reduced in thickness. From a knowledge of the original and final thicknesses and roll diameters the gripping angle α can be calculated as follows.

If h_1 is the initial thickness of the material and h_2 the thickness of the material at exit. The roll radius being R

$$\frac{h_1 - h_2}{2} = R(1 - \cos\alpha)$$

and for small α $$= R\left[1 - \left(1 - \frac{\alpha^2}{2} \cdots\right)\right] = \frac{R\alpha^2}{2}$$

$$\therefore \quad \alpha = \sqrt{\frac{h_1 - h_2}{R}}$$

When material is on point of being gripped Fig. 7.

$$P_{rr} \sin\alpha = F\cos\alpha = \mu$$

$$\therefore \quad \mu = \tan^{-1}\alpha$$

Measurements using this method have been made by Tafel (35).

Pavlov (36) attempted to measure the coefficient of friction under conditions found in rolling by applying, in effect, a back tension to a bar and reducing it to rest. The rolls then slip on the material which acts as a brake. Readings of roll force and back tension at the instant that the bar came to rest furnished data for calculating the

coefficient of friction.

A similar but more refined method has been used by Whitton and Ford (37). It can be shown that, if T is the rolling Torque, P the roll force and R the Roll radius then, when the neutral point is at exit, the coefficient of friction μ is given by

$$\mu = \frac{T}{PR}$$

The experimental method involves applying a gradually increasing back tension, which forces the neutral point towards exit, and taking simultaneous readings of roll force, roll torque and forward slip.

The value of μ when the forward slip becomes zero then gives the coefficient of friction.

Using this method for cold rolling experiments Whitton and Ford have measured the coefficient for a wide variety of materials and rolling lubricants.

Many investigators have attampted to measure the coefficient of friction by using tests where the pressures involved are of the same order as those found in rolling but where the experimental complications involved in rolling experiments are absent.

Siebel and Pomp (38) used a compression test to determine the coefficient of friction for various metals. Conical plattens were used with corresponding

conical depressions in the ends of the specimen. The angle of the cone was adjusted by trial and error until the specimens remained sensibly cylindrical while deforming plastically. With the conditions of homogeneous compression thus obtained it can be shown that the coefficient of friction $\mu = \cot \theta$ where θ is the semi-angle of the cone.

Alexander (21) using the plane strain compression test in which the conditions of pressure and motion are very similar to the rolling process, has shown that an estimate of the coefficient of friction can be made by using two sets of dies having differing die width to material thickness ratios.

In all the rolling experiments described the assumption is made that the coefficient of friction is constant throughout the arc of contact.

An attempt to check this assumption has been made by Rooyen and Backofen (39). Using a pair of pins, one radial and one inclined, let into the surface of the roll they were able to measure both the radial pressure and tangential force at the same point. The results are somewhat inconclusive as small errors in measuring the radial and tangential components lead to a substantial error in the calculated value of the coefficient of friction.

4. 5. DETERMINATION OF YIELD STRESS.

In cold rolling the yield stress varies

through the roll gap as the amount of plastic work increases. In hot rolling the yield stress is a function of the rate of strain and as this quantity varies through the roll gap it follows that there will be a variation in yield stress in this case also.

The earlier theories of rolling assume a constant yield stress through the arc of contact and although this assumption will not be too much in error in the case of cold rolling when the material has already undergone some work-hardening e.g. second and subsequent passes. It will not be a good approximation in the case of cold rolling of annealed material or for hot rolling.

Theories such as that of Orowan (3) allow the variation in yield stress to be taken into account and the problem arises as to how the yield stress variation with reduction can be determined.

Ford (40) has found that the yield stress at a particular reduction is higher than the yield stress of the same material undergoing the same reduction in an homogeneous compression test.

The yield stress can however be obtained by carrying out a homogeneous compression test such as that devised by Cook and Larke (41) and making a suitable correction for the inhomogeneity of the compression.

Another method suggested by Orowan (3)

and developed by Ford (40) is to deform the material between two plane plattens in such a way that the conditions of pressure and flow are very similar to those found in the cold rolling process.

The test has been investigated in great detail by Watts and Ford (42) who have shown that with suitable precautions the test is eminently suitable for determining yield stress curves for cold rolling.

5. DISCUSSION OF THEORIES OF ROLLING.

Consideration of the experiments designed to study flow patterns in the rolling process reveal a considerable measure of agreement on the principal features of the flow. Subject to the qualification, that the method adopted to enable the flow to be seen must, to a greater or lesser extent, have affected the conditions of the experiment and therefore the flow pattern it was intended to study, the conclusions are summarized in section 4.2. The assumptions ((a) - (f) section 3.1.) made in theories of rolling must now be examined in the light of the experimental results to assess their validity.

The assumption (a) of plane strain conditions made in all theories of rolling is supported by the experimental evidence. The experiments of Metz are typical and the results are supported by the findings of many other investigators. Non-planar conditions are confined to relatively narrow zones at the edges of the strip. The effect of these zones can be considered negligible where the width/thickness ratio of the rolled material is greater than about 10 (22). The flow pattern on the edge surface of the strip is not representative of the flow in the bulk of the material. Realization of this fact has led investigators e.g. Unckel, Siebel and Huhne to try and obtain the flow pattern in the interior of the material by splitting the specimen longitudinally

and then temporarily fixing the two halves together by various means while the specimen was rolled. It is evident from published evidence, and experience with this problem suggests, that plane strain conditions in these experiments was realized only very imperfectly.

Assumptions (b) that plane vertical sections remain plane is certainly not true for hot rolling as evidenced by the results of Metz, Unckel and Orowan. For cold rolling there is not a great deal of experimental evidence. What there is suggests that, except for heavy pass reductions, the distortion of originally vertical planes is not great. Indirect evidence is supplied by the analysis of experimental results given by Ford and Ellis which indicate that this assumption does not lead to large errors in calculating roll force and roll torque.

Assumption (c) and (d) are assumptions about material properties as opposed to assumptions about the process of rolling, and experience suggests that for metals the assumptions made are reasonable although for very large reductions marked anisotropy can develop in the rolled material (43).

As Orowan has pointed out the assumption (e) of slipping friction can only be valid when the product of the normal force and the coefficient of friction between roll face and material is less than the shear

yield stress of the material. It is therefore only likely to be true for cold rolling. Evidence for this concept is provided by the experiments of Capus and Cockcroft.

Assumption (f) is a very usual one but the only experimental measurements available are those of Rooyen and Backofen. Owing to the formidable problems involved, however, their results are somewhat inconclusive. Their experiments do seem to indicate that there is a variation in the coefficient of friction over the arc of contact. Measurements of the greatest gripping angle as used by Tafel give the coefficient of friction for one speed of rubbing and the conditions are not those found in rolling. The method used by Whitton and Ford reproduces the conditions found in rolling but if there is a variation in the coefficient through the arc of contact this method will measure the overall effect and give an average value for this parameter.

It can be seen therefore that the physical assumptions on which theories of rolling are based are reasonable for cold rolling but less so for hot rolling conditions.

The most usual test that has been carried out is to make measurements of roll force and torque for comparison with theory. A given roll force can, however, be produced by various distributions of roll

pressure and a more critical test of theory is provided by measurements of roll pressure distribution such as those of Siebel and Lueg and Smith et al.

By this criterion the theory due to Orowan predicts the form and magnitude of the roll pressure distribution very closely as do other theories based on that of Orowan, e.g. Bland and Ford.

As is evident from a comparison of calculated and experimental results (19) existing theories of rolling are able to cover with adequate accuracy for practical purposes, all cases of cold rolling. There are however a number of factors in the rolling process which are imperfectly understood and for a fuller understanding of the fundamentals of the process further investigation is required.

One of these factors concerns the coefficient of friction. Is it constant through the arc of contact, as is assumed in most theories, or does it vary and, if so, in what manner? Another factor is the manner in which the stress varies across a vertical section.

An assumption about the stress distribution across a vertical section is fundamental to all theories of rolling. With the exception of Orowan's theory, the assumption has usually been of a uniform distribution, but the only checks available to date have been roll pressure distribution measurements.

It is possible, however, that a given value of roll pressure at a point in the arc of contact could be produced by various stress distributions over the section. It is obviously desirable for a full understanding of the rolling process that the answer to this problem should be obtained.

The aim of the present work is an attempt to provide an answer to the questions posed above.

6. MEASUREMENT OF STRESS IN ROLL GAP.

6. 1. INTRODUCTION

Stresses in a material cannot be measured directly but can only be inferred by measuring the strains produce by such stresses and then using the stress-strain relation for the material. The strains in turn are obtained by calculation from an observed deformation.

For the rolling problem the deformation can be obtained by observing the deformation of an originally square network of fine lines or grid engraved on a plane which it is desired to study. The deformed grid provides data which enables the strain pattern to be evaluated. The translation of the strains to stresses is accomplished by applying the laws of plastic flow. The next section will be devoted to a brief discussion of that part of plasticity theory relevant to the problem of the rolling process.

6. 2. PLASTICITY THEORY.

It is usual in plasticity theory to neglect elastic strains as being negligible in comparison with the plastic strains. This neglect is certainly justifiable in the rolling process where the plastic strain developed is very great in comparison with elastic strains at yield point of the material. Before the material can flow plastically the yield point must have been reached. When a material is subject

to a complex stress system what is the condition which must be fulfilled before the first plastic yielding takes place? Various yield criteria have been put forward in an attempt to supply the answer.

The two most widely used are those of Tresca (17) and Von Mises (18). Both criteria have experimental support. The weight of evidence (44) suggests that the Mises criterion predicts the behaviour of ductile metals rather better than the Tresca criterion, although the latter is often easier to use mathematically.

The Tresca Criterion

The Tresca criterion postulates that plastic flow will first take place when the greatest difference of the principal stresses reaches a constant value.

Symbolically if p_1, p_2, and p_3 are principal stresses and $p_1 > p_2 > p_3$ then yield will first occur when

$$p_1 - p_3 = k \qquad (1)$$

where k is the yield stress in simple tension. Since $\frac{p_1 - p_3}{2}$ is the maximum shear stress this theory is sometimes known as the maximum shear stress criterion.

In this theory the intermediate ~~shear~~ principal stress

p_2 has no influence on the yielding and this is in agreement with the experimental evidence (45).

The Von Mises Criterion.

The criterion proposed by von Mises (18) can be written mathematically in the form

$$(p_1-p_2)^2+(p_2-p_3)^2+(p_3-p_1)^2 = 2k^2 \qquad (2)$$

Hencky (46) has pointed out that this criterion has a physical interpretation in that it represents the maximum elastic shear strain energy in the material.

Both theories predict that a hydrostatic stress will not produce plastic flow and this is in agreement with the experimental observations of Bridgman (47).

Any stress system can therefore be reduced to an equivalent system of a hydrostatic stress and a superposed stress system. The absolute stress level is dependent on the hydrostatic stress but yielding is governed by the magnitude of the superposed stresses only. The superposed stresses are known as the deviatoric stresses defined by

$$\begin{aligned} p_1' &= p_1 - p \\ p_2' &= p_2 - p \\ p_3' &= p_3 - p \end{aligned} \qquad (3)$$

where $p = \frac{p_1+p_2+p_3}{3}$ is the hydrostatic stress. Then it can be shown that the yield criteria in terms

of the deviatoric stresses are:-

$$p_1' - p_3' = k \quad \text{(Tresca)} \tag{4}$$

$$(p_1')^2 + (p_2')^2 + (p_3')^2 = \frac{2}{3}k^2 \quad \text{(Mises)} \tag{5}$$

Laws of plastic flow.

St. Venant (48) was the first to formulate satisfactory laws of plastic flow and with great insight postulated that the direction of the principal plastic strain increments (and not total strains) will coincide with the direction of the principal stresses.

If elastic strain increments are neglected and the components of a strain increment are de_1 de_2 and de_3, the St. Venant's postulate can be written mathematically as

$$\frac{de_1 - de_2}{p_1 - p_2} = \frac{de_2 - de_3}{p_2 - p_3} = \frac{de_3 - de_1}{p_3 - p_1} = \lambda \tag{6}$$

or in terms of the deviatoric stresses

$$\frac{de_1}{p_1'} = \frac{de_2}{p_2'} = \frac{de_3}{p_3'} = \lambda \tag{7}$$

where λ is a factor of proportionality which is not constant for all stages of the deformation but varies

with the strain history.

As is well known, systems of stress and strain can be represented graphically as Mohr stress and strain circles. The flow rules can be taken as equivalent to the statement that the circles of stress and strain remain geometrically similar.

The directions of the principal stresses can then be obtained from the principal strain increment directions by application of the flow rule.

The theory briefly outlined in the foregoing is generally applicable. When, however, the problem is one of plane strain, as in the case of rolling, somewhat simpler expressions result and the necessary modification to the equations will now be considered.

Plane Strain

In plane strain, flow in one of the three co-ordinate directions is prevented, and the problem is reduced to one of two-dimensional flow.

The general relations between principal stress and principal strain increments are given by

$$\begin{aligned} de_1 &= d\lambda\left[p_1 - \tfrac{1}{2}(p_2+p_3)\right] \\ de_2 &= d\lambda\left[p_2 - \tfrac{1}{2}(p_3+p_1)\right] \\ de_3 &= d\lambda\left[p_3 - \tfrac{1}{2}(p_1+p_2)\right] \end{aligned} \qquad (8)$$

where $d\lambda$ is a parameter which varies with the amount of work hardening which has taken place. The $\frac{1}{2}$ appears since elastic strains are neglected and the

deformation takes place without change in volume.

For the case of plane strain.

$$de_3 = 0$$

$$\therefore \qquad p_3 = \tfrac{1}{2}(p_1 + p_2) \tag{9}$$

The Tresca yield criterion then becomes

$$p_1 - p_2 = k \tag{10}$$

since p_3 is intermediate in value between p_1 and p_2. Substituting for the value of p_3, the Mises criterion becomes

$$(p_1 - p_2)^2 + \left(p_2 - \frac{p_1+p_2}{2}\right)^2 + \left(\frac{p_1+p_2}{2} - p_1\right)^2 = 2k^2$$

$$\text{or} \qquad p_1 - p_2 = \frac{2}{\sqrt{3}}k \tag{11}$$

The yield criterion by the two theories reduces to the same form for the case of plain strain, with a different constant. The ratio of the constants being 1.15. It can therefore be written as

$$p_1 - p_2 = C \tag{12}$$

Where C is given the appropriate value depending on the criteria of yielding adopted.

The equilibrium equations for plane strain in terms of cartesian co-ordinates are:-

$$\frac{\partial p_{xx}}{\partial x} + \frac{\partial p_{xy}}{\partial y} = 0$$

and

$$\frac{\partial p_{yy}}{\partial y} + \frac{\partial p_{yx}}{\partial x} = 0 \qquad (13)$$

The Slip Line Field.

For a plastic rigid material (i.e. a material which is assumed to have an infinite value of E so that deformation is absent under loading until yielding takes place. After yielding the yield stress is assumed to have a constant value irrespective of the imposed strain) the equilibrium conditions can be obtained in terms of the variation of the hydrostatic stress along a slip line, which is defined as a line whose tangent at every point coincides with the direction of maximum shear stress at that point. It follows, since at every point in a stressed material there are two planes at right angles on which the shear stress reaches a maximum value, that the slip line field is made up of a network of lines formed by two families of mutually orthogonal curves. If the slip line field can be found then the stress condition at any point in the field can easily be obtained.

It has become customary to refer to the two families of curves as α and β lines (22).

The equilibrium equations can then be written

in the form

$$p + 2k_s\phi = \text{constant along an } \alpha \text{ line}$$
$$p - 2k_s\phi = \text{constant along a } \beta \text{ line} \qquad (14)$$

where p = the hydrostatic stress

$2k_s$ = the yield stress in tension

ϕ = anticlockwise angle turned through by a slip line with respect to some fixed direction.

The value of the constant can be determined for a given slip line if the value of the hydrostatic stress is known at a point on the slip line. In general this will be known at a boundary and hence can be found for all other points within the field.

6. 3. OUTLINE OF TECHNIQUE USED.

It is now possible to indicate the method adopted to obtain the stress distribution in the roll gap.

The deformation pattern is obtained by measuring the deformation of an originally square network or grid incorporated in a part of the specimen undergoing plane strain. In order to obtain the strain history of an element of the material a complete roll gap pattern is required. This can be done by stopping the mill while the specimen is still within the roll gap. A quick release device, which will be described later, overcomes the objectionsto this method which have already been noted in section 4.2.

By analysing the deformed grid the direction of the principal strain increments can be obtained and therefore, by application of the flow rule, the directions of the principal stresses and the maximum shear stresses. Since stress free boundaries are known it is possible to calculate the stress distribution at all points in the roll gap.

6. 4. PRODUCTION OF GRID.

There are a number of techniques available for producing grids to enable deformation patterns to be studied. The photo grid method as described by Haven and Harding (49) is typical and the method is capable of high accuracy. Experience with this technique revealed that under the type and amount of deformation found in rolling and similar processes the emulsion film did not adhere satisfactorily to the specimen. It was decided therefore to use a grid of the engraved type. It was originally intended to use two types of grid one square formed by a network of straight lines and the other a system of closely spaced circles.

For producing a grid of circles a standard light milling-machine was used. A special tool was made and after considerable experiment it was found possible to produce closely spaced circles having a diameter of approximately 0·020 in with the necessary fineness of line and consistency of diameter.

The machine indices were used for the spacing of the circles. An example is shown in Fig. 8. It was thought that the distortion of a circle into an ellipse would enable the principal strain directions to be obtained relatively simply but owing to the small deformations involved the accuracy proved insufficient and this type of grid was abandoned. The amount of distortion of a specimen with a circular grid which was given a reduction of approximately 15% is indicated in Fig. 9.

The square grid was produced on a standard horizontal milling machine used as a dividing engine. The tool was attached to the locked arbor and the traversing of the slides carried out by hand.

The graduated indices of the machine were not used for spacing but direct readings of the movement of the work table were made with a dial gauge graduated 0•0001 in/division. The machine set up for dividing is shown in Fig. 10.

The engraving tool was ground and lapped from a hardened and tempered strip of high speed steel. The included angle of the vee-shaped tool was approximately 30° with a small radius at the apex of the vee. For use on copper a rake angle of approximately 20° was found to give the best results.

A special tool holder was made to fit on to

the milling machine arbor and to provide adequate support for the cutting tool which owing to its proportions lacks lateral rigidity. This holder can be seen in place on the arbor in Fig. 10.

The procedure adopted was as follows. The specimen was clamped in a universal machine vice and the edge, which was to receive the grid, ground on a surface grinder. The vice was then removed, without disturbing the specimen, to the milling machine on which the engraving was carried out. An example of the grid produced is shown in Fig. 11. The spacing of the lines in this example is 0·010 in and the depth of cut 0·001 in.

6. 5. SPECIMEN REQUIREMENTS.

Having obtained a grid it is then necessary to incorporate it in a plane of flow and in a zone where conditions of plane strain are found. This precludes zones near the edge of the strip. The most useful plane would appear to be that in the middle of the specimen, where it is farthest from the edges and considerations of symmetry assist in obtaining conditions of plane strain.

The method of incorporation must fulfil the following requirement:

(a) The grid itself and the method of incorporating it in a plane of flow must affect the homogeneity of the specimen as little as possible.

(b) Since the method of analysis involves the measurement of the grid before and after rolling the method of joining the two halves of the specimen must not distort the grid.

(c) The strength of the joint must be sufficient to resist the forces tending to separate the parts during the deformation.

(d) After the deformation process has been completed it must be possible to part the joint, for examination of the distorted grid, without introducing any further deformation.

With a reasonably fine grid the method of joining is more likely to affect the homogeneity than the grid itself. Various methods of joining were tried. The use of dowels and bolts, as used by a number of investigators presented practical difficulties as this involved fitting the bolts into material 2 in. wide and nominally $\frac{1}{8}$ in. thick. It was felt that the largest diameter of bolt should not exceed $\frac{1}{16}$ in.. This requirement presents a formidable drilling problem. A more fundamental objection to this method arises from the spacing required. It was found that to get a reasonable approximation to plane strain conditions the spacing of the bolts was such as to completely destroy the homogeneity of the specimen. This difficulty has been apparent in published work and is borne out by the experience of other workers dealing with similar problems involving the creation of plane

strain conditions at an interface.

The use of a resin based bonding agent, "Araldite", was tried. A strong joint was obtained but the amount of plastic strain that the resin can sustain appears to be small and the joint failed when the specimen was rolled and reduced by an amount which was of the order of 10%.

Attention was then turned to welding processes. Fusion welding is ruled out since the grid would be wholly or partly destroyed by the welding process and since the joint produced is a permanent one subsequent examination of the grid would be impossible.

A number of metals can be welded by a technique known as pressure welding. The common metals to which this process can be applied are aluminium and copper. Aluminium and its alloys can be welded by the application of pressure alone. A very full study of the possibilities of this process together with an investigation of the necessary conditions has been made by Tylecote (50).

Some tests to ascertain the suitability of the pressure welding process as applied to copper have been made by Cook and Davis (51) while a more comprehensive series of tests to find the optimum conditions for satisfactory welding were undertaken by Cook and Holmes (52).

The pressure welding of aluminium is accomplished by inducing a large amount of local deformation between the two surfaces in contact. The relative movement between the surfaces breaks down the tenacious oxide film and satisfactory welding takes place.

Pressure welding of copper requires the simultaneous application of pressure and heat. The temperatures involved are well below the fusion temperature for copper. A weld which has an U.T.S. comparable with that of the parent metal also requires a certain amount of local deformation but considerably less than that required for aluminium.

The very heavy local, in this case interfacial, deformation that is required to weld aluminium ruled out the use of this metal. H.C. copper was found to be most suitable and by using a combination of the correct temperature and pressure a joint could be produced which fulfilled all the requirements laid down above.

Existing data on pressure welding of copper is confined to the range necessary to obtain a joint which is comparable in strength to the parent metal. The relatively low joint strength wanted for the present application required an investigation into the effects of pressure and temperature at the lowest range of values at which pressure welding was possible at all.

To investigate the pressure welding of copper a large number of specimens, similar in properties and dimensions, to the ones used for the rolling tests were prepared. These specimens were welded under different conditions and the suitability of the joint assessed.

6. 6. PREPARATION OF SPECIMENS.

The specimens were prepared from strips of H. C. copper of $1\frac{1}{4}$" x $\frac{1}{8}$" section and having a length of 6". A specimen consisted of two such strips placed edge to edge to form a specimen $2\frac{1}{2}$" wide. A grid was engraved on the edge of one strip to enable the distortion, if any, produced by the welding process to be measured.

The preliminary treatment of each specimen before welding was similar. The ground edges which were to be joined were first treated with No 0. emery paper to produce a matt appearance. Great care was taken to avoid rounding of the edges. After the removal of grease by washing with carbon tetrachloride and drying, the edge was immersed in concentrated nitric acid for 5 seconds and then washed in running water.

The two strips forming a specimen were then placed with the prepared edges in contact in the jig shown in Fig. 12. A jig is necessary to maintain alignment of the two halves during the welding process.

The two steel blocks A.A. which lightly nip the two halves of the specimen B.B. between them by means of the bolts at the ends serve to align the specimen. The blocks C.C. which have shallow grooves machined along their length to suit the specimen thickness allow the load, applied by a standard compression testing machine, to be distributed over the length of the specimen. Dowels D. align blocks C.C. This is arranged by having the dowels an interference fit in one block and a sliding fit in the other. The frame E enables vertical alignment to be maintained when the load is applied through block F.

Determination of Optimum Conditions for Welding.

Heating was carried out in a furnace fitted with thermostatic control. The complete assembly consisting of specimen B.B. and blocks A.A. and C.C. was transferred to the furnace and the amount of oxidation reduced by covering the assembly during heating with a light gauge steel box sealed with asbestos string. On reaching the required temperature the assembly was placed in the frame E., which had already been lined up in the testing machine, and the load applied. The load was held constant while the specimen cooled down.

An indirect method was used to assess the temperature at which the load was applied. A specimen was prepared with a thermocouple embedded in the

interface. The whole assembly of B., A. and C. was then inserted into the furnace at a fixed temperature and a heating curve of temperature against time plotted. On removal from the furnace the jig was quickly removed to the frame E. which was in place in the testing machine and a cooling curve plotted. (Typical examples are plotted in Fig. 13.).

By suitable choice of furnace temperatures and heating time and a knowledge of the rate of cooling, various temperatures of specimen could be obtained by allowing a suitable lapse of time before applying pressure to the specimen. Using this technique welding was carried out with various combinations of pressure and temperature.

The initial testing of the weld was carried out by a plane strain compression test as described by Watts and Ford (42). The specimen was given a deformation of approximately 40%. For those welds which passed this test satisfactorily a portion of the specimen was removed to form a tensile test piece to determine the tensile strength of the joint and a further portion rolled in the rolling mill. The joint in the remainder of the specimen was broken for examination and measurement of the grid.

Pressure between 1 and 3 ton/sq. in. were applied and temperatures between 600° and 900° C.

It was found that below 700° C no welding

took place at all and at approximately 850° C welding was so effective, with considerable grain growth across the interface, that portions of the grid were destroyed when the joint was broken.

It appeared that the quality of the weld is more sensitive to variations in the temperature than to variations in the pressure.

As a result of these tests the conditions of welding, for the material being used, were standardized at 720° C and a pressure of 1 Ton/sq. in..

Under these condtions no measurable distortion of the grid took place during welding. The grid was measured both before and after welding on an O.M.T. toolmakers microscope. The movement of the worktable of the microscope is controlled by micrometer screws with drums graduated in 0·0001 in. divisions. Measurements could consistently be estimated to half a division.

The specimens for the rolling tests were made from $\frac{1}{8}$" thick H.C. copper sheet and were prepared using the conditions specified above. After welding, the surfaces were ground on a surface grinder to ensure uniformity of thickness. The nominal thickness was 0·120 in..

A tensile test piece was cut from each of 6 specimens, the position being indicated in Fig. 14. The tensile tests were carried out in a Hounsfield

Tensometer and the results of these tests are recorded in Table 1.

TABLE I.

Test Piece No.	Breaking Load lb.	C.S.A. sq.in.		Breaking Stress lb/sq.in.
1	56	·1205 x ·501	·0604	930
2	286	·1202 x ·500	·0601	4760
3	260	·1200 x ·499	·0599	4350
4	61	·1205 x ·498	·0600	1020
5	248	·1203 x ·502	·0604	4110
6	236	.1203 x ·502	.0604	3910

It will be observed that two of the test pieces broke at considerably lower stresses than the others. On examination the weld was found to be poor. This poor welding, which occurred with a number of the specimens, was confined to small areas near the ends of the specimen. This 'end effect' was observed in some of the earlier experiments to determine optimum conditions for welding. It is thought to be due to the difficulty of obtaining a uniform distribution of pressure over the whole length of the specimen. For this reason, approximately half an inch was cut off each end of all specimens and discarded before rolling tests were carried out.

To assess the possibilities of the method of joining, a portion of one specimen was given a

reduction of 85% in 10 passes. When the joint was broken the interface was found to have remained absolutely plane and the heavily distorted grid still plainly visible.

Various methods were tried for breaking the joint after rolling. The most satisfactory method was found to be by holding the specimen in a machine vice with the joint in line with the top of the jaws. A bending moment applied to the portion of the specimen outside the vice jaws resulted in a clean parting of the joint without distortion of the grid.

6. 7. OBTAINING THE ROLL-GAP PATTERN.

The method that has been adopted by nearly all investigators to obtain the deformation in the roll gap is as follows.

The material to be rolled is inserted between the rolls with the mill running and the length of strip chosen such that the mill can be stopped with the material still within the roll gap. As soon as the mill has stopped the upper roll is lifted as quickly as possible and the material removed for an examination of the pattern of the roll gap left on the strip.

This method is open to two objections. One is that the problem, which is a dynamic one, is reduced, as soon as the mill stops, to a static one and the shape of the roll gap may differ in the two cases. The other objection arises from the fact that

the raising of the top roll using the normal screw down is a fairly slow process and, especially in annealed material, the possibility of creep affecting the shape of the roll gap cannot be ruled out.

The measurements carried out by Orowan (3) to determine the shape of the deformed roll are open to this objection and he admits that the profile may require modification to allow for the creep which may have taken place between the stopping of the mill and the raising of the upper roll.

6. 8. QUICK RELEASE MECHANISM.

The most obvious solution to the problem of obtaining a rapid release of load is to introduce a component between the end of the screw on the screw down and the bearing chock, such that the thickness can be reduced very rapidly thereby producing the necessary rapid release of load.

The rolling mill used for all experiments was a commercial two high mill manufactured by W. H. Robertson of Bedford having 4in. diameter rolls with a 6in. face and driven by a 7 H.P., constant speed, D.C. Motor. General views of the mill are shown in Figs. 15. and 16.

The mill was designed for a maximum roll force of 20 tons and therefore to enable the full capacity of the machine to be used the quick release elements must each be capable of removing a load of

10 ton. The space available in this mill for fitting the quick release element is very limited being approximately a cube of 2in. side.

The use of a small hydraulic cylinder and ram was first considered but with the size of cylinder possible in the available space very high pressures would be required. The problems of control and sealing at the pressure involved were thought to be too great and this type of quick release mechanism was not considered further.

The mechanical device eventually used consists of two short cylinders, each having a number of projections or "teeth" at one end. In the working position these "teeth" are opposite each other as shown in Fig. 17 (a). A partial rotation of one cylinder relative to the other allows the teeth on one to drop into the spaces on the other giving the required reduction in height as shown in Fig. 17 (b), thus giving a relaxation of the load.

The relaxation will be complete if the reduction in height is greater than the combined elastic recovery of housing, rolls and strip. Owing to the restricted space available the reduction in height was limited to $\frac{1}{8}$in. but this proved to be sufficient for the greatest pass reduction that could be made with rough rolls on a strip having an initial thickness of 0·12".

A pair of experimental cylinders similar to those shown in Fig. 17 were made and loaded in a standard testing machine. They were found to operate satisfactorily for low loads but for loads above approximately 2 tons a considerable torque was required for operation.

The restrictions on size between screw and bearing chock already mentioned are also applicable to the mill generally and for this reason the mechanism for operating the load release elements would have to be of relatively light construction.

To reduce the operating torque to a value that could be applied by a light mechanism the cylinders were modified by machining a helix on the faces of the teeth such that the load supplied a component tending to "unload" the release cylinders. The shape can be clearly seen in Fig. 18.

The angle of the helix was calculated to be the equilibrium angle for an assumed value of the coefficient of friction between upper and lower blocks and was then modified by trial and error until the full load could be released by the application of a small torque. The reduction in torque also has the advantage that a sensitive control of release is obtained.

Fig. 19 shows the complete quick release device with the operating mechanism. All the components in this Fig. are in the correct relative position. Two

views of the mechanism in place on the mill are shown in Figs. 15 and 16.

A drawing of the assembly showing details is given in Fig. 20.

The two halves of the release block A_1 and A_2 are kept in the correct relative position by a pin which is a press fit in A_2 and a sliding fit in A_1, The complete block is located in positon by a recess machined in the top of A_1, to accomodate the end of the screwdown screw and by a pad C which is recessed, partly into the top of the bearing chock and partly into A_2.

The operating mechanism is carried on a sub-frame J bolted to the rolling mill housing.

Operation of the hand lever G produces a longitudinal movement of the bar E. By means of pin F, attached to E, movement of the slotted arm D is obtained and hence partial rotation of A_1 is produced with the consequent release of load.

Rotation of the lower half of the release block A_2 is prevented by tie tod H. With the handle G in the working position shown, the mechanism is self locking. Rotation of G through 90° produces complete release.

Complete adjustment is provided and adjustment points can be clearly seen on the drawing.

To ensure positive lifting of the rolls when

the quick release mechanism is operated the upper bearing chocks are spring loaded. The springs are visible on top of the mill housing in the general views of the mill, Figs 15 and 16.

6. 9. OPERATION AND PERFORMANCE OF THE QUICK RELEASE MECHANISM.

To ensure a satisfactory roll gap impression on the specimen, when the quick release mechanism is operated, requires the application of a back tension great enough to overcome the forward force resulting from the weight of the specimen and the coefficient of friction between specimen and roll.

To one end of each specimen a small ring was soft soldered and the ring attached to a "soft" spring (stiffness approx. ·05 lb/in). The other end of the spring was attached to a suitable point on the entry side of the rolling mill. The spring can be seen in Figs. 15 and 16.

The length of material rolled before the quick release mechanism was operated, was about 3" and the spring tension adjusted to give an initial tension of 1 lb. On release of the roll force this back tension was sufficient to withdraw the specimen from the roll gap.

It is thus possible, using this technique, to obtain a pattern of the roll gap under dynamic conditions.

The effect of using the quick release mechanism can be seen in Fig. 21. Specimen (a) was rolled using the quick release mechanism and (b) using the technique of stopping the mill and raising the top roll as quickly as possible (in this case 3 - 4 secs) by the screw down gear.

Talysurf records of the two specimens photographed in Fig. 21 are plotted in Fig. 22. The records were obtained by traversing the stylus over both sides of the specimen and then taking the mean reading at each section to obtain one half of the true profile.

Fig. 22 shows that the quick release mechanism does effectively get rid of the 'creep' which is present when the technique of obtaining a roll gap impression by stopping the mill with the material in the roll gap is adopted.

6. 10. MEASUREMENT OF ROLL FORCE AND ROLL TORQUE.

As a check on the results obtained it was decided to measure both roll force and torque. The roll force was measured by a load cell introduced between the screw and bearing chock. The output from the cell is indicated on a microammeter and the calibration for the two cells used is given in Fig. 23. The roll torque was measured by using an electrical wire resistance network affixed to the spindles of the mill drive. The measurement of both

roll force and roll torque by this method has been described by Rankine et al (4). The output from these is again taken to microammeters. The calibration for the torque meters is given in Fig. 24.

The microammeters indicating both roll force and roll torque are grouped on one panel and a cine film record of the meter readings was taken during a test. The microammeter readings are then read back from the developed film.

It would have been desirable to make measurements of roll force with the quick release mechanism in place but the space restrictions made this impossible. Measurements of roll force and torque were made as follows.

Strips of high conductivity copper taken from the same sheet of material as the test specimens, were machined to the same width and thickness as these specimens and subjected to the same heat treatment. Each strip was approximately 18" long.

These strips were then passed through the rolling mill with an increase in reduction for each strip. Cine film records of the tests were taken and the variation of roll force and roll torque with reduction is given in Fig. 25.

An estimate of the frictional torque was obtained by forcing the rolls together by means of the screwdown without material between the rolls and

measuring the torque for each value of roll force.

6. 11. ROLLING OF SPECIMENS.

The rolling programme for the test specimens containing a grid on the central plane envisaged a series of passes ranging from a reduction of about 10% to the maximum reduction that could be obtained in one pass. For each test specimen a number of dummy specimens were prepared having identical dimensions to the test specimens and having been subjected to the same heat treatment. These were used for initial setting of the rolling mill to ensure parallelism of the rolls and that the required reduction would be obtained.

Great difficulty was experienced in obtaining specimens with a roll gap impression symmetrically disposed about the centre line of the specimen.

In spite of extensive experiment and variations in technique this particular problem was not completely solved and a large proportion of test specimens had to be discarded because of gross lack of symmetry in the roll gap impression. The behaviour appeared to be completely random and the obtaining of a symmetrical roll gap pattern a matter of chance.

7. ANALYSIS OF DEFORMED NETWORK.

7. 1. INTRODUCTION.

In the most general case of deformation in a homogeneous strain field a cube will deform into a parallelopiped or a spherical element will deform into an ellipsoid. For the case of plane strain the problem is reduced to one of two dimensions and the corresponding transformation is from a square to a parallelogram or alternatively from a circle to an ellipse.

The change in direction of the principal axes during deformation is easier to visualize by considering the change from a circle to an ellipse, the major and minor axes of the ellipse giving the directions of the principal strains. For quantitative analysis, however, a square network is more convenient to use.

In the present problem the deformation pattern in the roll gap is obtained by the technique, already described, of releasing the roll force with the material still between the rolls. The impression thus obtained enables the complete strain history at any point to be examined. This is important since the stress at any point is a function of the strain history and not of the total strain finally

developed at that point.

Considering one square of the network in Fig. 26. (a). During its passage through the roll gap it will, in general, suffer a rigid body displacement, rotation and deformation Fig. 26 (b) relative to a set of axes fixed in the material and moving with it.

If the strain field is homogeneous, or alternatively, if the strain field is not uniform but the square is made small enough so that the strain in the region surrounding the square can be considered to be sensibly homogeneous, then the deformation will be the type already described and the square will deform into a parallelogram.

If the strain pattern changes rapidly, in a distance comparable with the grid spacing being used, the assumption of homogeneity of strain is no longer valid. In this case the assumption can only be sustained if the grid line spacing is considerably reduced. There is however a limit to the reduction in spacing which can be effected, for the error of the measuring equipment remains constant and as the spacing is reduced there is a corresponding increase in the percentage error.

It is possible to devise a method of analysis to be described later, which enables the data required for the calculation of the magnitude and

direction of the principal strains to be evaluated at a point.

Thus, however rapidly the strain pattern changes over a region, in the vicinity of a point it can be taken as being homogeneous, and it is possible to apply to it an analysis developed for a homogeneous strain field.

7. 2. MEASURING EQUIPMENT.

All measurements were made on an O.M.T. Toolmakers Microscope. A view of the instrument is shown in Fig. 27.

The table on which the specimen is placed is free to move in a horizontal plane in two co-ordinate directions. The movement is controlled by micrometer heads graduated in 0•0001 in divisions and having a total movement of lin.. By using slip gauges the maximum travel in the longitudinal direction is 6in. and at right angles to this 2 in.. In conjunction with cross wires in the ocular of the fixed microscope it is thus possible to obtain the co-ordinate readings for specified points on the surface of the specimen. Angular measurements can be made either by rotating the cross-wires in the microscope ocular or by rotating the table. The amount of rotation being measured on the appropriate scale. Whether the ocular or table is used for angular measurement depends on the particular

application.

Interchangeable objectives enable magnifications up to X 100 to be obtained.

7.3. METHOD OF MEASUREMENT.

After trying various techniques of measurement to assess the accuracy obtainable it was decided to measure the co-ordinate positions of nodal points in the deformed grid and to obtain the necessary data, involving lineal and angular measurements, by calculation from the co-ordinate readings.

Each specimen was measured three times before pressure welding and three times after a successful roll gap impression had been obtained. Any point for which there was poor agreement between the three readings was re-checked.

The specimen, clamped in position on the microscope, was orientated by rotating the table until one of the grid lines in an undeformed area was parallel to the line of travel of the table. The table was then locked against rotation and co-ordinate readings of the nodal points taken.

Readings could be estimated to ·000025 in. and consistent readings to ·0001 in. were obtainable. The consistency of readings, to a large extent, depending on the fineness of the engraved line.

7. 4. METHOD OF ANALYSIS.

As already indicated, the analysis is directly applicable only to a homogeneous strain field where a square deforms into a parallelogram or a circle into an ellipse Fig. 28.

Then if the sides of the parallelogram are 2a and 2b and the included angle between them is θ, the angle α, which the principal strain direction makes with the longer side 2a, can be shown to be :-

(see Appendix I)

$$\alpha = \frac{1}{2}\tan^{-1}\frac{\sin 2\theta}{\left(\frac{a}{b}\right)^2 + \cos 2\theta} \qquad \text{Eq(1)}$$

and the magnitude of the principal strains e_1 by,

$$e_1 = \frac{\sin\theta}{\left\{\sin^2(\theta-\alpha) + \left(\frac{a}{b}\right)^2 \sin^2\alpha\right\}^{\frac{1}{2}}} - 1 \qquad \text{Eq(2)}$$

Equations (1) and (2) enable the direction and magnitude of the principal strains to be calculated if a, b and θ can be measured. If the direction of the principal strain increment is known the principal stress direction follows and hence the maximum shear stress direction. These shear stress directions form an orthogenal network - the slip line

field.

The importance of the slip line field has been dealt with in section 6.2.

The calculations for α and e_1 are somewhat tedious and it is more convenient to carry out systematic calculations giving the variation in α for a range of values of Θ and the ratio $(a/b)^2$ and present the results in the form of graphs.

The detailed calculations are given in appendix I and the results of the calculations tabulated in Tables II and III.

Graphs enabling the direction of the principal strains to be obtained are given in Figs. 29 and 30 (a) and 30 (b). Graphs for determining the magnitude of the principal strains are given in Figs. 31. and 32..

Figs. 29. and 31. give values of α and e_1, for a range of Θ between 90° and 86° and for $(a/b)^2$ between 1·0 and 4·0.. For most applications where an incremental theory is to be used Θ and a/b will vary over a very much more restricted range of values and, therefore, Figs. 30 (a) and 30 (b), have been prepared for a range of Θ of 1° and values of $(a/b)^2$ between 1·000 and 1·100 and 1·10 and 2·00.

Fig. 32 enables values of strain to be determined for a range of Θ of 1° and values

of $(a/b)^2$ between 1·001 and 1·050. This graph has been plotted in a different way for convenience in use.

It will be seen from Figs. 29, 30(a) and 30(b), that for small increments of deformation, i.e., for values of Θ differing only slightly from 90° and ratios of a/b close to unity, the direction of the principal strain is very sensitive to small changes both in the angle Θ and the ratio a/b and interpolation is not easy.

In this range, practically the most important one, it was found that the original equation could be modified by making certain approximations to give graphs which are more convenient to use, since interpolation is easier and gives satisfactory accuracy for the range of variables met in practice.

The modifications necessary to equation 1. are discussed in Appendix II. The modified graphs are given in Figs. 33, 34(a) and 34(b).

Values which differ by 1% from the exact expression are indicated on the graphs. This value was chosen since it was thought that the data from the measurements could not be relied upon to a greater degree of accuracy than this.

It will be seen that in the most useful region the difference between the approximate and the

more exact expression is considerably less than 1%.

The calculations for these modified graphs are given in table IV, Appendix II and the calculations for limits of accuracy in Table V.

When examining the distortion of the square network the analysis must proceed in a step-wise manner. The size of each step being determined by the rapidity with which the strain pattern changes in that region.

Strain increments must be obtained in terms of increments of deformation. The strain increment associated with a given increment of deformation is computed by using as a reference configuration the configuration of the system immediately before the application of that particular increment of deformation.

This is illustrated, for a homogeneous strain field, in Fig. 35. After one increment of deformation the original square 35(a) is deformed into the parallelogram 35(b). A further increment of deformation produces the parallelogram shown in 35(c). To obtain the increment of strain between stages (b) and (c) the appropriate increment of deformation which has taken place between (b) and (c) must be considered. This can most easily be done by considering the deformation which would be

impressed on a square element PQRS in stage (b). In stage (c) this would become a parallelogram P'Q'R'S' whose sides have the ratio $\frac{a''}{b''} \cdot \frac{b'}{a'}$ and an included angle $90 - (\Theta'' - \Theta')$. It is to be understood that the increments of deformation are small.

When the strain field is not homogeneous the original square network will deform into a network of quadrilaterals. The method of analysis adopted in this case is as follows.

Reference is made to Fig. 36.

A vertical element aa and a horizontal element bb, defined in each case by the nodal points of the network, are considered. For the vertical element aa progressive deformation as the material passes through the roll gap will result in changes of length and rotation, as shown, from aa to a'a' and then to a''a''. The angle this element makes with a reference direction changing from ϕ' to ϕ''. Similar arguments apply to the horizontal element bb which progressively takes up the positions indicated by b'b' and b''b'' and rotates through ψ' to ψ''. In both cases the changes in length and orientation will be continuous except in regions where discontinuities occur.

By plotting the data obtained from measurement of the nodal points it is therefore

possible to obtain the length and direction of an element at any point in the field.

In general the original straight lines of the network will deform into the form shown in Fig. 37. For clarity the diagram is greatly distorted.

The initial network size must be chosen so that the curvilinear sides can be replaced by the chords 12, 23, 34 and 41 without great error.

The side 12 changes continuously through aa and a'a', (these two being taken very close together and therefore can be considered parallel,) to 34. The angle these lines make with a reference direction changing from ϕ_1, through ϕ to ϕ_2.

Similarly 14 changes through bb b'b' to 23. The angle changing from ψ_1, through ψ to ψ_2.

The element at the centre of the figure is a parellelogram whose sides have the ratio aa/bb and an included angle of $90° + \Psi - \Phi$. These approximations enable the analysis already developed for the case of a homogeneous strain field to be applied to this case.

To test the assumptions made in the theory some tests were carried out on flat specimens which were loaded in such a way that the direction of principal stress was accurately known. The direction

was calculated from the distortion of a network engraved on the surface. These tests and the results are described in Appendix III. Very satisfactory agreement was obtained. The method has been used subsequently by Lianis (53) to obtain slip line fields for the bending of notched bars and by Shah (54) to analyse the problem of machining.

8. RESULTS.

8. 1. THE ROLLING SCHEDULE.

The original intention was to obtain roll gap impressions for a range of reductions and for various frictional conditions between strip and roll. Owing to the difficulties of obtaining a satisfactory impression the intention of rolling a number of specimens with various lubricants was abandoned and all rolling was carried out clean and dry. It was considered that the frictional conditions would be more reproducible than in the presence of a lubricant. In each case immediately before rolling both strip and roll face were thoroughly degreased with carbon tetrachloride and allowed to dry. The frictional conditions between roll and strip were varied by altering the surface finish of the roll. Early passes were made with rolls having a finely ground finish. Further series of passes were carried out using rougher rolls obtained by rolling emery cloth through the mill. This method of roughening the rolls was used by Whitton and Ford (37) and the roughness of surface finish produced by this method is discussed in their paper.

All roll gap impressions were obtained by using the quick release mechanism described in sections 6. 8. and 6. 9.

Although great care was taken with the rolling

technique the majority of specimens had to be discarded through one or other of two faults, curvature of the specimen and gross lack of symmetry about the geometric centre line of the roll gap impression. In some specimens these two faults were combined.

Of the satisfactory specimens three were from those rolled with the rolls in the roughest condition and as these were the only ones giving a range of reduction for one frictional condition they were used for analysis.

The reductions obtained were 21·8%, 35·4% and 50·2% all in one pass. Although a greater range of reductions would have been desirable the practical range was restricted by the following factors.

The upper limit of reduction is reached when the geometry of the roll pass is such that when the strip is presented to the roll gripping of the strip does not occur. For the present experiments, with a strip thickness of approximately 0·120", this limit was reached at a reduction of about 40%. By tapering the edge presented to the roll it was found that a reduction of approximately 50% could be obtained.

The lower limit of reduction is determined by the accuracy of the measuring apparatus available. It was found for reductions below about 20% that the deformations over the greater part of the roll gap

impression were so small that meaningful results could not be obtained with the accuracy of measurement possible with the equipment used.

The three specimens obtained were considered suitable for analysis as they covered a reasonable range of reduction values for the same frictional conditions.

The relatively high value found for the coefficient of friction accentuates the effect of this variable on the roll pressure distribution and therefore makes comparison with the theoretical predictions easier.

8. 2. THE DEFORMATION PATTERN.

Examination of the photographs, Fig. 38, which illustrate the rolled specimens for the reductions used, show that the assumption of plane sections remaining plane, made in so many of the theories, is a very reasonable one for cold rolling, even for reductions in one pass as high as 50% and with a relatively high coefficient of friction, for the vertical lines indicate only a small amount of distortion. Owing to the necessary small size of the specimens further analysis of the deformation pattern could only be made after careful measurement of the grid had been carried out.

The measurements of grid spacing were carried out as explained in section 7. 3. The

co-ordinate values of the nodal points are tabulated in Tables VI - VIII. Where curvature of the specimen was present the co-ordinate readings were adjusted to give a straight centre line and it is the corrected values which have been tabulated. This procedure was adopted only for specimens with small curvature. Small curvature, in this connection, was taken as being a departure from the geometric centre line of the roll gap by the actual centre line of the specimen of not more than 0·002" in the length of the roll gap impression. As already mentioned specimens with pronounced curvature were rejected.

Further information about the deformation pattern is revealed in Fig. 39. In these diagrams the vertical lines of a half section above the centre line of the specimen have been plotted with an exaggerated horizontal scale and uniform spacing along the centre line to bring out the variations in spacing which occur as the vertical sections pass through the roll gap. The appearance of these lines when plotted with vertical and horizontal scales given the same weight and with the correct spacing can be seen by referring to Figs. 40, 41 and 42.

The pattern of deformation as revealed in Fig. 39 shows marked similarities between the three

reductions and indicates that the geometry of the pass does not greatly affect the pattern. It is clear that the largest deformations are reached at the surface of the material and that the characteristic pattern is as follows. Immediately after entry there is a marked increase in the spacing of the vertical lines with a slight bending convex to entry. This increase in spacing is followed by a tendency for the spacing to decrease. A zone of fairly uniform spacing is succeeded by a reduced spacing accompanied by a double curvature of the lines with a portion of the lines becoming slightly convex to exit.

The pattern as just described is most clearly seen for specimen A Fig. 30., but is apparent in both specimens B and C. A point of interest with specimen B is that although the reduction is greater than that produced on A, 35.4% as opposed to 21.3%, the magnitude of the deformations is noticeably smaller. The characteristic deformation pattern as already described can, however, be discerned.

This pattern would appear to support the theories of rolling (section 3) which postulate that relative slip between material and roll face takes place over the greater part of the arc of contact and that the direction of slipping at any point is dependent on the relation of that point to the neutral point. At entry the direction of slip is toward the

neutral point and the tangential stresses at the surface would tend to increase the spacing of the lines and produce the curvature. Near exit the direction of the tangential stresses changes and the tendency is to reduce the spacing of the lines and alter the sense of the curvature already produced earlier in the deformation. The region over which the spacing appears to be fairly constant spans the point at which the occurence of a 'neutral point' is predicted by theory. A consideration of the slip-line field suggests that there is in fact a zone in the arc of contact within which the deformation is essentially homogeneous compression but discussion of this point will be postponed until the analysis leading to the construction of the slip line field has been described.

8. 3. THE ELASTIC-PLASTIC BOUNDARY.

The lines of the grid initially parallel to the direction of rolling become distorted on entering the zone within the roll gap in which plastic deformation takes place. They then follow the "stream lines" in this region and again become parallel to the direction of rolling after leaving the roll gap. The point at which the direction of such a grid line changes direction defines the boundary between the elastic and plastic zones in the material. In the ideal rigid-plastic material this change is abrupt and the two zones are separated by a line but in real

materials, and particularly in the present case where the material is in the annealed state and initially undergoes rapid work hardening, the boundary is no longer a line but is a zone through which the behaviour changes from elastic to preponderently plastic.

The method of obtaining this boundary is illustrated in Fig. 43. for specimen A. The data for plotting is taken from Table VI and plotted to scales which accentuate the difference in slope between a "stream line" within the plastic zone and the same line outside this zone. The actual change in direction takes place over a small distance and is a gradual transition from one slope to the other. For the purpose of fixing the boundary the two lines were extrapolated with the appropriate slope and the point of intersection taken as defining the boundary between elastic and plastic behaviour on that stream line.

A similar construction was used for specimens B and C. The boundaries in each case have been plotted on Figs. 40, 41, and 42.

The shape of the boundary both on the entry and exit side for all three specimens is very similar in shape with a tendency for the shape to become more pronounced with the greater reduction.

It is evident, on the entry side, that plastic deformation extends right to the centre line of the specimen in a distance from the plane of entry which is

a function of the reduction and decreases with increasing reduction. For 21·3% reduction this distance is 0·039" while for 50·2% reduction this has decreased to 0·024".

8. 4. OBTAINING a/b AND Θ.

The method of analysis has already been outlined in section 7. 4. and reference to Fig. 23 indicates that the quantities required to enable the direction of the principle strain directions to be obtained are Θ, the angle between elements of the grid which were initially parallel and normal to the direction of rolling, and the ratio a/b of the sides of the element. Θ can be obtained by measureing ψ and ϕ as can be seen by referring to Fig. 37. ψ is the angle which a tangent to a "stream-line" at any point makes with the rolling direction and ϕ is the angle which the tangent to an element of the grid at any point which was initially normal to the direction of rolling, makes with this normal direction. The angles ψ and ϕ are illustrated in Fig. 36. The values of 2a and 2b, the sides of the deformed square grid and the angle ϕ are obtained by calculation from the co-ordinate readings of Tables VI - VIII. The angle ψ is more conveniently calculated from a plot of the type used for Fig. 43.

Typical calculations are given for specimen A.

The results for ψ, 2a, 2b and ϕ are given in Tables IX, X and XI respectively.

In all cases the variation in these quantities is most conveniently calculated along the "stream lines". The dimension of the specimens and spacing of the grid gave eleven of these stream lines across the thickness. These grid lines were designated 1 - 13, 1 - 6 lying on one side of the centre line and 7 - 13 on the other. 1 and 13 are, in fact, the boundaries, that is, the trace of the surface of the specimen. Since the specimens are symmetrical the analysis was carried out over the half covered by grid lines 7 - 13.

The variation in ψ along the stream lines 8 - 12 for each of the specimens A, B and C is plotted in Figs. 44, 45 and 46 respectively.

Similarity of pattern is apparent for the three specimens. The angle on a given stream line at a given distance from the entry plane increases, as might be expected, with increasing reduction. It is also apparent from a consideration of the shape of these stream lines that the deformation shows some departure from homogeneous compression. Deformation of the latter type would require that the stream lines be circular arcs, as is the boundary, with a uniform reduction in the slope of the tangent, and hence ψ,

from entry to exit. The inflexion present in the curves Fig. 44 - 46 indicates that the lack of homogeneity in the compression is quite small but increases with increasing reduction and is also more pronounced nearer the surface.

The variations in the length 2a and 2b for the three specimens are plotted in Figs 47 - 49 for 2a and Figs. 50 - 52 for 2b. The variation in these two quantities appears uniform from entry to exit, 2a increasing and 2b decreasing. The final dimensions agree closely with those which would be predicted from considerations of constancy of volume and plane strain. It is also apparent that the variation in 2a and 2b is uniform across the thickness of the specimen since the points for all streamlines in one specimen plot on to one curve.

As in the case of ψ the angle ϕ was calculated for variation along a stream line and the results are plotted in Figs. 53, 54 and 55. The pattern revealed in these three figures shows a general similarity. The crossing of the curves for the various streamlines plotted in Fig. 55 is explained by reference to Fig. 39. It will be noted that as the reduction increases the inflexion in the vertical sections as exit is approached becomes more marked.

With the variation in the quantities 2a, 2b, ψ and ϕ plotted along the stream lines it is now

possible to read off the values for co-ordinate points in the specimen. For convenience the co-ordinates were taken at the nodal points of the deformed grid pattern. At each nodal point the lengths 2a and 2b are read off and hence the ratio a/b obtained. A knowledge of the values of ψ and ϕ at the same nodal point enables the included angle Θ to be obtained.

8. 5. DETAILS OF CALCULATIONS FOR ONE SPECIMEN.

The fully tabulated results for specimen A are set out in Table XII and the course of the calculations will now be followed in detail.

Reference is made to Table XII. Columns (1) and (2) give the co-ordinate readings for the nodal points along a particular stream line. Columns (3) to (6) are obtained from graphs already plotted Figs. 44 - 55.

The general method of analysis has been set out in section 7. 4. but the specific method used for the present specimens is illustrated in Fig. 56. It will be seen by reference to this figure that Θ in column (9) is obtained from a knowledge of $\phi_2 - \phi_1$, and $\psi_2 - \psi_1$. These values are tabulated in columns (7) and (8).

The method is illustrated in the table below

x	ϕ	ψ	$\phi_2 - \phi_1$	$\psi_2 - \psi_1$
x'	ϕ'	ψ'		
x''	ϕ''	ψ''	$\phi'' - \phi'$	$\psi'' - \psi'$
x'''	ϕ'''	ψ'''	$\phi''' - \phi''$	$\psi''' - \psi''$
x^{IV}	ϕ^{IV}	ψ^{IV}	$\phi^{IV} - \phi'''$	$\psi^{IV} - \psi'''$

etc

Column (10) tabulates the ratio a/b and it is obvious from the geometry of the deformation that this ratio increases steadily from entry to exit. Since however incremental deformations are involved the ratio required is that corresponding to a ratio of $1/1$, i.e., a square, immediately prior to the increment under consideration. This ratio has been designated a'/b' and is obtained by dividing the current value of a/b by the value of this ratio in the immediately preceding stage of the deformation. The values are tabulated in column (11).

The angle α which the greater principal strain makes with the side 2a of the element, is a function of $(a'/b')^2$ and the value of this parameter is tabulated in column (12). The value of α in column (13) is obtained from Θ, column (9), and $(a'/b')^2$, column (12), and the graphs of Figs. 33 and 34. The angle designated α_1, and tabulated in column (14), is the angle the principal strain direction makes with the axis of the specimen. The relation between α, α_1 and $\psi_2 - \psi_1$, will be clear from Fig. 56. The maximum shear stress directions bisect the principal strain directions and are tabulated in column (15).

These maximum shear stresses directions are then set out on Fig. 40 and the slip line field sketched in such that the direction of each slip line

is tangential to the maximum shear direction at every point.

In a similar way the slip line field has been obtained for specimens B and C and are plotted in Figs. 41 and 42. respectively.

It will be seen that the slip line field has a similar pattern for all three specimens. The shaded area indicates a region within which a neutral point or zone exists as evidenced by the slope of the bounding slip lines. The accuracy of the measurements were such that it was not possible to fix, without ambiguity, the position of the neutral point or zone. For this reason the average stresses on the surface of the shaded region were obtained by considering the equilibrium of the material between the limiting slip lines defining the region and the surface of the specimen.

This shaded region is not a rigid zone, as is often found in plasticity problems, for examination of the plots of 2a and 2b, Figs. 47 - 52, indicates that the deformation is a continuous process from entry to exit and at no point do these parameters have constant values, a condition necessary if a rigid zone is to exist.

Having established the shape of the slip line field it is now necessary to determine the yield stress for the material in order to calculate the roll pressure distribution and the coefficient of friction between

material and roll face. This determination will be considered in the next section.

8. 6. DETERMINATION OF YIELD STRESS.

The yield stress curve for the material used for the rolling specimens was measured by using the plane strain compression test described by Watts and Ford (42). Specimens were prepared as for rolling, as described in Section 6. 6., except that no grid was engraved on the welded interface. A series of impressions with increasing reduction were then made on the specimen using the plane strain apparatus. Care was taken with the lubrication of the plattens to reduce the effects of friction. The die width was also changed as the reduction increased to conform to the die breadth/specimen thickness ratio limits suggested in the paper by Watts and Ford. After covering the range of reductions used in the rolling experiments the plane strain compression specimen was broken in half along the welded joint and Vickers hardness measurements made on the interior edge of the specimen within the zone deformed by the plattens of the plane strain apparatus. In most of the impressions it was found possible, by using a 5 Kgm load to obtain three readings and no significant difference in hardness number could be detected within the deformed zone. Two specimens were tested in this way and the results for both, which were in very close agreement,

are plotted in Figs. 57 and 58.

This yield stress-hardness correlation was then used to determine the variation of yield stress along the length of the specimen through the roll gap.

A hardness traverse of what was originally, an interior edge of the specimen was made, after grid measurements had been completed, by mounting each specimen on a co-ordinate table fixed to a Vickers hardness testing machine. In this way hardness indentations were carried out spaced at approximately 0·02" in the direction of rolling and with four readings across the thickness of each specimen. The load used was 5 kg and one diagonal of the diamond was oriented to lie parallel to the centre line of the specimen. Typical readings for specimen B are given in table XIII.

Variations in hardness number across the thickness of the specimen are seen to lie within the normal experimental variation found for a homogeneous material and this tends to lend support to the idea, already put forward from other considerations, that the departure from homogeneous compression in cold rolling is not very great. The variation in yield stress through the roll gap obtained from these hardness measurements is plotted on Figs. 40 - 42. It will be noted that, even for such a material as annealed copper which, initially possesses a great capacity for work hardening,

the yield stress over a very large part of the arc of contact is sensibly constant and therefore the theory of the slip-line field can be applied with some confidence.

8. 7. INVESTIGATION OF "REDUNDANT SHEAR".

In the rolling process the deformation which takes place is greater than that undergone in homogeneous compression to produce the same change in thickness. This additional deformation in rolling, and the consequent greater amount of work hardening, results in the noticed effect of a slightly greater yield stress than that found in a plane strain compression test for the same reduction in thickness. This effect is often referred to as "redundant shearing" and Whitton and Ford (37) have suggested that the increase in yield stress may be as much as 5% although reference to their paper shows that for copper, up to reductions of 30% at least, the effect is very much less being of the order of 1 - 2%.

An attempt was made to estimate the amount of redundant shear in the present case by adding the increments of principle strain through the roll gap from entry to exit.

Reference to section 7. 4. will show that equations are given for the direction of the principal strains, Eq.1. and for the magnitude of these principal strains Eq. 2. The latter equation enables the ratio r/a to be found in terms of the measured parameters.

The actual strain increment is then $^{r}/_{a} - 1$.

The length of side of an element of the grid 2a, increases from entry to exit and at exit the length has increased, as reference to Figs. 47 -49 will show, to a value required from considerations of constancy of volume. There is however an additional work hardening effect due to the additional deformation represented by the summation of the principal strain increments $^{r}/_{a} - 1$.

The quantity $^{r}/_{a} - 1$ for specimen A, obtained from the graphs Figs. 31 - 32, is tabulated in column (16) of Table XII. It will be seen that sum of these increments is between 1 - 2% for each streamline and is similar for specimens B and C. It would appear that these results are in line with those found by Whitton and Ford in the paper mentioned above. The hardness measurements do not provide a sensitive enough method to detect the magnitude of the differences in yield stress involved.

8. 8. THE ROLL PRESSURE DISTRIBUTION.

Having established the slip line field, which has been drawn on Figs. 40 - 42, it is then possible to determine the roll pressure distribution.

The first step is to establish the value of the hydrostatic stress p on the limiting slip lines at entry and exit. Since there is zero force transmitted across these slip lines in the direction of rolling and

the value of the shear stress along these lines is known it is possible to determine the value of p as follows. Reference is made to Fig. 59. A. B. represents an entry slip line. It is convenient to think of this slip line as being stepped, as indicated in the inset, then for zero transmitted force in the x direction across this line

$$\int_0^{\frac{h_1}{2}} p_{xx}\,dy + \int_0^{a} p_{xy}\,dx = 0$$

A similar argument will hold for the exit slip line. This enables the hydrostatic stress p to be determined at any point along these limiting slip lines and hence by use of the equations of equilibrium discussed in Section 6.2.

$$p + 2k_s\phi \quad \text{constant}$$

$$\text{and} \quad p - 2k_s\phi \quad \text{constant}$$

The value of p at any other point in the field can be determined. The equilibrium equations used above are valid for material with a constant yield stress $2k_s$ and are therefore not strictly applicable to regions near the entry point where the material is undergoing rapid work hardening. The method adopted in this region was to assume that the shear yield stress k_s could be considered constant over a short length of the slip line and therefore the change of hydrostatic stress along this

short length could be calculated. In this way the variation in stress states along a complete slip line was built up by a step by step process. The variation in shear yield stress were obtained from the hardness measurements as described in section 8. 6.

It is thus possible to establish the value of the hydrostatic stress, and hence the stress state, for a number of points along the boundary of the roll gap impression. Such a point is illustrated at C Fig. 60. Since the hydrostatic stress p_c is known at this point the centre of the Mohr Circle is fixed in relation to the origin. The radius of the circle is the shear stress k. The pole of the Mohr Circle is found by drawing a line, through the point of maximum shear stress S, parallel to the slip line at C. The normal stress p_n at C on the roll surface and the tangential stress p_t are given by the co-ordinates on the Mohr Circle of the point q found by drawing a line, q p, through the pole parallel to the tangent to the roll surface at C. The ratio of p_t/p_n gives the value of the coefficient of friction at the same point.

The shaded regions shown in Figs. 40 - 42 separating the entry and exit sides of the slip line field were treated, for the purpose of obtaining the pressure on the surface, as being rigid. That is the mean pressure on the surface was obtained by considering the equilibrium of the shaded region C D E Fig. 61.

If $\bar{p}$ is the mean pressure over C E then

$$\bar{p}_{CE} = \int_0^a p_{yy}\,dx + \int_a^b p_{yy}\,dx + \int_0^{\frac{h}{2}} p_{xy}\,dy + \int_0^{\frac{h'}{2}} p_{xy}\,dy$$

Knowing the variation of p_{yy} and p_{xy} along the boundaries $\bar{p}$ can be found. The fact that $\bar{p}$ is normal to the roll surface and therefore makes a small angle with the y direction was neglected.

The roll pressure distributions for the three specimens are plotted in Figs. 62, 63 and 64. For comparison the roll pressure distribution was calculated by the Bland and Ford theory. It has already been noted that for cold rolling the distribution given by this theory agrees very closely with that given by Orowan, and as it allows consistant values of deformed roll radius and roll pressure to be obtained more easily was used in preference. Details of the calculations are given in Appendix IV.

It will be seen that the roll pressure distribution obtained from analysis of the slip line field and that predicted from theory show a marked similarity. The peak pressure predicted by theory occurs within the region over which a mean pressure was calculated. It is possible with greater accuracy of measurement that such a peak would be found - possibly slightly rounded. At exit the two curves are very

close together. It is at entry that the greatest difference is found. The roll pressure obtained from the slip line field solution is significantly lower than the theoretical and is indeed below the yield stress of the material. The pressure then increases more rapidly as the neutral region is approached and the total area under the two curves is closely comparable and agrees very well with the experimentally determined value of roll force for each specimen. This characteristic applies to all three specimens.

It is possible that the discrepancy in roll pressure at entry is due to the very rapid rate of work hardening of the material at this point and the method of taking an average value of the shear stress over a small length is not sufficiently accurate. Another possibility is that the pattern of deformation is such as to produce compressive stresses near the centre line of the specimen at entry with a compensating pattern of tensile stresses near the surface. If these tensile stresses are high enough the roll pressure to cause yielding could be appreciably reduced in a manner analogous to the reduction in roll pressure which results from the application of tensions to the strip.

To obtain consistency between roll pressure and deformed roll radius it was necessary to use values of coefficient of friction between 0·25 and 0·35. These are rather higher than those normally associated

with cold rolling conditions. Whitton and Ford in their paper on friction in cold rolling found that for "clean and dry" rolls and strip the coefficient of friction was about 0·12. In the present case conditions were "clean and dry" and a deliberate attempt made to obtain a high coefficient by rolling folded emery cloth. It appears that this method was very efficacious for the calculated values of roll force and roll torque using these high values of coefficient of friction agree very closely with the experimental values as reference to Appendix IV will confirm. The values of coefficient of friction obtained by calculating the ratio of normal to shear stress along the surface are also plotted in Figs. 62 - 64. It will be seen that apart from a high value near entry the mean value along the arc of contact lies between 0·2 and 0·3 which confirms the values arrived at on theoretical grounds.

The product of the coefficient of friction and normal pressure p_{rr} cannot exceed the yield shear stress k of the material and the ratio $\frac{\mu p_{rr}}{k}$ is plotted on Figs. 62 - 64. It will be noted that over a small length for A and C this ratio exceeds 1. For B, as might be expected with the higher coefficient of friction the length over which "sticking" takes place is somewhat greater. This condition implies that the slip lines are normal and tangential to the surface over this region but this condition was not found in

plotting the slip line field. The direction in fact was much nearer 45° to the roll surface than normal and tangential. This can only occur when no tangential stresses are developed at the surface and the material has the same velocity as the roll surface. Theoretically this condition only exists at one point, the neutral point.

The form of the slip line field found suggests, however, that the "neutral point" is a zone rather than a point. This concept requires some consideration.

Since the thickness of the specimen decreases towards exit as the material passes through the zone, considerations of constancy of volume and plane strain require an increase in velocity. If, in fact, the velocity remains constant it can only mean that flow has taken place parallel to the roll axes and conditions of plane strain are not maintained over this region. It is probable that the increase in width of the strip, which although small is always present, takes place while the material passes through the neutral zone.

The effect of the lateral spread will be to modify the stresses in this zone and introduce a complex three dimensional stress system. The third stress acting in a direction parallel to the roll axes is no longer the mean value of the stresses in the other

co-ordinate directions but is increased by the resistance to lateral flow imposed by the friction between the roll and material. The consequence is very likely to be a rounding of the peak of the roll pressure distribution curve.

Rounding of the peak of the roll pressure curve has been found in those experiments in which a pin inserted into the roll face was used to measure the roll pressure. This phenomena has always been ascribed to the finite size of the measuring pin but in the light of the present work it appears that it may be a genuine effect due to deviation from plane strain conditions over a small length of the arc of contact near the theoretical neutral point.

8. 9. THE DEFORMED ROLL PROFILE.

The shape of the roll surface in contact with the strip during rolling has, as already been mentioned, been the subject of much speculation. It has usually been assumed that Hitchcock's formula could be applied without much error and this formula has invariably been used in theoretical work. The assumption is made that the roll surface remains in the form of a circular arc but with an increased radius compared with the unloaded state. Orowan (3) suggested that this assumption, of a circular arc, was far from true and in his paper gave graphs which indicated definite depressions in the roll surface under load

which departed very much from the circular arc. The measurements made by Orowan are open to objection and it was decided to try and obtain the roll gap profile when the roll pressure was instantaneously released and creep effects would be absent.

The profiles of the three specimens are plotted in Figs. 65 -67. The co-ordinates are those used in the original measurements given in Tables VI - VIII. Also plotted on the graphs Figs. 65 - 67 are the points corresponding to the deformed roll radius required to give consistency with the roll pressure, as given by calculation and experiment. For specimen C the agreement is very good and reasonably so for specimen A. The assumed roll radius for specimen B shows a much greater divergence from the actual profile and is in agreement with the anomalous behaviour of this specimen in other respects.

In carrying out the calculations, to obtain the co-ordinate points for the deformed roll radius, it was assumed that the centre remained on the line joining the roll centres but since the roll pressure is not symmetrical it is possible that the centre is displaced from this position. To investigate this possibility, in the case of specimen B, co-ordinate points for a roll radius of 2·14 in. with the centre displaced 0·15in. toward the entry side have been

plotted in Fig. 66. It will be seen that this configuration is somewhat closer to the actual profile than the assumption that the centre of the deformed roll remains in the plane of exit.

The effect of variations in roll radius, with the centre in the plane of exit, were also investigated for specimen B and the results for a radius of 2·80in. are plotted in Fig. 66. A deformed radius of this value would, however, for the measured arc length result in a smaller reduction, 33% against the actual reduction of 35·4%, or conversely the actual reduction would require an arc length of 0·344 in. as opposed to the measured value of 0.336 in.. The points for a radius of 2·80 in. lie very close to the actual profile. A similar investigation for specimen A revealed that a radius which coincided with the actual profile at entry and exit diverged at intermediate points by as much as the points plotted for a radius of 2·16 in.. This suggests that the profile for specimen A is, in fact, not a circular arc although the departure from circularity is not very great.

8. 10. DISCUSSION OF RESULTS.

Detailed discussion of the results obtained has taken place, where appropriate, in sections 8. 1. to 8. 9. and it is only necessary in this section to consider the general conclusions to be drawn from the present investigation.

One of the most striking facts to emerge is the remarkable insight of the early workers in this field, in particular Von Karman, whose assumptions concerning the physical behaviour of the material in strip rolling, were remarkably near the truth. Even for reductions in one pass, as high as 50%, and with a relatively high coefficient of friction between roll and strip, the departure from the condition of homogeneous compression is, has been shown, quite small. A necessary consquence of this assumption of homogeneous compression is the uniform distribution of the horizontal stress over a vertical section. Examination of the experimental slip line field indicates that over the greater portion of the thickness of the material in the roll gap the change in curvature of the slip lines is small and therefore the stress is very nearly uniform. As the surface of the specimen is approached there is a more rapid increase in the curvature and hence a significant increase in the stress on the vertical section. This pattern can be discerned for all three specimens.

It appears, therefore, that the actual stress distribution on a vertical section is between the uniformity assumed by Von Karman, and the parabolic type assumed by Orowan. Since the variation of stress is confined to relatively small zones near the surface the Von Karman assumption is not greatly

in error and explains the success of the theories based on this assumption in predicting values of roll force and roll torque.

The form of the distribution of roll pressure in the arc of contact predicted by the theories of Orowan and Bland and Ford find support in the results of this investigation. Unfortunately, the pressure distribution near the neutral point has not been obtained without ambiguity. The weight of evidence accumulated in this investigation supports the concept of a neutral zone rather than a neutral point and a consequent rounding of the peak of the roll pressure distribution curve. The tentative nature of this conclusion arises from the difficulty of obtaining the necessary accuracy of measurement. This can be increased either by increasing the size of the specimen used or by increasing the accuracy of measurement. The second course would seem to be the more promising for the investigation of the rolling process, for an increase in size of specimen would introduce considerable practical difficulties. This applies in particular to the problem of devising a suitable quick release mechanism for use with the high loads associated with large mills.

For investigation of other processes the limitations on size of specimen are not so severe and in such cases very satisfactory results have been

obtained. Lianis (53) using large specimens and the methods of analysis described in section 7, has investigated the form of the slip line field for the bending of notched bars with great success.

The coefficient of friction, plotted in Figs 62-64 is reasonably constant over the greater portion of the arc of contact although very high values are reached near the entry plane. These high values are confined to a small part of the arc of contact and their contribution to the total frictional effect will be small. The assumption, made in most theories of rolling, that the coefficient of friction is constant through the arc of contact is, therefore, a reasonable one.

The values found for the coefficient of friction are somewhat higher than those usually associated with cold rolling conditions and legitimate doubt could be thrown on the results obtained from the slip line field solution in isolation but calculations for roll force require co-efficients of friction of this order to obtain consistency between deformed roll radius and roll force. Additional evidence for accepting these values is provided by the close agreement between experimental and calculated values of roll force and roll torque.

Another aspect of the rolling problem which was investigated was the shape of the roll surface in contact with the deforming material. No evidence was found for

the suggestion put forward by Orowan that the roll surface was often distorted into a shape which effectively produced a surface equivalent to two rolls of smaller diameter. On the contrary the shape in every case was represented by a smooth curve and the shape approached the circular arc predicted by Hitchcock's theory. This agreement probably explains why the use of this concept in many rolling theories does not lead to any serious discrepancies between experimental and calculated values of roll force and roll torque.

The techniques and analyses described in this investigation have been applied to the specific problem of investigating some of the problems associated with the process of cold rolling but they are of general applicability where conditions of plane strain are encountered. As has already been noted the analysis has already been applied to problems of the bending of notched bars and to that of orthogonal machining.

The technique of pressure welding adopted enables plane strain conditions to be accurately maintained but it does suffer from the disadvantage that the material, due to the necessary heating and cooling cycle, is far removed from the ideal rigid-plastic material of plasticity theory. It has been shown in the present work that even with this limitation it is possible to obtain a great deal of information about the nature of the deformation process in the cold rolling of strip.

REFERENCES.

1. SIEBEL E.
Berichte des Walzwerksausschusses. Verein Deutscher Eisenhuttenleute. No. 37 1924.
Also Stahl und Eisen V 45 1925 p 1563-6.

2. KARMAN T.
'On the Theory of Rolling'. Zeitschrift fur Angewandte Mathematck und Mechanik V 5 1925 p 139.

3. OROWAN E.
'The Calculation of Roll Pressure in Hot and Cold Flat Rolling' Proc. I Mech. E. V 150 1943 pp 140-167.

4. RANKINE J. BAILEY W.H. STANTON F. P.
Resistance Strain Gauges for the Measurement of Roll Force Torque and Strip Tension J.I.S.I V. 160 1948 pp 381-387.

5. SIEBEL E. LUEG W.
Investigations into the Distribution of Pressure at the Surface of the Material in Contact with the Rolls. Mitt K. W. Inst. Eisenforschung V. 15 1933 pp 1-14.

6. SMITH C.L SCOTT F.H. SYLWESTROWICZ W.
Pressure Distribution between Stock and Rolls in Hot and Cold Flat Rolling. J.I.S.I. V 170 1952 pp 347-359.

7. HANSON D. WHEELER M.A.
Deformation of Metals under Prolonged Loading. Journal of Inst. Metals V 45 1931 p 229.

8. CAPUS J.M. COCKCROFT M.G.
A New Technique for investigating Flow in Metal Working Processes. Letter to 'Nature' May 1st V 173 No. 4409 1954.

9. PRANDTL L.
Zeitschrift fur Angewandte Mathematik. Vol. 3.

10. NADAI A.
"Plasticity" Mc Graw Hill 1931.

11. EKELUND S.
"Analysis of Factors Influencing Roll Pressure and Power Consumption in the Hot Rolling of Steel". Steel. V. 93 1933.

12. TSELIKOV A.I.
"Effect of External Friction and Tension on the Pressure of the Metal on the Rolls in Rolling" Metallurg No 6 1939.

13. TRINKS W.
"Pressures and Roll Flattening in Cold Rolling Blast Furness and Steel Plant" V. 25 1937.

14. NADAI A.
The Forces Required for Rolling Steel Strip Under Tension. Journal of App. Mech. June, 1939.

15. BLAND D.R. FORD H.
The Calculation of Roll Force and Torque in Cold Strip Rolling with Tensions. Proc. 1. Mech. E. V 159. 1948 pp 144.

16. SIMS R.B.
Calculation of Roll Force and Toque in Hot Rolling Mills. Proc. I Mech. E. V 168 1954 pp 191-200.

17. TRESCA H.
Memoir on the Deformation of Solid Bodies. V 18 1868 p 733-799 Mem. pres. Acad. Sci. Paris.

18. MISES V.
Mechanics of Solid Bodies under Conditions of Plastic Flow. Nachrichten von der Gesellschaft der Wissenschafter zu Gottengen. Math. Physik Klasse 1913.

19. FORD H. ELLIS F. BLAND D.
Cold Rolling with Strip Tension. A New Approximate Method of Calculation and a Comparision with Other Methods. J.I.S.I. V. 1951 pp 57 - 72 and V 171 1952.

20. LEE E.H.
Contribution to Discussion on Paper by Orowan (3) Proc I Mech. E V 152 1945. pp 319.

21. ALEXANDER J.M.
Effect of Coulomb Friction in the Plane Strain Compression of a Plastic-Rigid Material. Journal of Mechanics and Physics of Solids V 3 1955 pp 233-245.

22. HILL R.
The Mathematical Theory of Plasticity. O.U.P 1950

23. COOK M. LARKE E.C.
Computation of Rolling Load, Torque and Roll Face Pressure in Metal Strip Rolling. Journal Inst. of Metals V 71 1945 pp 557.

24. HOLLENBURG A.
Observations on the Rolling of Iron. Stahl und Eisen V.3. 1883.

25. METZ N.
Experimental Investigations into the Flow of Metals During Rolling.
Archiv. Fur Das Eisenhuttenwesen. Sept 1927 pp 193-204.

26. UNCKEL H.
A Contribtution to the Theory of Material Flow during Rolling. Archiv. fur das Eisenhuttenvesen V 10 1936 pp 13-18.

27. WEISS L.
Flow Lines in Rolling. Zeitschrift fur Metallkunde. V 20 1928 pp 302.

28. WEISS L.
Calculation of Output in Rolling. Zeitschrift fur Metallkunde. V 20 1928 pp 302.

29. SIEBEL E. OSENBORG E.
On the Influence of Friction and Cross-sectional Dimensions on the Flow of Material in Rolling.
Mitt. K.W. Inst. Eisent. V.16 1934 pp 33.

30. SIEBEL E. HUNNE
Investigation of Plastic Deformation in Technical Forming Processes. Mitt K. W. Inst. Eisenf V. 13 1931 pp 43-62.

31. GREEN A.P.
Use of Plasticene Models to Simulate Plastic Flow of Metal. Philosophical Magazine V 42 1951 pp 365-373.

32. SIMS R.B. PLACE J.A. MORLEY A.D.
Load Meter for Industrial Mills Engineering V 173 No. 4487-88 1952.

33. MACGREGOR C.W. PALMER R.B.
Contact Stresses in Rolling of Metals. Journal of Applied Mechanics V 70 1948 pp 297-302.

34 POMP A. LUEG W.
The Influence of Roll Diameter on the Cold Rolling of Strip Steel. Mitt. K.W. Inst. Eisent. V 17 1935 pp 63-76.

35. TAFEL W.
The Relation between Gripping Angle and Roll Speed. Stahl und Eisen. V 4A 1924.

36. PAVLOV P.
Metallurg. 1934.

37. WHITTON P.W. FORD H.
Surface Friction and Lubrication in Cold Strip Rolling. Proc. 1 Mech. E. V 169 1955 pp 123.

38. SIEBEL E. POMP A.
Roll Pressure and Work in the Cold Rolling of Metals. Mitt. K.W. Inst. Eisenf. V 9. 1927 p 157.

39. VAN ROOYEN G.T. BACKOFEN W.A.
Friction in Cold Rolling. Journal Iron and Steel Inst. June, 1957. pp 235-244.

40. FORD H.
Researches into the Deformation of Metals by Cold Rolling. Proc. 1 Mech. E. V 159 1948 p 115.

41. COOK M. LARKE E.C.
Resistance of Copper and Copper Alloys to Homogeneous Deformation in Compression. J. J. Inst. of Metals V 71 1945 pp 371-390.

42. WATTS A.B. FORD H.
An Experimental Investigation of the Yielding of Strip between Smooth Dies. Proc. Inst. of Mech. E. V 169 1955 p 123.

43. COOK M.
Directional Properties in Rolled Brass Strip. J. Inst. of Metals V 60 1937 p 159.

44. TAYLOR G.I. QUINNEY H.
Plastic Distortion of Metals Phil. Trans. Roy. Soc. A. V 230. 1932 p 323.

45. BRIDGMAN P.W.
Series of Papers in :- Journal Applied Physics V 17 1946, V 18 1947.

46. HENCKY H.
Zeits ang Math. Mech. Vol 4. 1924 p 323.

47. BRIDGMAN P.W.
as for Ref (45).

48. SAINT-VENANT B de
Comptes Rendus Acad. Sci. Paris. V 70 1870 p 473.

49. HAVEN C. P., HARDING J.F.
Studies of Plastic Flow Problems by Photo Grid Methods. Experimental Stress Analysis V2 No 2 p 59.

50. TYLECOTE R. F.
Recent developments in Pressure Welding of Light Alloys. Sheet Metal Industries. V 26 1949 p 161.

51. COOK M. DAVIS E.
Welding of Copper and Copper Alloys. Trans. Inst. of Welding V 10 1947 p 178.

52. DAVIS E.
Pressure Welding Characteristics of some Copper Base Alloys. Journal of Institute of Metals. V 77 1950.

53. LIANIS G.
Ph.d. Thesis U of L 1956. See also Lianis G. and Ford H. Plastic Yielding of Single Notched Bars Due to Bending J. Mech. and Phys. of Solids V. 7 1958 p1-21.

54. SHAH
M. Sc. Thesis U. of L. 1959.

APPENDIX I.

If a square, in which is inscribed a circle, Fig. 68(a), is deformed into a parallelogram with sides 2a and 2b, Fig. 68(b), the the circle becomes an ellipse.

For the system of oblique co-ordinates the equation of the ellipse is:-

$$\frac{x^2}{a^2} + \frac{y^2}{b^2} = 1$$

For any point P on the ellipse

$$y = r\,\mathrm{Sin}\alpha \times \frac{1}{\mathrm{Sin}\,\theta}$$

$$x = r\,\mathrm{Cos}\alpha - y\,\mathrm{Cos}\theta$$

$$\therefore \quad \frac{(r\,\mathrm{Cos}\alpha - r\,\mathrm{Sin}\alpha\,\mathrm{Cot}\theta)^2}{a^2} + \frac{(r\frac{\mathrm{Sin}\alpha}{\mathrm{Sin}\,\theta})^2}{b^2} = 1$$

$$\text{or} \quad b^2r^2(\mathrm{Cos}\alpha - \mathrm{Sin}\alpha\,\mathrm{Cot}\theta)^2 + a^2r^2\left(\frac{\mathrm{Sin}\alpha}{\mathrm{Sin}\,\theta}\right)^2 = a^2b^2$$

$$\therefore \quad r^2\left\{b^2(\mathrm{Cos}\alpha - \mathrm{Sin}\alpha\,\mathrm{Cot}\theta)^2 + \frac{a^2\,\mathrm{Sin}^2\alpha}{\mathrm{Sin}^2\theta}\right\} = a^2b^2$$

then

$$r = ab\left\{b^2(\mathrm{Cos}\alpha - \mathrm{Sin}\alpha\,\mathrm{Cot}\theta)^2 + \frac{a^2\,\mathrm{Sin}^2\alpha}{\mathrm{Sin}^2\theta}\right\}^{-\frac{1}{2}} \qquad (1)$$

For major axis, r is a maximum and therefore

$$\frac{dr}{d\alpha} = 0$$

Now

$$\frac{dr}{d\alpha} = -\frac{1}{2}ab\left\{b^2(\cos\alpha - \sin\alpha\cot\theta)^2 + \frac{a^2\sin^2\alpha}{\sin^2\theta}\right\}^{-\frac{3}{2}}$$
$$\left\{2b^2(\cos\alpha - \cot\theta\sin\alpha)(-\sin\alpha - \cot\theta\cos\alpha) + \frac{a^2\sin 2\alpha}{\sin^2\theta}\right\}$$

$$\therefore\ -2b^2(\cos\alpha - \cot\theta\sin\alpha)(\sin\alpha + \cot\theta\cos\alpha) + \frac{a^2\sin 2\alpha}{\sin^2\theta} = 0$$

and

$$a^2\sin 2\alpha = 2b^2(\sin\alpha\cos\alpha - \cot\theta\sin^2\alpha + \cot\theta\cos^2\alpha - \cot^2\theta\sin\alpha\cos\alpha)$$

$$= b^2\left\{\sin 2\alpha(1-\cot^2\theta) + 2\cot\theta\cos 2\alpha\right\}$$

$$\therefore\ \sin 2\alpha\left\{\frac{a^2}{\sin^2\theta} - b^2(1-\cot^2\theta)\right\} = 2b^2\cot\theta\cos 2\alpha$$

and $$\tan 2\alpha = \frac{2b^2\cot\theta}{\frac{a^2}{\sin^2\theta} - b^2(1-\cot^2\theta)}$$

$$= \frac{2b^2\,\frac{\cos\theta}{\sin\theta}}{\frac{a^2}{\sin^2\theta} - \frac{b^2(\sin^2\theta - \cos^2\theta)}{\sin^2\theta}}$$

$$\therefore \quad \tan 2\alpha = \frac{2b^2 \sin\theta \cos\theta}{a^2 + b^2 \cos 2\theta}$$

and

$$\alpha = \tfrac{1}{2} \tan^{-1} \frac{b^2 \sin 2\theta}{a^2 + b^2 \cos 2\theta}$$

or

$$\alpha = \tfrac{1}{2} \tan^{-1} \frac{\sin 2\theta}{\left(\frac{a}{b}\right)^2 + \cos 2\theta}$$

Since a', b' appear as a ratio it is more convenient to take the length of side of the parallelogram in all calculations. The equation is therefore used in the form

$$\alpha = \tfrac{1}{2} \tan^{-1} \frac{\sin 2\theta}{\left(\frac{a}{b}\right)^2 + \cos 2\theta} \qquad (2)$$

Where a is understood to be the length of the longer side of the parallelogram and b the length of the shorter side.

The two values of α given by (2) give the directions of the major and minor axes, i.e. the principal strain increment directions.

To obtain the magnitude of the strain increment the value of α found in (2) can be used in (1) to obtain the value of r. The resulting expression is very cumbersome and the most satisfactory procedure is to insert numerical values into (1) simplified

in the following way.

from (1)

$$r = ab\left\{b^2(\cos\alpha - \cot\theta \sin\alpha)^2 + \frac{a^2 \sin^2\alpha}{\sin^2\theta}\right\}^{-\frac{1}{2}}$$

or

$$\frac{r}{a} = \left\{\left(\frac{\cos\alpha \sin\theta - \cos\theta \sin\alpha}{\sin\theta}\right)^2 + \left(\frac{a}{b}\right)^2 \frac{\sin^2\alpha}{\sin^2\theta}\right\}^{-\frac{1}{2}}$$

$$\therefore \quad \frac{r}{a} = \frac{\sin\theta}{\left\{\sin^2(\theta-\alpha) + \left(\frac{a}{b}\right)^2 \sin^2\alpha\right\}^{\frac{1}{2}}} \qquad (3)$$

By substituting values of α from (2) into (3) the ratio r/a can be obtained and hence the principal strain increment.

The solution to equations (2) and (3) is most conveniently presented in the form of graphs Figs. 29-32.

Typical calculations for α and r/a for one value of a/b are given in Tables II(a) and III(a) and summarized results used in plotting Figs. 29-32 are given in Tables II(b) and III(b).

APPENDIX II.

Taking Equation (2) Appendix I

$$\tan 2\alpha = \frac{\sin 2\theta}{\left(\frac{a}{b}\right)^2 + \cos 2\theta}$$

Writing $A = (a/b)^2$ and noting that θ very rarely lies outside the limits $90° > \theta > 85°$ and in most cases $90° > \theta > 89$.

Put $\phi = 90° - \theta$

$$\therefore \quad 0 < \phi < 1°$$

Then

$$\tan 2\alpha = \frac{\sin 2(90-\phi)}{A + \cos 2(90-\phi)}$$

$$= \frac{\sin 2\phi}{A - \cos 2\phi}$$

Expanding

$$\tan 2\alpha = \frac{2\phi - \frac{(2\phi)^3}{3!} + \cdots}{A - 1 + \frac{(2\phi)^2}{2!} - \frac{(2\phi)^4}{4!} + \cdots}$$

$$= \frac{1 - \frac{4\phi^2}{3!} + \cdots}{\frac{A-1}{2\phi} + \frac{2\phi}{2!} - \cdots}$$

When ϕ is small $\frac{4\phi^2}{3!}$ can be neglected in comparison with 1

$$\therefore \quad \tan 2\alpha \simeq \frac{1}{\frac{A-1}{2\phi} + \frac{2\phi}{2}} = \frac{2\phi}{(A-1) + 2\phi^2}$$

$\therefore$ To a very close approximation

$$\tan 2\alpha = \frac{2\phi}{(A-1)+2\phi^2} \qquad (4)$$

Further simplication is possible, for in most practical cases, $\phi \ll 1$ and for cases where A is small say $A < 1{\cdot}001$, the associated value of ϕ is also small, say $\phi < 0{\cdot}2^\circ$, therefore for such cases $2\phi^2$ is small compared with A-1.

and $$\tan 2\alpha \simeq \frac{2\phi}{A-1}$$

$$\therefore \quad A-1 = \frac{2\phi}{\tan 2\alpha}$$

$$\text{or} \quad A = \frac{2}{\tan 2\alpha}\cdot\phi + 1 \qquad (5)$$

i.e. If A is plotted against ϕ a straight line of slope $2/\tan 2\alpha$ results. Substituting $0 < \alpha < 45^\circ$ gives a family of curves.

The results are tabulated in Table IV and the complete curves are plotted in Fig. 34 (a) and (b).

ACCURACY OF EXPRESSIONS USED.

The accuracy obtained by using equation (5) was judged by reference to equation (4) but since this latter is also an approximation it is first necessary to establish the order of error that might arise by using this expression.

The greatest errors will arise when Θ

differs considerably from 90° and A is small.

Taking the extreme case where A = 1·001 (which corresponds to a ratio of a/b = 1·0005, a case where the direct strains involved are of elastic order.) and Θ = 85° (A large shear component. A change in Θ of 5° in one step is large and in practice a smaller increment would be taken so that this case is a very extreme one.)

When Θ = 85° A = 1·001

The exact expression $\tan 2\alpha = \frac{\sin 2\Theta}{A+\cos 2\Theta}$

gives $\frac{0.17365}{1.001-0.9848} = \frac{0.17365}{0.0162} = 10.71$

The approximate expression is

$$\tan 2\alpha = \frac{2\phi}{(A-1)+2\phi^2}$$

$$= \frac{0.1745}{0.001+0.0152} = \frac{0.1745}{0.0162} = 10.77$$

and the error is 0·6%

It is therfore permissible for all practical cases to use equation (4) as a standard for comparison.

Now for all values of ϕ

$$\frac{2\phi}{A-1} > \frac{2\phi}{(A-1)+2\phi^2}$$

$\therefore$ Error is

$$\frac{\frac{2\phi}{A-1} - \frac{2\phi}{(A-1)+2\phi^2}}{\frac{2\phi}{(A-1)+2\phi^2}}$$

$$= \frac{(A-1)+2\phi^2}{A-1} - 1$$

$$= \frac{2\phi^2}{A-1}$$

The error in this case is in tan 2α

When α is small $\approx 1^\circ$ an error of 1% in tan 2α gives approximately a 1% error in angle. The error in angle rapidly diminishes and at 6° an error of 1% in tan 2α corresponds to an error os less than 0·3% in the value of the angle.

It is thus possible to locate on the curves of ϕ against A, Figs. ~~35(a) and (b)~~, the co-ordinates of the points to give a certain error in tan 2α. The calculations for errors of 1%, 0·5% and 0·1% are given in table V(a).

The error in the angle α rather than tan 2α is of more direct interest and what is required is an expression giving the value of ϕ for a given value

of α to give a required degree of accuracy.

If α is the angle and $d\alpha$ is the error then

$$\frac{d\alpha}{\alpha} = e$$

The error in $\tan 2\alpha = \frac{2\phi^2}{A-1}$

i.e. $$\frac{\tan(2\alpha + 2d\alpha) - \tan 2\alpha}{\tan 2\alpha} = \frac{2\phi^2}{A-1} \qquad (6)$$

Also $$\tan 2\alpha = \frac{2\phi}{(A-1) + 2\phi^2} \qquad (7)$$

Let $$\frac{\tan 2(\alpha + d\alpha) - \tan 2\alpha}{\tan 2\alpha} = C$$

then from (6) $$A - 1 = \frac{2\phi^2}{C}$$

Substituting in (7)

$$\tan 2\alpha = \frac{2\phi}{\frac{2\phi^2}{C} + 2\phi^2}$$

$$= \frac{2\phi}{2\phi^2(\frac{1}{C}+1)} = \frac{1}{\phi(\frac{1+C}{C})}$$

$$\therefore \phi = \frac{C}{1+C} \cdot \frac{1}{\tan 2\alpha}$$

or

$$\phi = \frac{\frac{\tan 2(\alpha + d\alpha) - \tan 2\alpha}{\tan 2\alpha}}{\left[\left\{\frac{\tan 2(\alpha + d\alpha) - \tan 2\alpha}{\tan 2\alpha}\right\} + 1\right] \tan 2\alpha}$$

$$\therefore \phi = \frac{\tan 2(\alpha+d\alpha) - \tan 2\alpha}{\tan 2(\alpha+d\alpha)\tan 2\alpha}$$

$$= \frac{1}{\tan 2\alpha} - \frac{1}{\tan 2(\alpha+d\alpha)}$$

$$= \cot 2\alpha - \cot 2\alpha(1+e) \qquad (8)$$

For each value of α the angle ϕ for a given accuracy e can be computed.

The results of the computations are given in Table V(b) for an error of 1% in α.

APPENDIX III.

The analysis developed in Section 7 depends solely on geometrical considerations and should therefore be applicable to any two dimensional strain field. To test the analysis a specimen was prepared as follows. A strip of $\frac{1}{8}$" copper approximately 18" long x 3" wide was machined into the form of a specimen. See Fig. 69. Near the centre a small area of square grid was engraved by hand using a precision adjustable square. The spacing of the lines was done by rule and was therefore only nominal but care was taken to keep lines parallel. The nodal points were carefully measured by the OMT microscope using the technique already described in Section 7.2.

The specimen was then subject to uniaxial tension and a small amount of plastic deformation induced. The nodal points were then measured again.

From the large specimen a smaller one was made such that the original grid was also at the centre of the smaller specimen. The orientation is obtained by having a stress free projection on the original section on which was engraved a reference line.

The smaller specimen was then subject to uniaxial tension again inducing a small but indeterminate amount of plastic deformation. The nodal points were then measured.

From the measurements the principal stress

directions were obtained and compared with the known directions.

A number of elements of the grid were analysed and the calculations relating to one ofthe grid elements are indicated in Fig. 69(a) (b) and (c), diagrams on which are marked the actual measurements of angle and lengths. 69(a) refers to the original undeformed configuration. It will be seen that the grid was a retangular one and the included angle 89° 33'. (d) and (e) illustrate the changes in configuration from an original square. e.g. (d) illustrates the lengths of sides and included angle that a square of side ·0577 in. would become if subjected to the same change of deformation which produced (b) from (a). Similarly (e) illustrates the configuration of an element which is in the form of a square at stage (b) when subject to deformation which produces (c) from (b).

To obtain (d)

The measured included angle is:-

$180° - (41° 15' + 51° 54') = 86° 51'$

Side c'd' becomes $\frac{\cdot 0789}{\cdot 0763} \times \cdot 0577'' = \cdot 0597''$

$$a/b = \frac{\cdot 0597}{\cdot 0592} = 1 \cdot 009 \qquad \left(\frac{a}{b}\right)^2 = 1 \cdot 018$$

True included angle

$90° - (89° 33' - 86° 51')$

$= 87° 18'$

From graph (Fig. 29)

For $(a/b)^2 = 1{\cdot}018$

and $\Theta = 87^\circ\ 18'$

$\alpha = 38{\cdot}2^\circ = 38^\circ\ 12'$

Angle which principal stress makes with reference direction A = $38^\circ\ 12' + 51^\circ\ 54' = 90^\circ\ 6'$

Known direction 90° with A

To obtain (e)

The measured included angle at (c) is

$180^\circ - (40^\circ\ 42' + 49^\circ\ 51') = 89^\circ\ 27'$

The side c" d" becomes

$\frac{\cdot 0761}{\cdot 0789} \times \cdot 0592'' = \cdot 0579''$

$(a/b) = \frac{\cdot 0610}{\cdot 0579} = 1{\cdot}055 \qquad (a/b)^2 = 1{\cdot}11$

True included angle = $90^\circ - (86^\circ 51' - 89^\circ 27') = 92^\circ\ 36'$

From graph (Fig. 29)

For $(a/b)^2 = 1{\cdot}11$

and $\Theta = 87^\circ\ 24'$

$\alpha = 20{\cdot}6^\circ = 20^\circ\ 36'$

Angle which principal stress makes with reference direction A = $40^\circ\ 42' - 20^\circ\ 36' = 20^\circ\ 6'$

Known direction of principal stress 20° with A.

APPENDIX IV.

SPECIMEN A 21·8% red.

$h_1 = 0.1215$, $h_2 = 0.0950$, $\delta = 0.0265$, $P_e = 6.5$ Ton/in, $\mu = 0.35$

$$R' = 2\left(1 + \frac{2\times1.67\times10^{-4}\times6.5}{.0265}\right) = 2.164 \text{ in}$$

$$\phi_1 = \sqrt{\frac{\delta}{R'}} = \sqrt{\frac{.0265}{2.164}} = \sqrt{.01228} = 0.111$$

$$\sqrt{\frac{R'}{h_2}} = \sqrt{\frac{2.164}{.095}} = 4.77$$

$$H_1 = 2\sqrt{\frac{R'}{h_2}}\tan^{-1}\left(\sqrt{\frac{R'}{h_2}}\phi_1\right) = 2\times4.77\tan(4.77\times.111) = 4.65$$

$$H_n = \frac{H_1}{2} - \frac{1}{2\mu}\ln\frac{h_1}{h_2} = 2.325 - \frac{1}{2\times.35}\times.247 = 1.977$$

$$\phi_n = \sqrt{\frac{h_2}{R'}}\tan\left(\sqrt{\frac{h_2}{R'}}\times\frac{H_n}{2}\right) = \frac{1}{4.77}\tan\frac{.989}{4.77} = 0.042^c$$

N.P.

x	0	·0454	·0905	·1278	·1670	·2040	·2410
ϕ	0	·021	·042	·059	·077	·094	·111
$\sqrt{\frac{R'}{h_2}}\phi$	0	·100	·200	·281	·367	·449	·529
$\tan^{-1}\sqrt{\frac{R'}{h_2}}\phi$	0	·100	·197	·274	·352	·422	·487
$H = 2\sqrt{\frac{R'}{h_2}}\tan^{-1}\sqrt{\frac{R'}{h_2}}\phi$	0	·954	1·88	2·61	3·35	4·02	4·65
$H_1 - H$			2·77	2·04	1·30	0·63	0
μH	0	·334	·659				
$\mu(H_1-H)$			·970	·715	·455	·220	0
$e^{\mu H}$	1·0	1·40	1·95				
$e^{\mu(H_1-H)}$			2·62	2·04	1·58	1·25	1·0
h	·0950	·0960	·0988	·1026	·1078	·1141	·1216
% red	21·8	21·0	18·6	15·5	11·2	6·0	0
$2k$ Ton/in^2	21·8	21·4	20·5	19·0	16·2	11·5	3·0
$p_{rr} = 2k\frac{h}{h_2}e^{\mu H}$	21·8	30·3	42·1				
$p_{rr} = 2k\frac{h}{h_1}e^{\mu(H_1-H)}$			42·1	32·7	22·7	13·5	3·0
$\frac{\mu p_{rr}}{k}$	0·70	·99	1·47	1·20	·98	·82	·70
$p_{rr}\phi$	0	·64	1·80				
$p_{rr}\phi$			1·80	1·92	1·73	1·27	·33

$$\int_0^{\phi_n} p_{rr}\, d\phi = \frac{.042}{6}\left[21.8 + 41.2 + 4(30.3)\right] = 1.29$$

$$\int_{\phi_n}^{\phi_1} p_{rr}\, d\phi = \frac{.069}{12}\left[44.0 + 4(32.7 + 13.5) + 2 \times 22.7 + 3\right] = 1.59$$

$$P_T = R' \int_0^{\phi_1} p_{rr}\, d\phi = 2.164(1.29 + 1.59) = 6.3 \text{ Ton/in}$$

Experimental Roll Force P_E = 6.5 Ton/in

$$\int_0^{\phi_n} p_{rr}\, \phi\, d\phi = \frac{.042}{6}\left[0 + 4 \times .635 + 1.8\right] = .0303$$

$$\int_{\phi_n}^{\phi_1} p_{rr}\, \phi\, d\phi = \frac{.069}{12}\left[1.8 + .333 + 4(1.92 + 1.27) + 2 \times 1.73\right] = .1055$$

$$T_T = R R' \int_0^{\phi_1} p_{rr}\, \phi\, d\phi = 2.0 \times 2.16 \times .1358 = .585 \text{ Ton/in/in}$$

$$= 1310 \text{ lbin/in}$$

Experimental Roll Torque 21.8% red = 1300 lbin/in

SPECIMEN B 35.2% red.

$h_1 = 0.1200, h_2 = 0.0778, \delta = 0.0422, P_E = 8.8$ Ton/in, $\mu = 0.27$

$\therefore \quad R' = 2.14$ in

N.P

x	0	·0499	·1000	·1491	·2000	·2490	·300
ϕ	0	·0233	·0466	·0699	·0933	·1166	·140
% red	35·2	34·0	31·1	26·4	19·6	11·0	0
$2k$ Ton/in^2	25·0	24·7	24·0	23·0	20·8	16·0	3·0
$p_{rr} = 2k\frac{h}{h_2}e^{\mu H}$	25·0	35·4	50·4				
$p_{rr} = 2k\frac{h}{h_1}e^{\mu(H_1-H)}$			50·4	37·8	27·5	18·2	3·0
$\frac{\mu p_{rr}}{k}$	·54	·77	1·13	·89	·715	·615	·54
$p_{rr}\phi$	0	·83	2·35				
$p_{rr}\phi$			2·35	2·64	2·56	2·12	·42

P_T = 9·1 Ton/in

Experimental Roll Force P_E = 8·8 Ton/in

T_T = 1·09 Ton in/in = 2440 lb.in./in.

Experimental Roll Torque 35·2% red = 2460 lb.in./in.

SPECIMEN C 50·2% red.

$h_1 = 0·1205$, $h_2 = 0·0600$, $\delta = 0·0605$, $P_E = 12·5$ Ton/in, $\mu = 0·25$

$\therefore R' = 2·14$ in.

N. P.

x	0	·0485	·097	·162	·228	·294	·359
ϕ	0	·0227	·0454	·0760	·1067	·1373	·1680
% red	50·2	49·3	46·6	40·0	30·0	16·5	0
$2k$ Ton/in^2	27·0	27·0	26·5	25·8	24·0	19·3	3·0
$p_{rr} = 2k\frac{h}{h_2}e^{\mu H}$	27·0	36·8	62·5				
$p_{rr} = 2k\frac{h}{h_1}e^{\mu(H_1-H)}$			62·5	45·2	32·4	21·6	3·0
$\frac{\mu p_{rr}}{k}$	·50	·68	1·20	·88	·68	·56	·50
$p_{rr}\phi$	0	·84	2·86				
$p_{rr}\phi$			2·86	3·42	3·46	2·97	·50

$$P_T = 12{\cdot}5 \text{ Ton/in}$$

Experimental Roll Force $P_E = 12{\cdot}5$ Ton/in

$$T_T = 1{\cdot}77 \text{ Ton in/in} = 3960 \text{ lb.in./in.}$$

Experimental Roll Torque 50·2% red = 3800 lb.in/in.

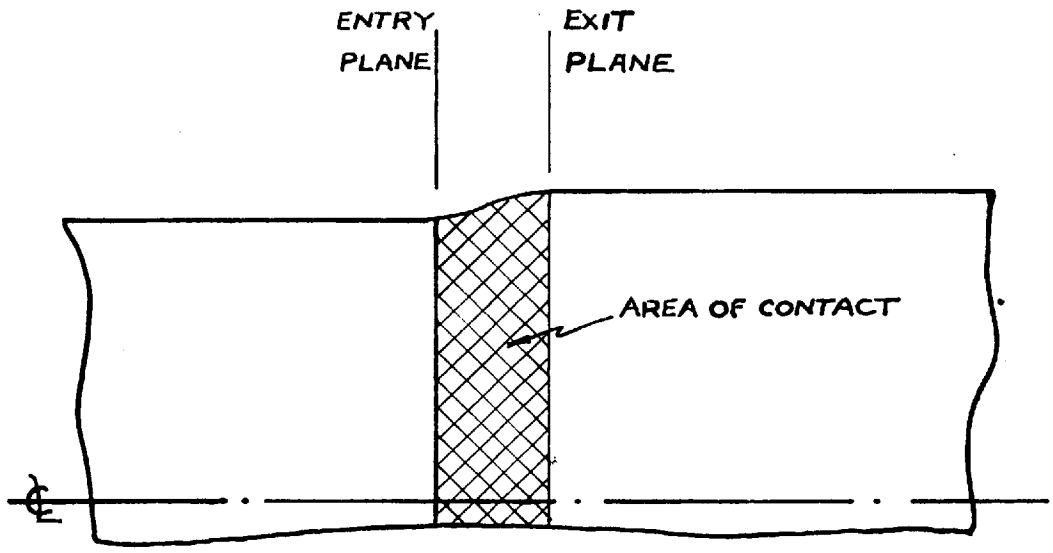


Fig. 1. Spread in Rolling.

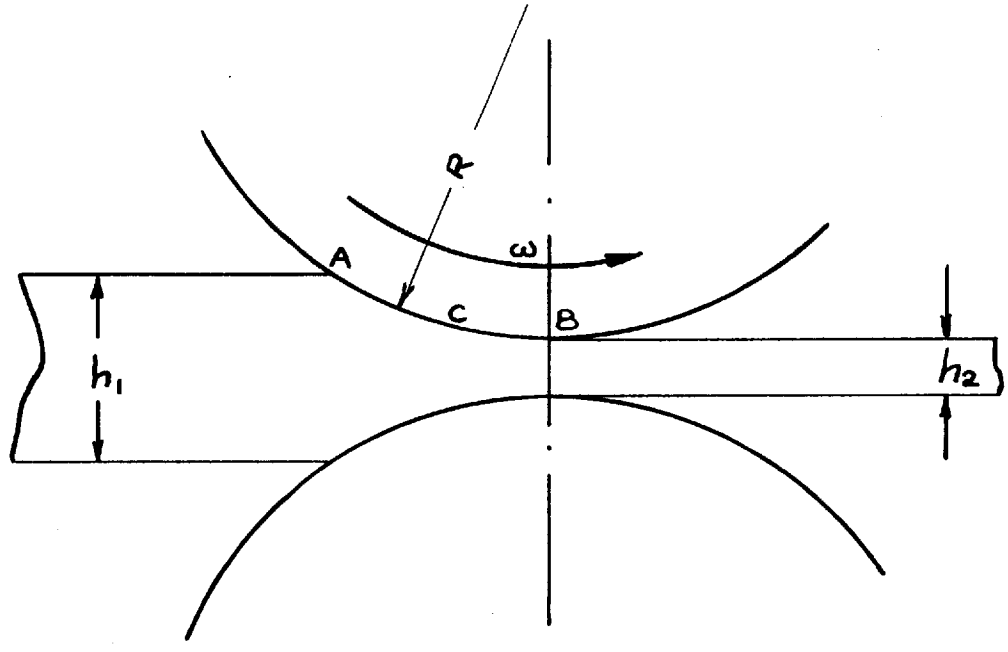


Fig. 2. Material in Roll Gap.

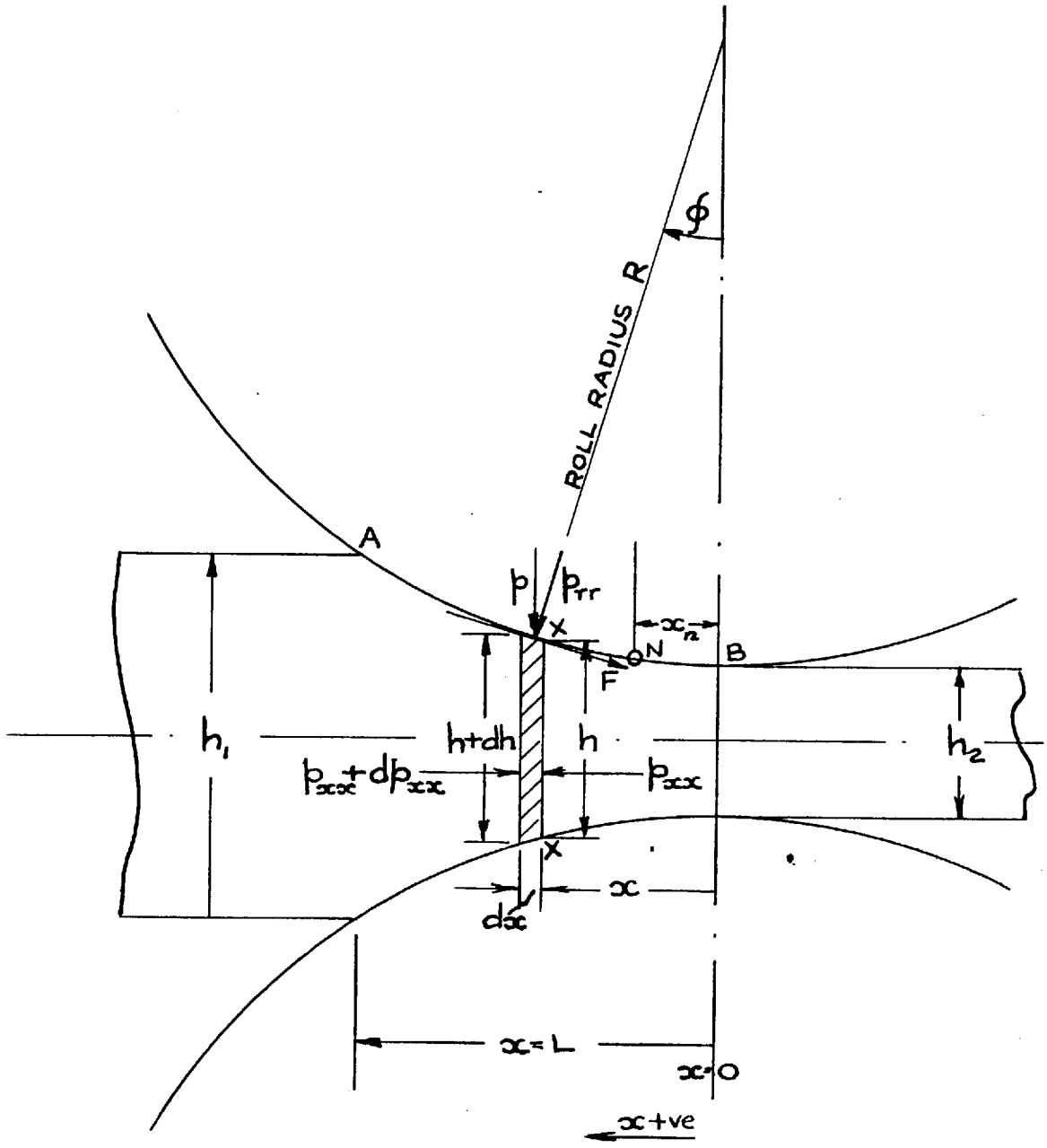


Fig. 3. Section through Roll Gap.

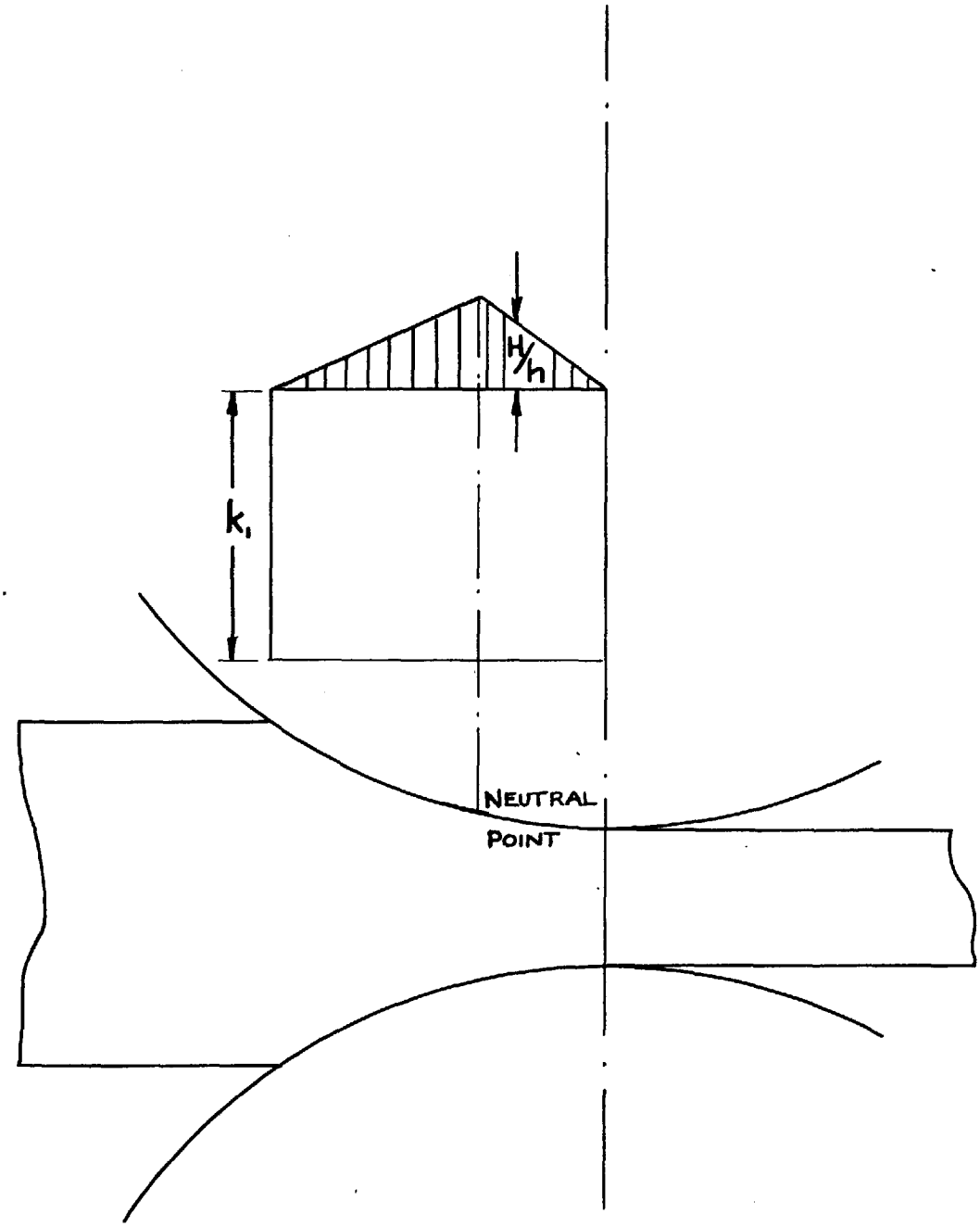


Fig. 4. Siebel's Friction Hill.

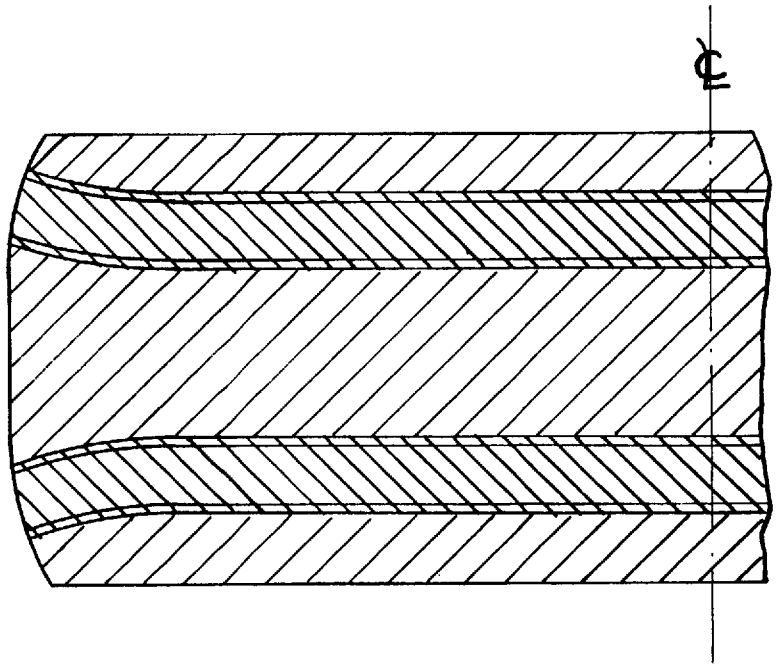


Fig. 5. Pattern of Deformation Across Width (after Metz)

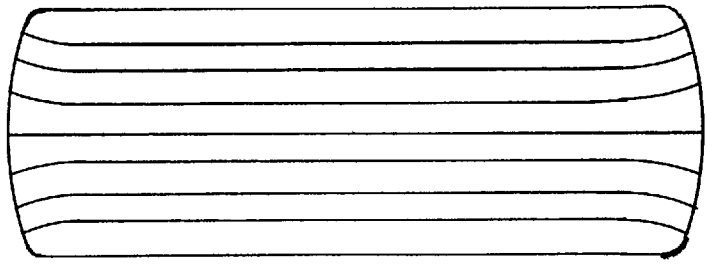


Fig. 6. Pattern of Deformation Across Width. (after Weiss)

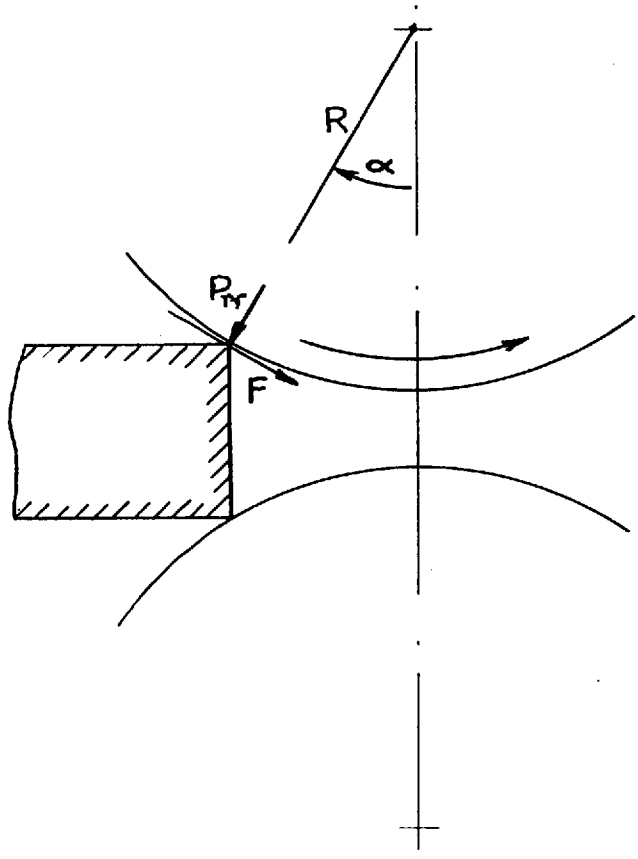


Fig. 7. Greatest Gripping Angle.

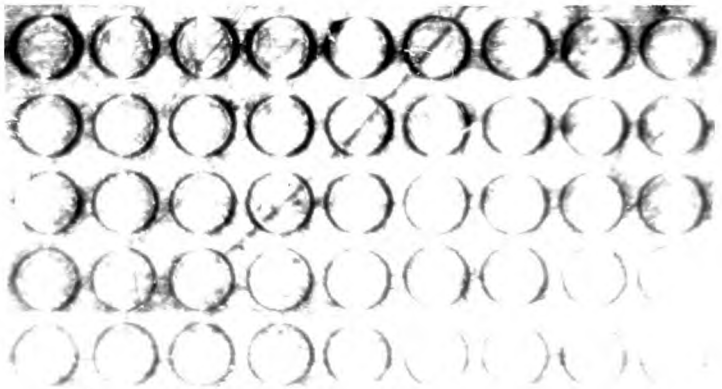


Fig. 8. Photograph of Circular Grid. X 15

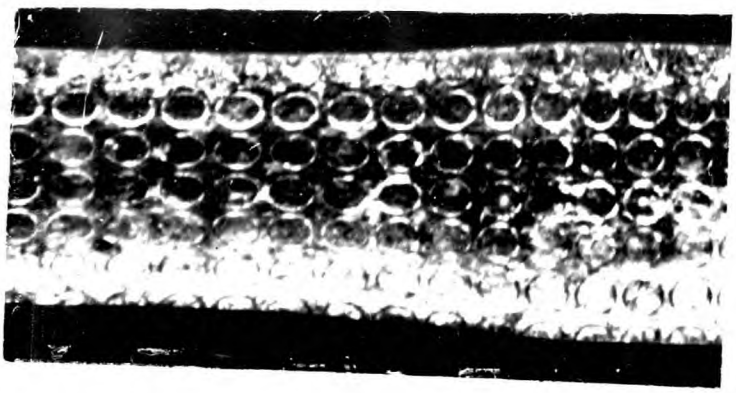


Fig. 9. Photograph of Distorted Circular Grid.



Fig. 10. Milling Machine set up for Engraving Grid.

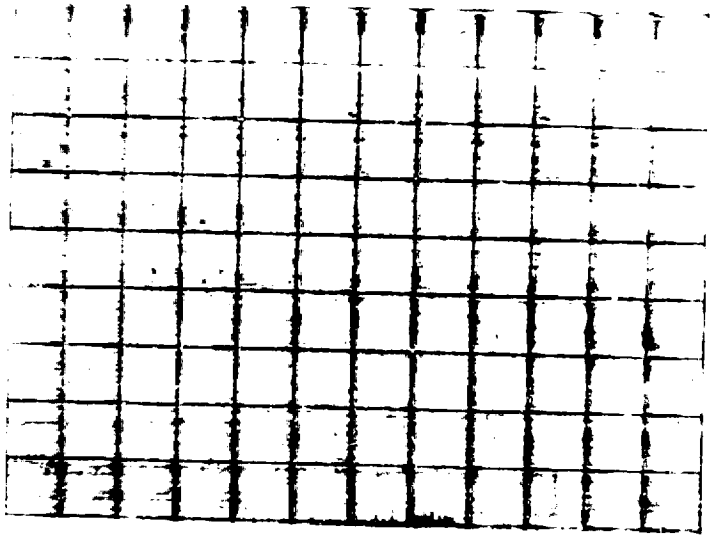


Fig. 11. Photograph of Square Grid. X 30

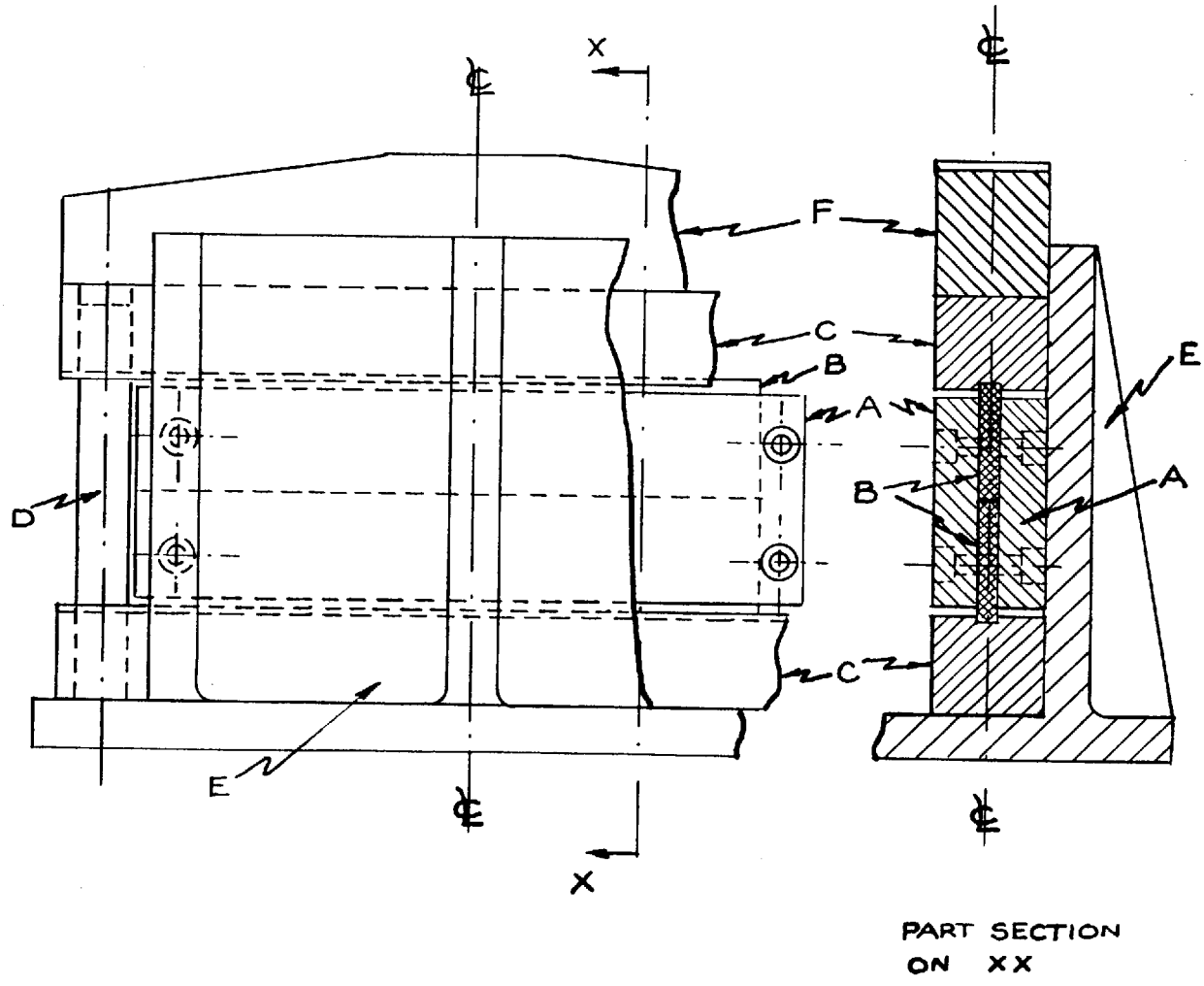


Fig. 12. Welding Jig.

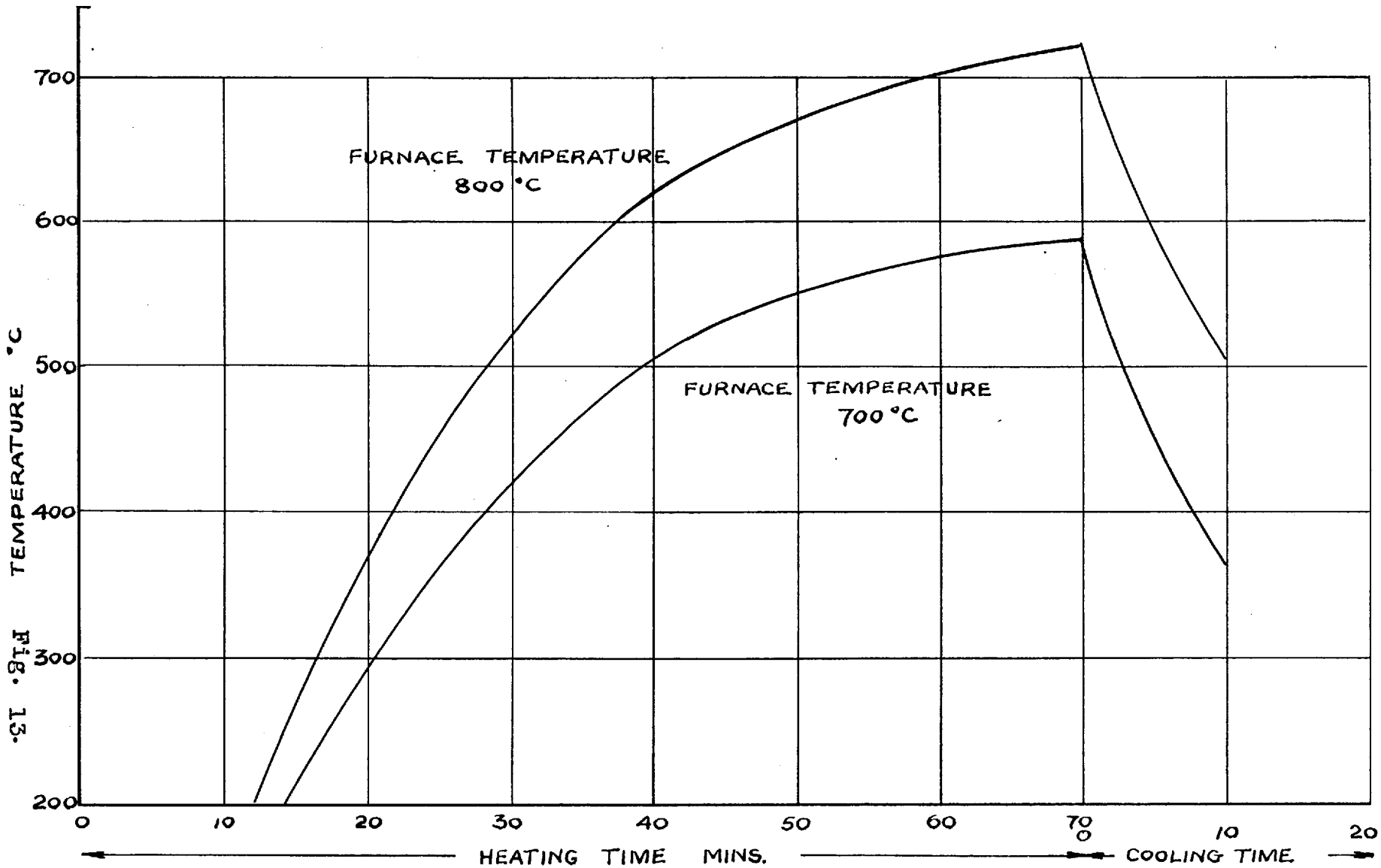

FURNACE TEMPERATURE
800 °C
FURNACE TEMPERATURE
700 °C
700
600
500
400
300
200
TEMPERATURE °C
0
10
20
30
40
50
60
70
10
20
HEATING TIME MINS.
COOLING TIME

FIG. 13.

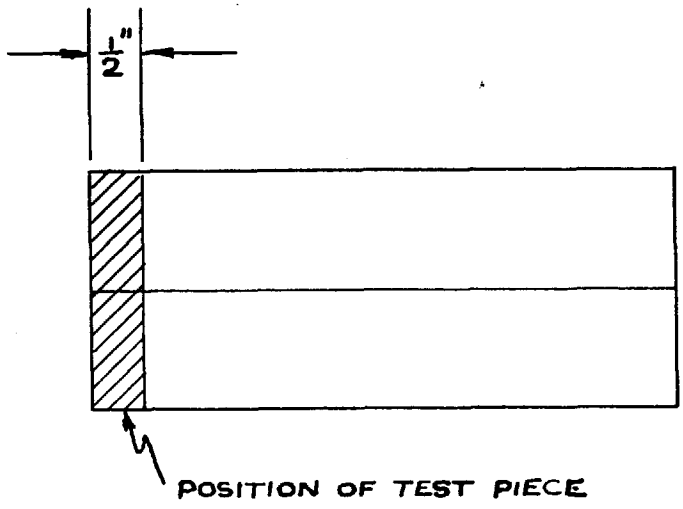


Fig. 14. Position of Tensile Test Specimens.



Fig. 15. General View of Rolling Mill.



Fig. 16. General View of Rolling Mill.

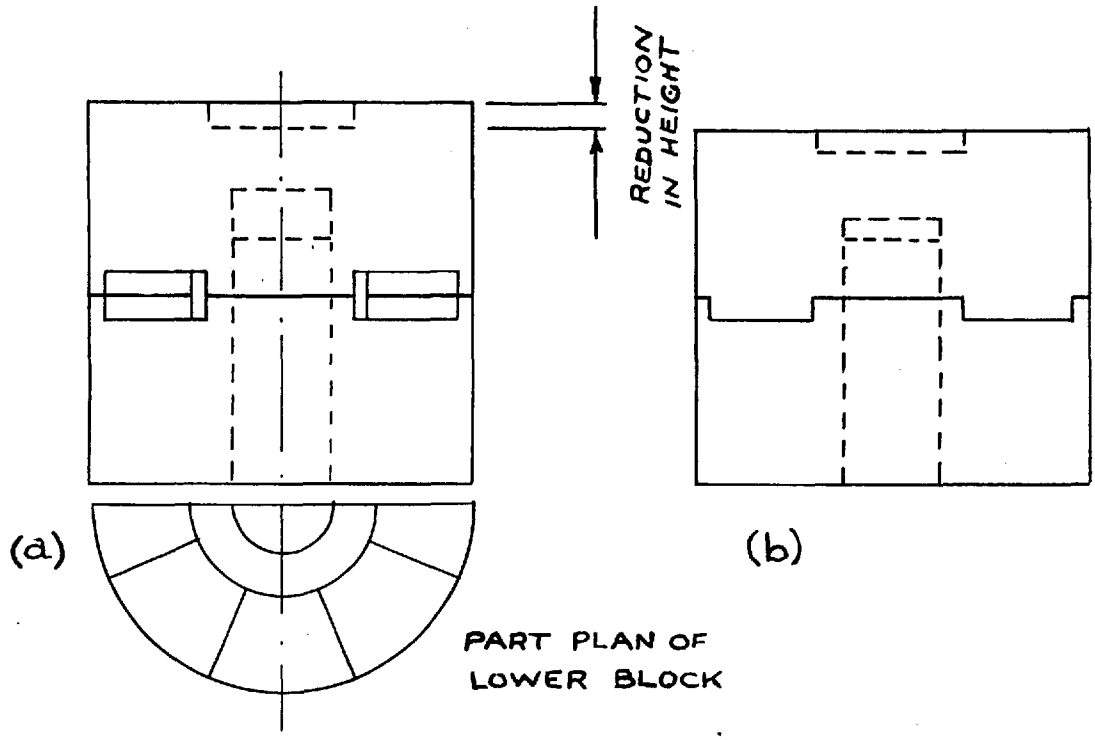


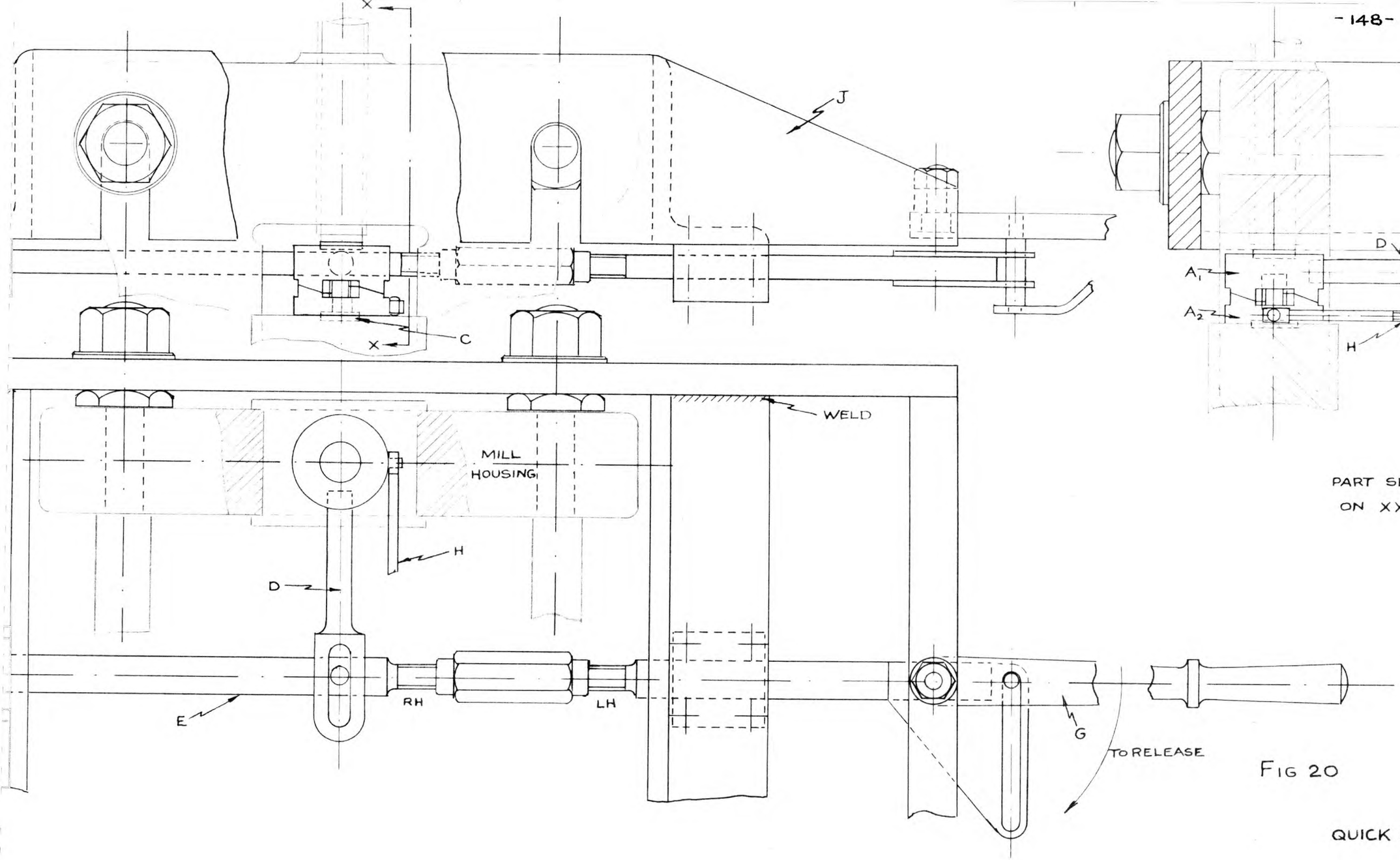
Fig. 17. Principle of Quick Release Blocks.



Fig. 18. Quick Release Element.



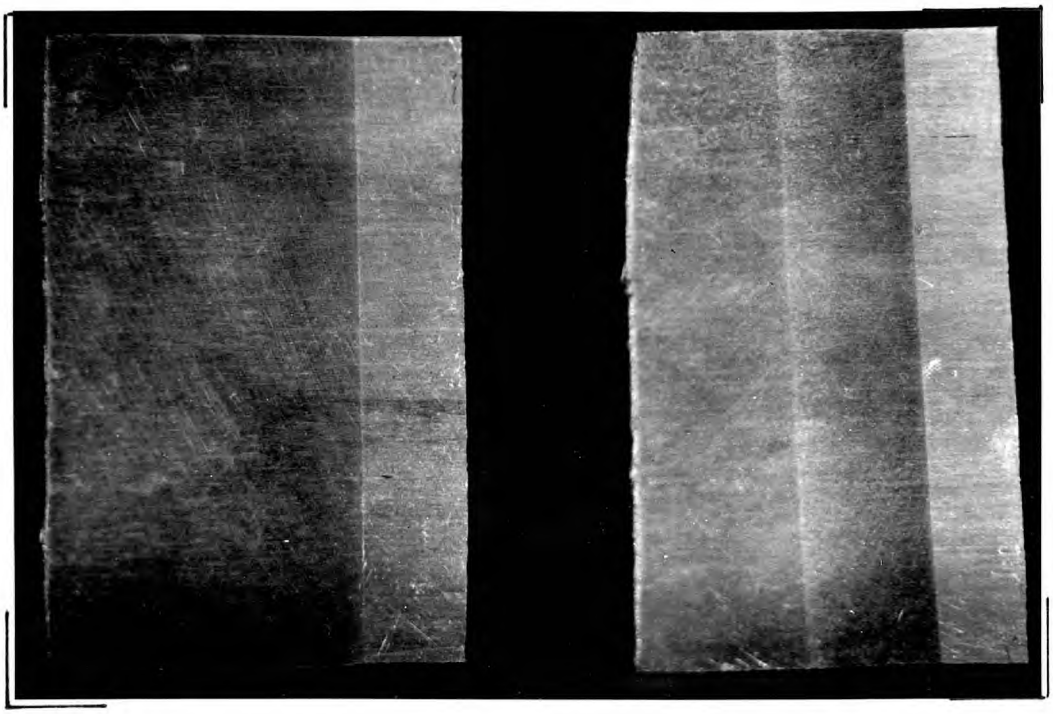
Fig. 19. Complete Quick Release Mechanism.



PART SECTION
ON XX

FIG 20

QUICK RELEASE MECHANISM.



A B

Fig. 21. Roll Gap Impression.

A with Quick Release.
B without Quick Release.

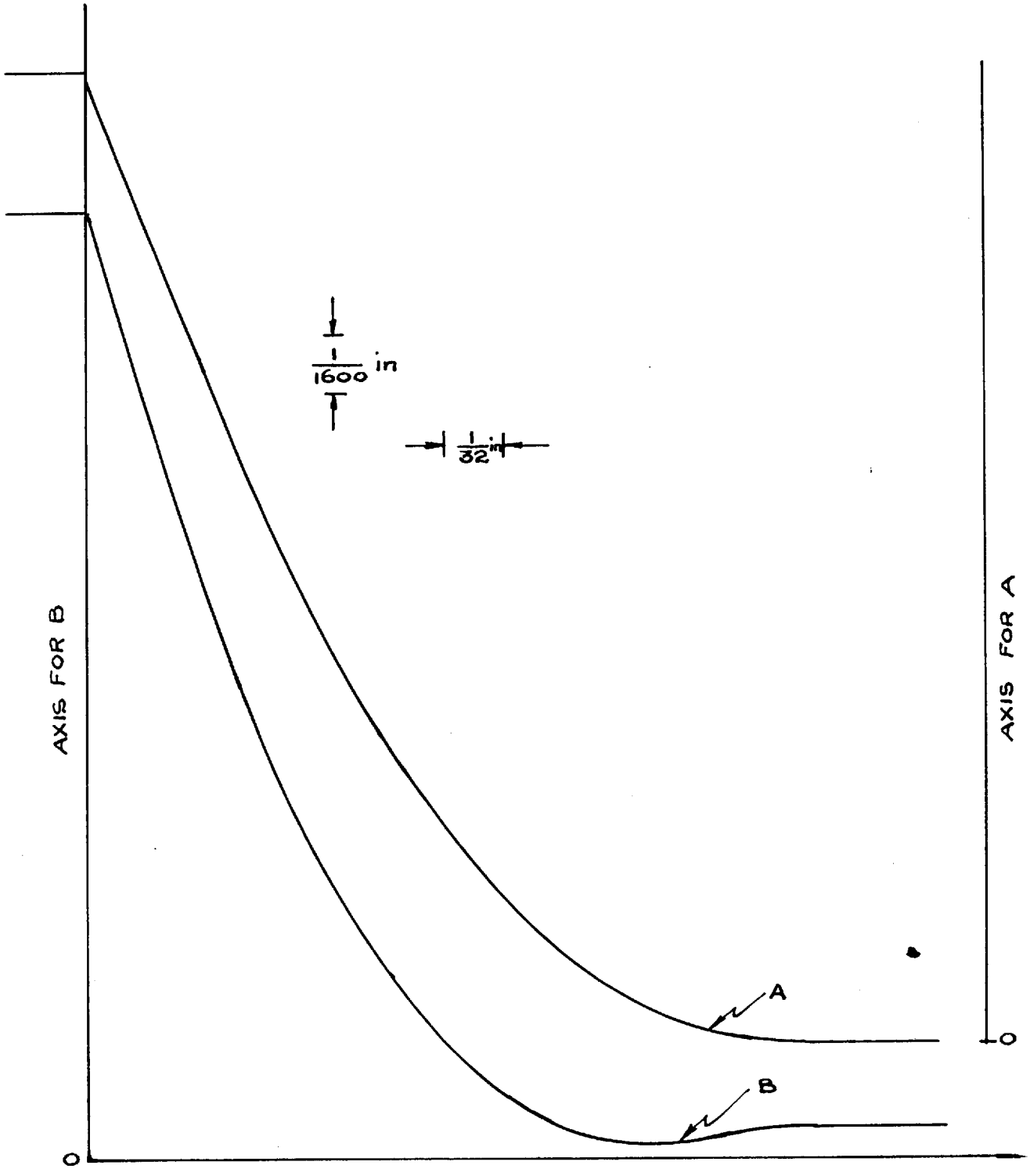


Fig. 22. Roll Gap Profile.

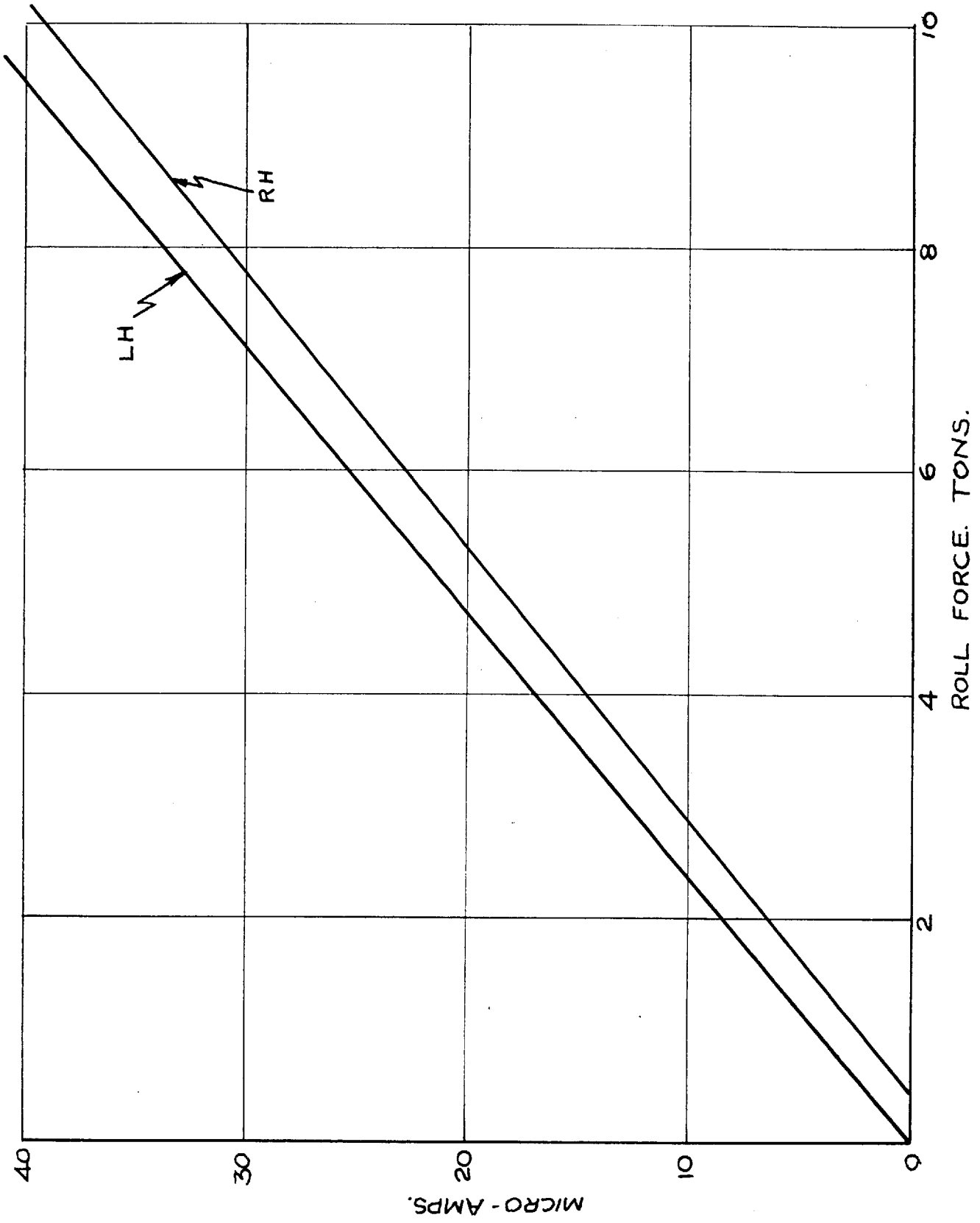


Fig. 23. Calibration Graph for Load Cell.

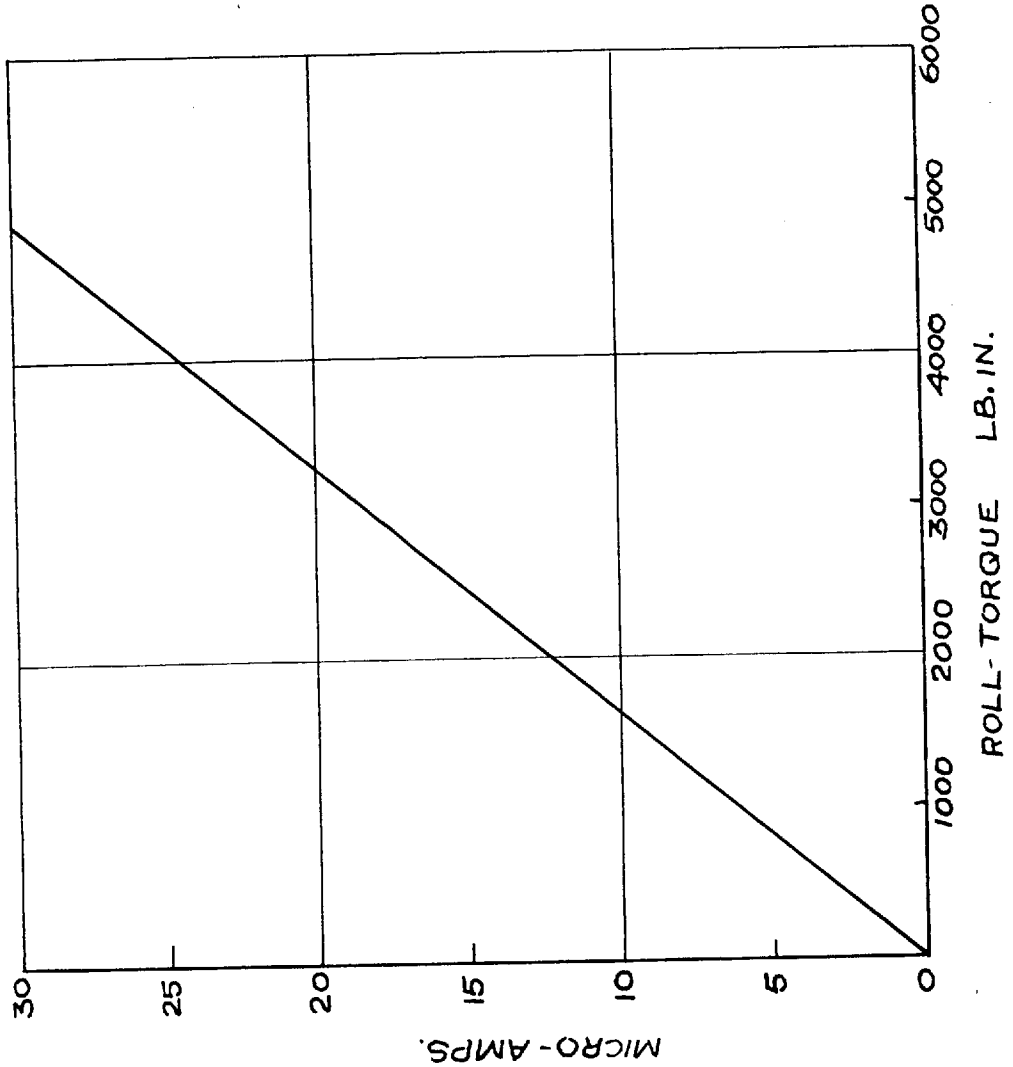


Fig. 24. Calibration Graph for Torque Meters.

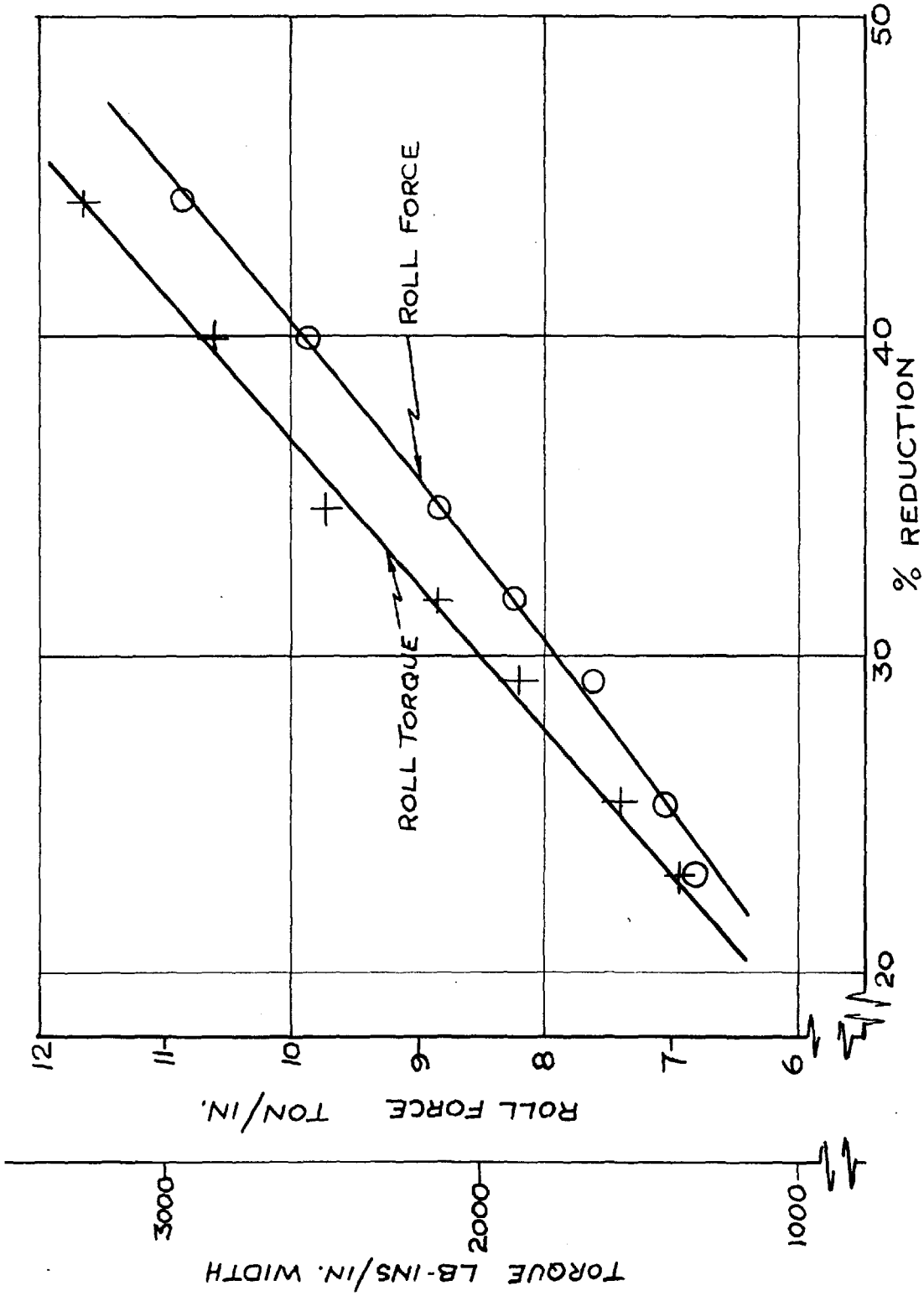


Fig. 25. Roll Force and Torque v. Reduction.

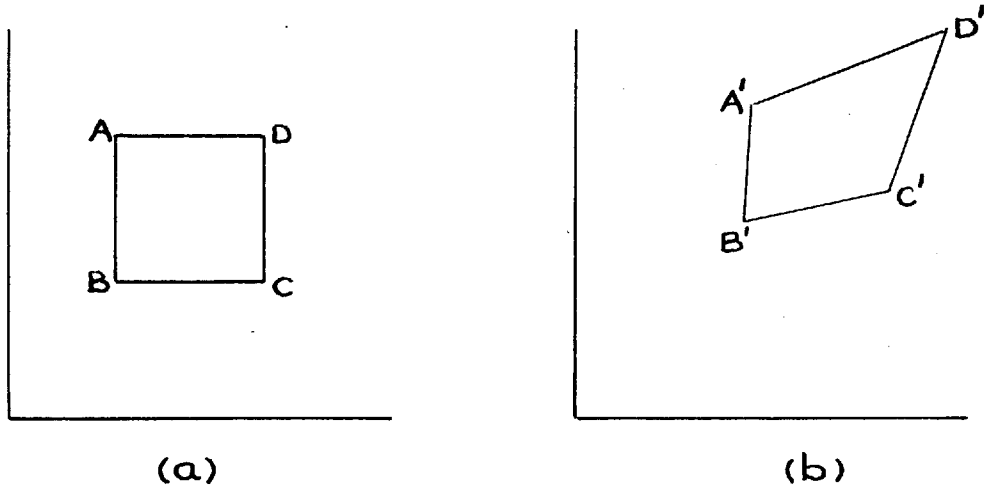


Fig. 26. Deformation of Square Grid.

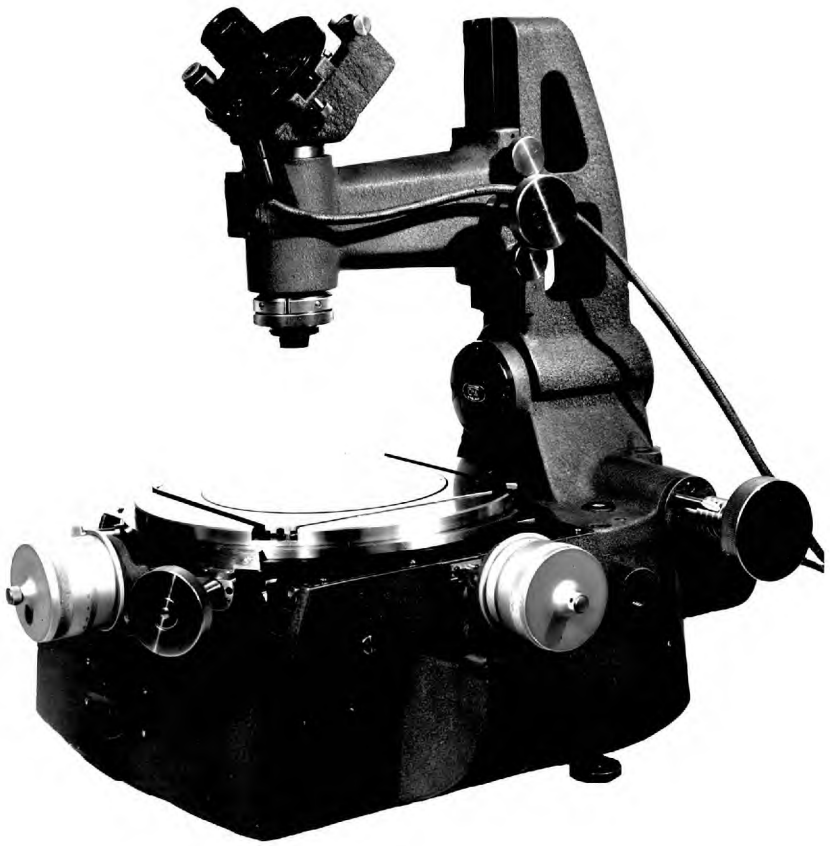


Fig. 27. O.M.T. Toolmaker's Microscope.

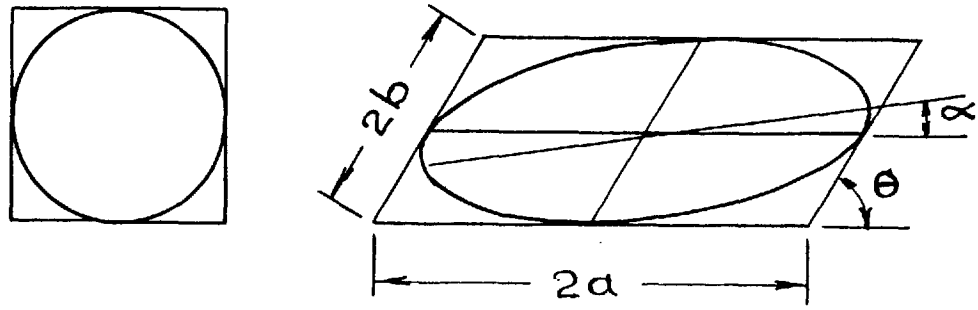


Fig. 28. Deformation of Circular Element.

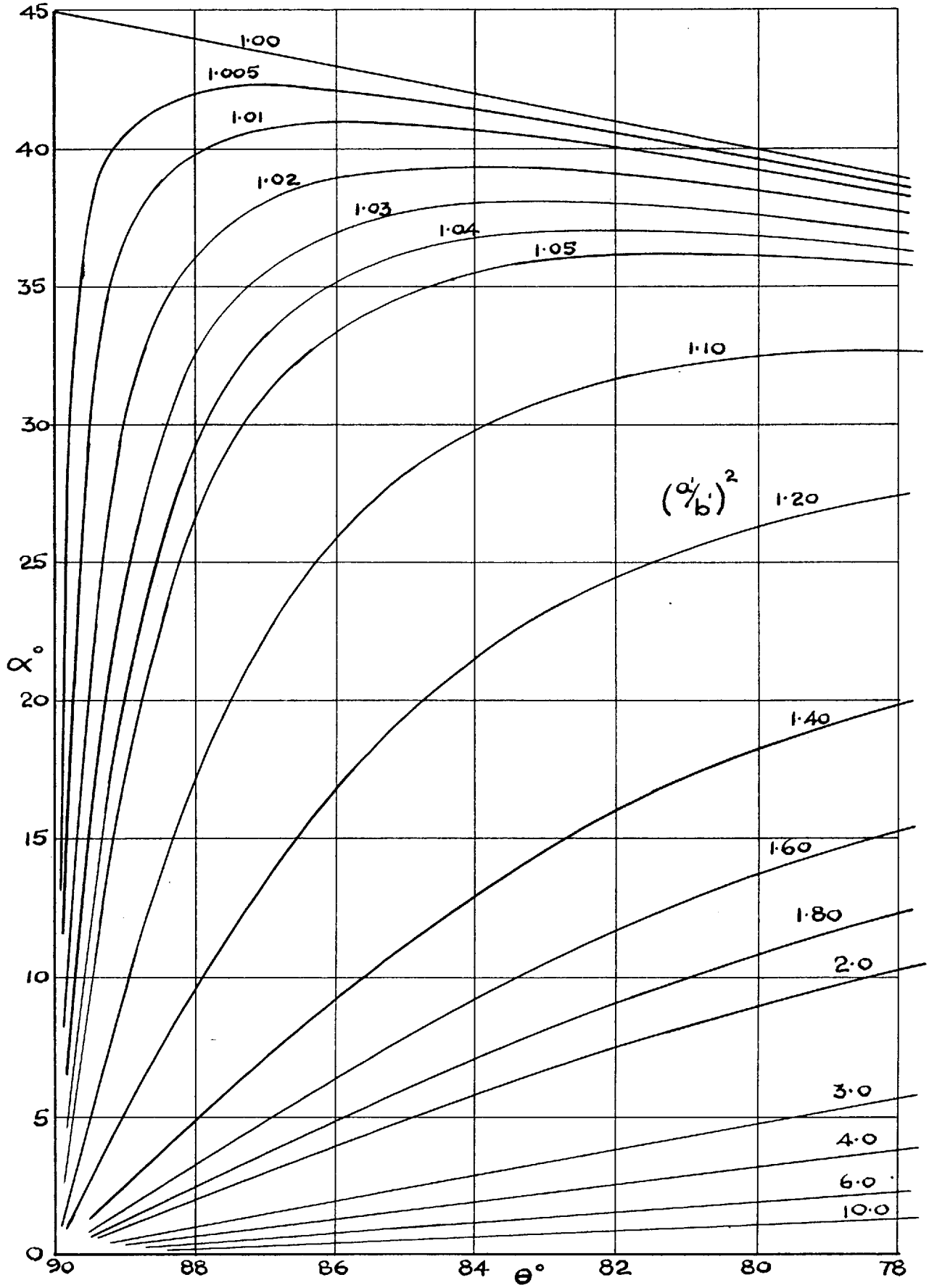

45
40
35
30
25
20
15
10
5
0
α°
90
88
86
84
θ°
82
80
78
1·00
1·005
1·01
1·02
1·03
1·04
1·05
1·10
1·20
1·40
1·60
1·80
2·0
3·0
4·0
6·0
10·0
(a'/b')²

Fig. 29.

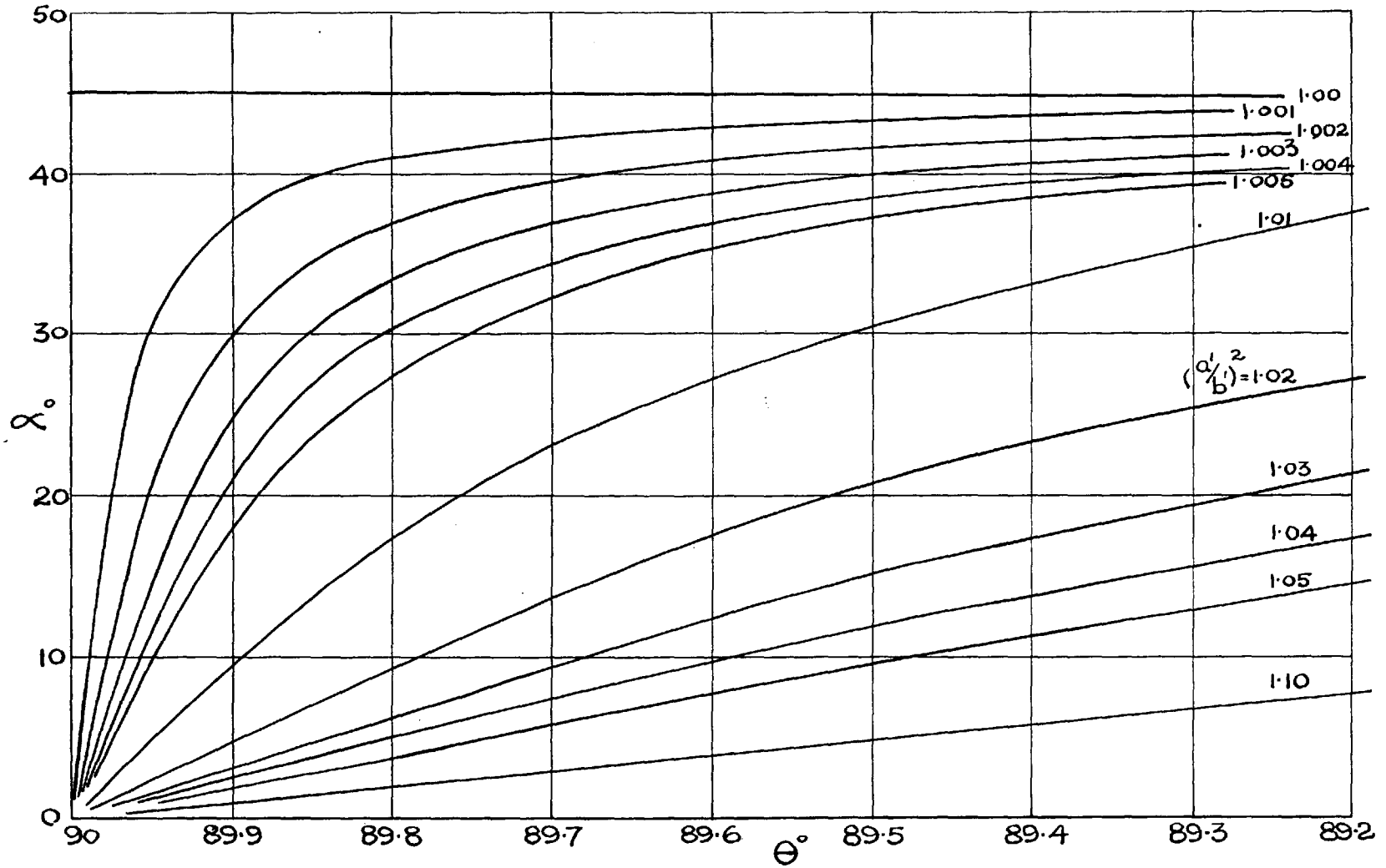

50
40
30
20
10
0
χ°
90
89·9
89·8
89·7
89·6
θ°
89·5
89·4
89·3
89·2
1·00
1·001
1·002
1·003
1·004
1·005
1·01
(a'/b')² = 1·02
1·03
1·04
1·05
1·10

Fig. 30(a)

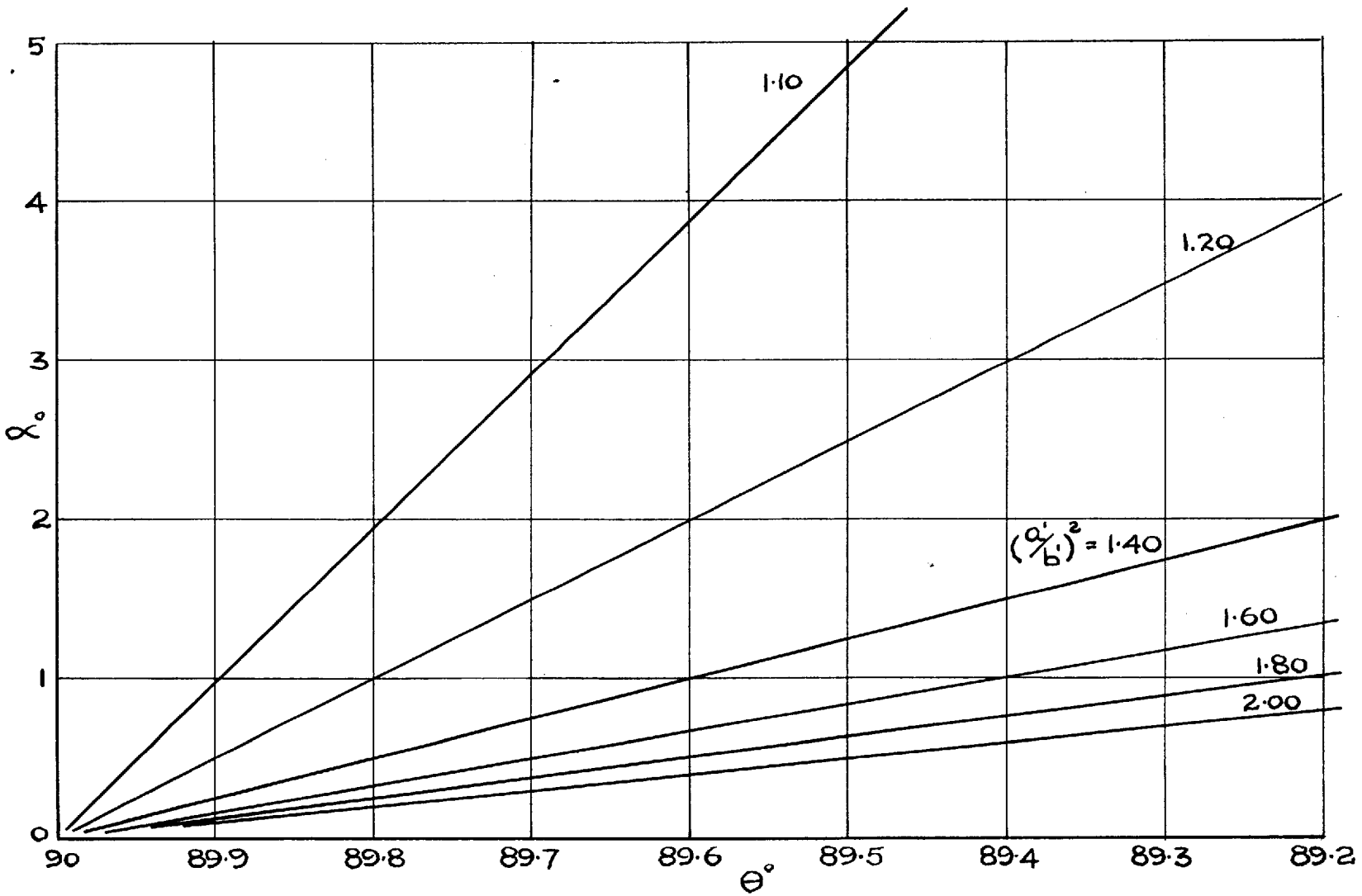

5
4
3
2
1
0
χ°
90
89·9
89·8
89·7
89·6
89·5
89·4
89·3
89·2
θ°
1·10
1.20
(a'/b')² = 1·40
1·60
1·80
2·00

Fig. 30(b).

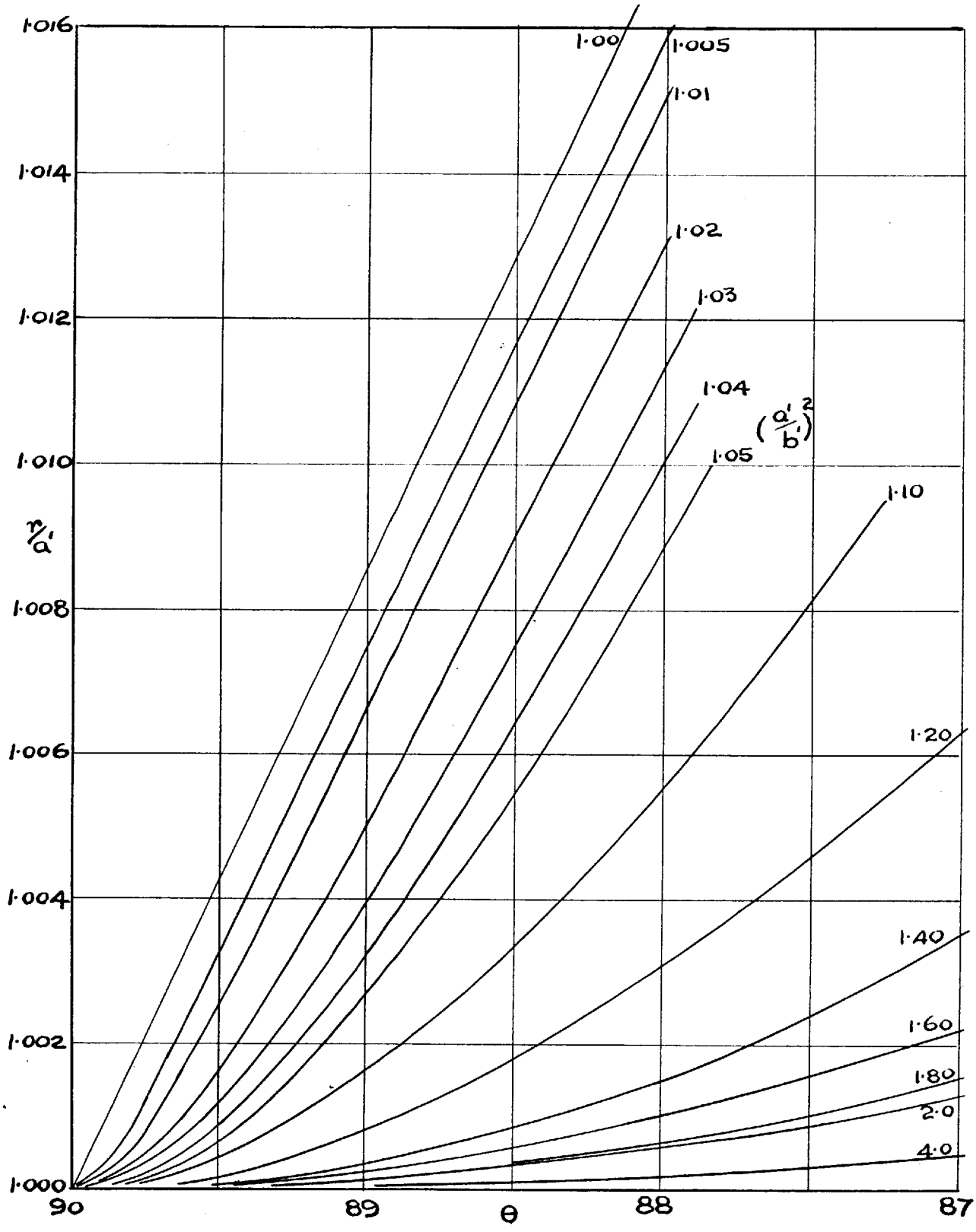

1·016
1·014
1·012
1·010
1·008
1·006
1·004
1·002
1·000
r/a'
90
89
θ
88
87
1·00
1·005
1·01
1·02
1·03
1·04
1·05
1·10
1·20
1·40
1·60
1·80
2·0
4·0
(a'/b')²

Fig. 31.

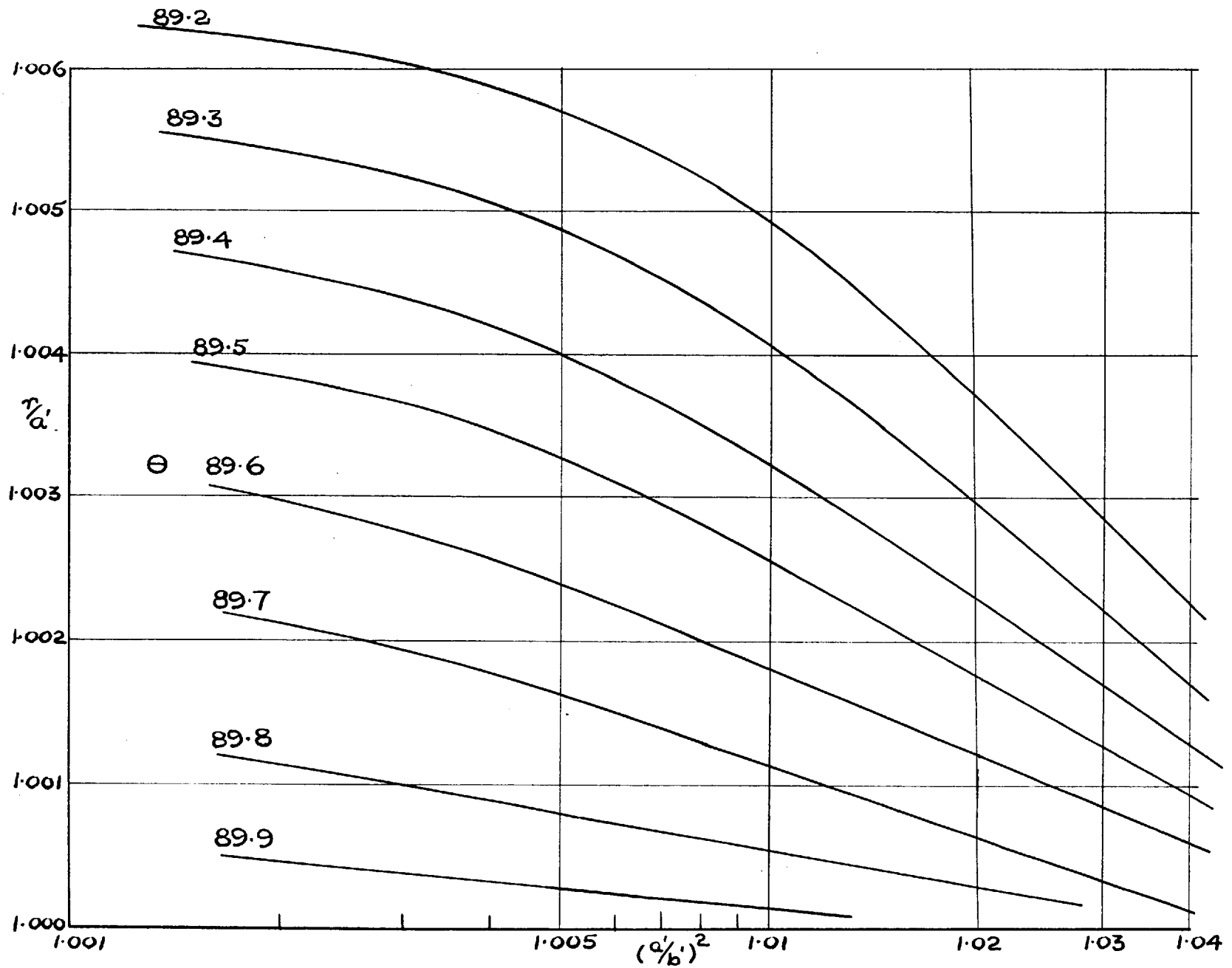

89·2
89·3
89·4
89·5
89·6
89·7
89·8
89·9
θ
r/a'
1·006
1·005
1·004
1·003
1·002
1·001
1·000
1·001
1·005
1·01
1·02
1·03
1·04
(a'/b')²

Fig. 32.

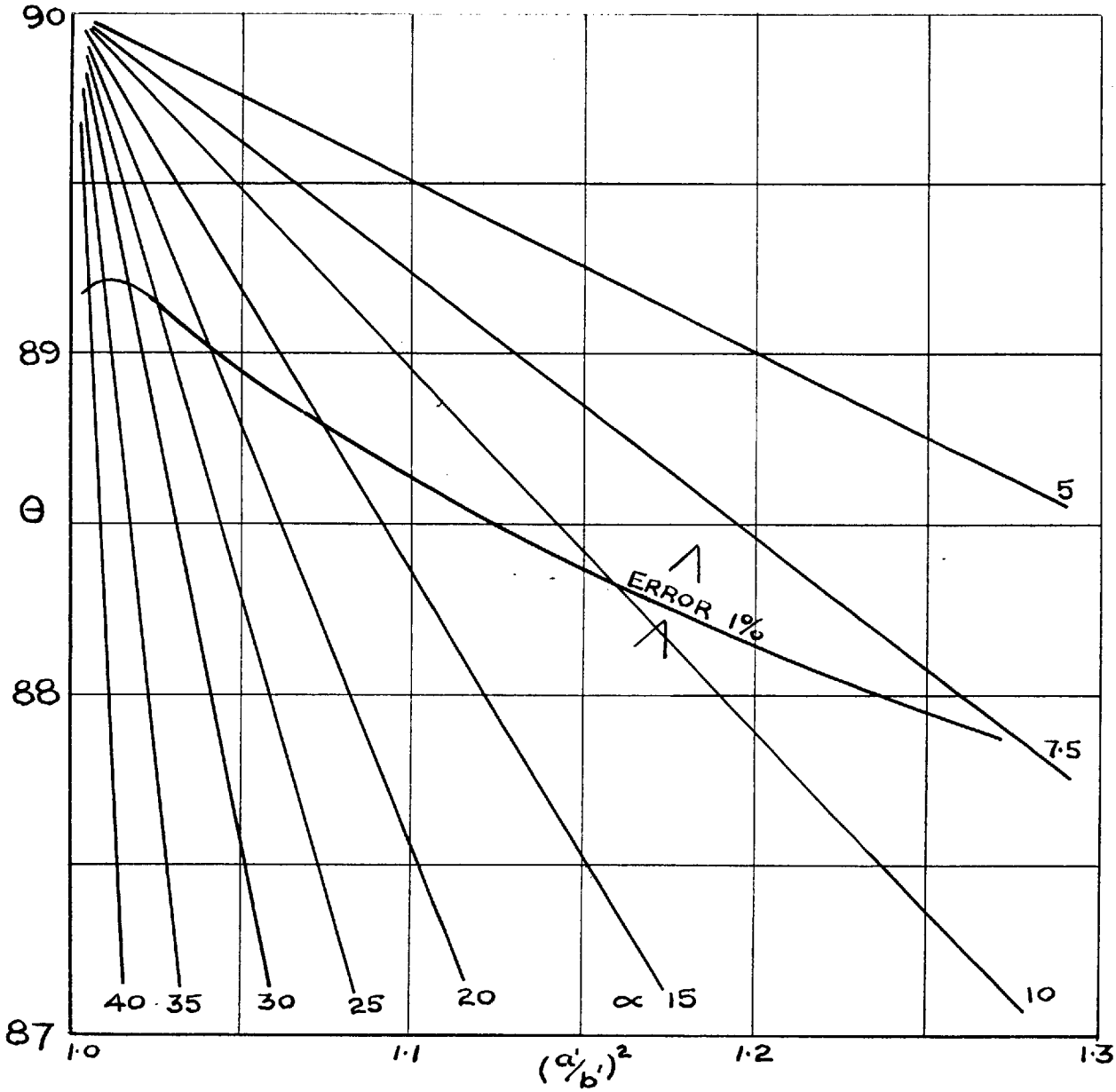


Fig. 33

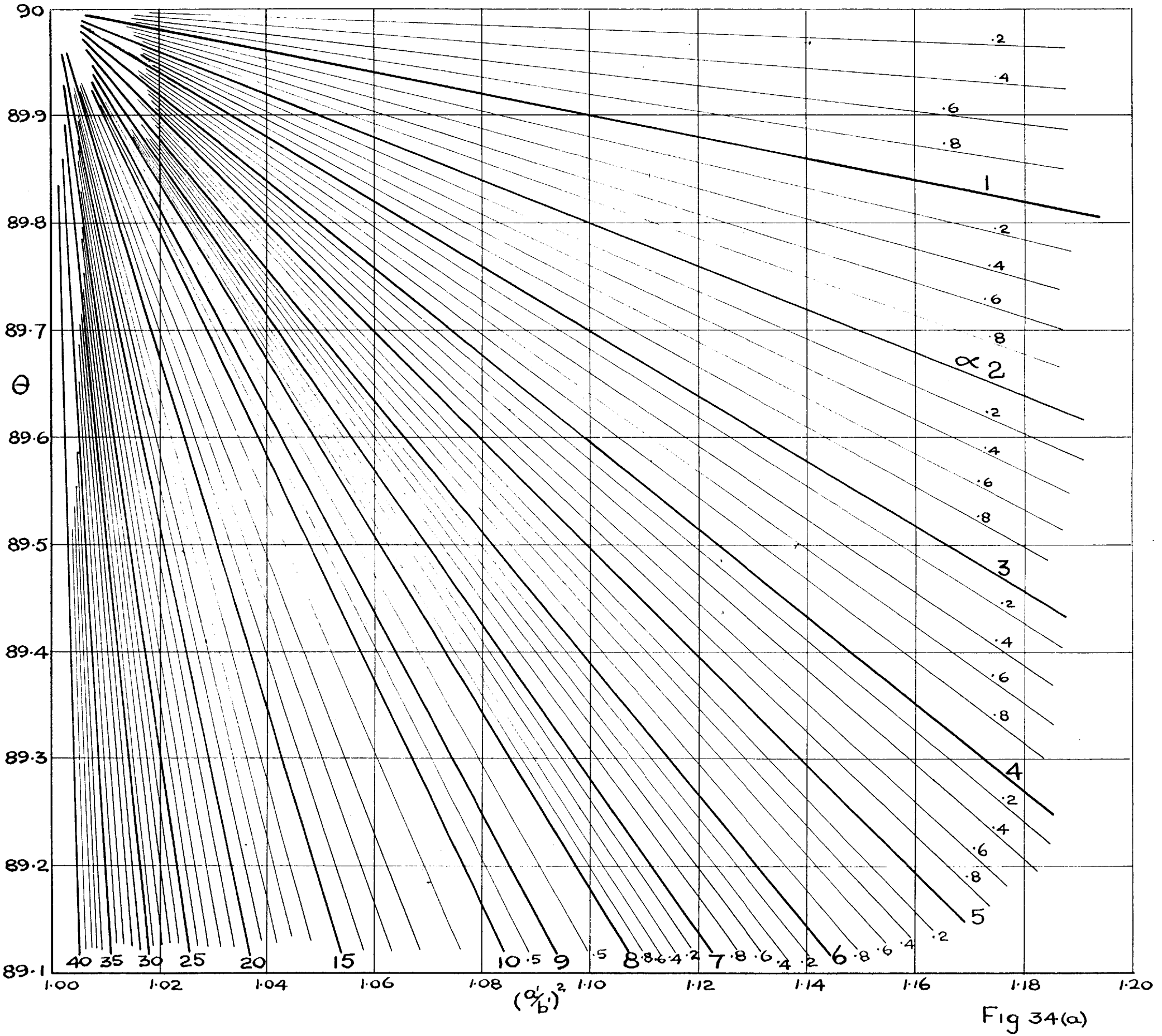

90
89·9
89·8
89·7
θ
89·6
89·5
89·4
89·3
89·2
89·1
1·00
1·02
1·04
1·06
1·08
1·10
1·12
1·14
1·16
1·18
1·20
(a'/b')²
40 35 30 25 20 15 10 ·5 9 ·5 8 ·8 ·6 ·4 ·2 7 ·8 ·6 ·4 ·2 6 ·8 ·6 ·4 ·2 5 ·8 ·6 ·4 ·2 4 ·8 ·6 ·4 ·2 3 ·8 ·6 ·4 ·2 1 ·8 ·6 ·4 ·2
α 2

Fig 34(a)

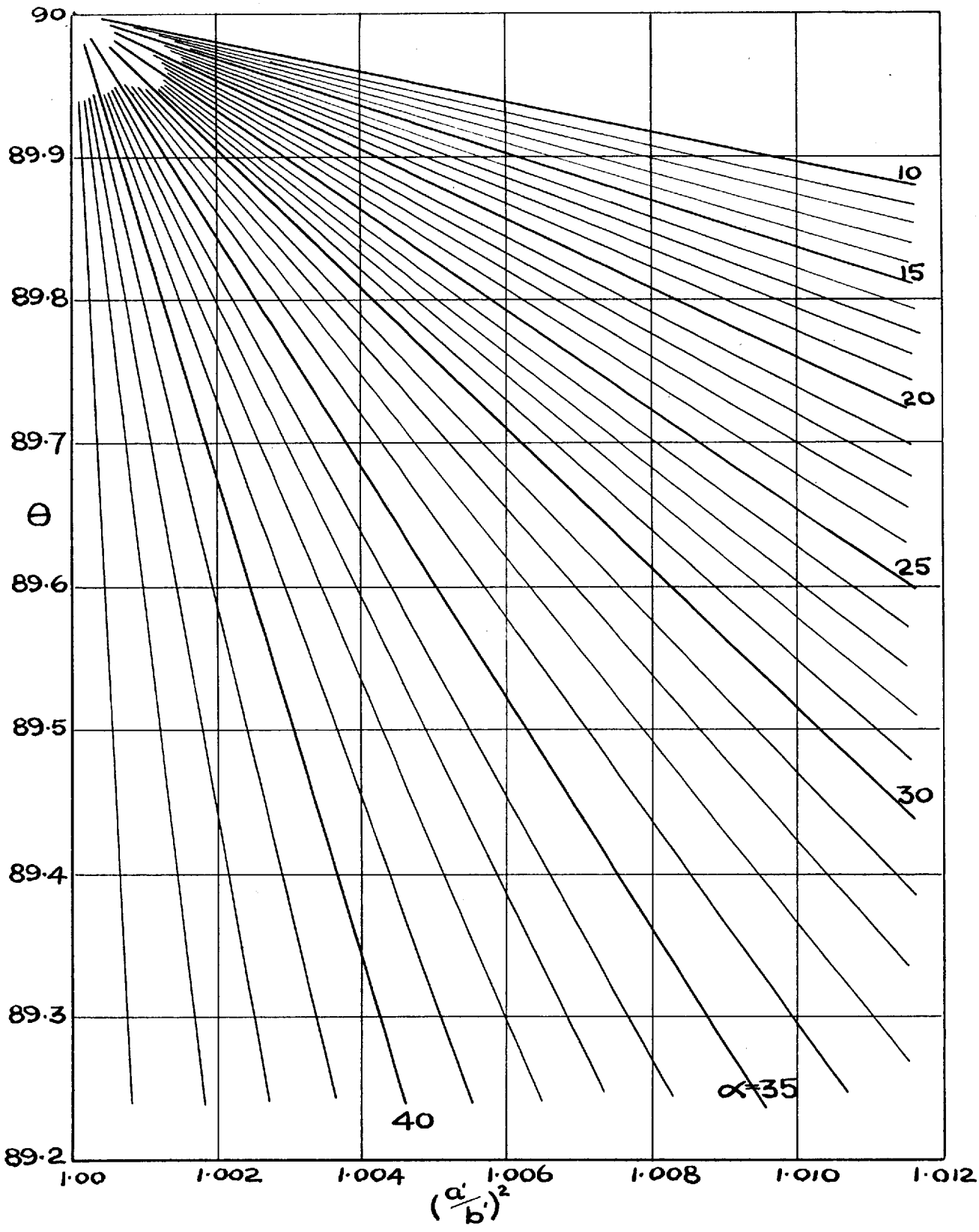

90
89·9
89·8
89·7
θ
89·6
89·5
89·4
89·3
89·2
1·00
1·002
1·004
1·006
1·008
1·010
1·012
$(\frac{a'}{b'})^2$
10
15
20
25
30
40
α=35

Fig. 34(b).

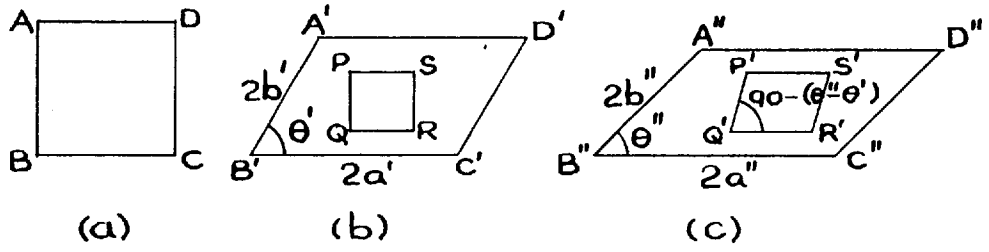


Fig. 35. Incremental Deformation of Element.

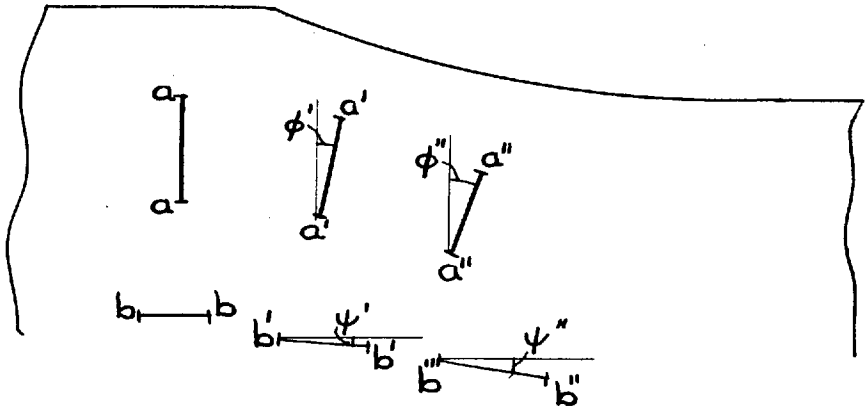


Fig. 36. Angular Changes in Element in Roll Gap.

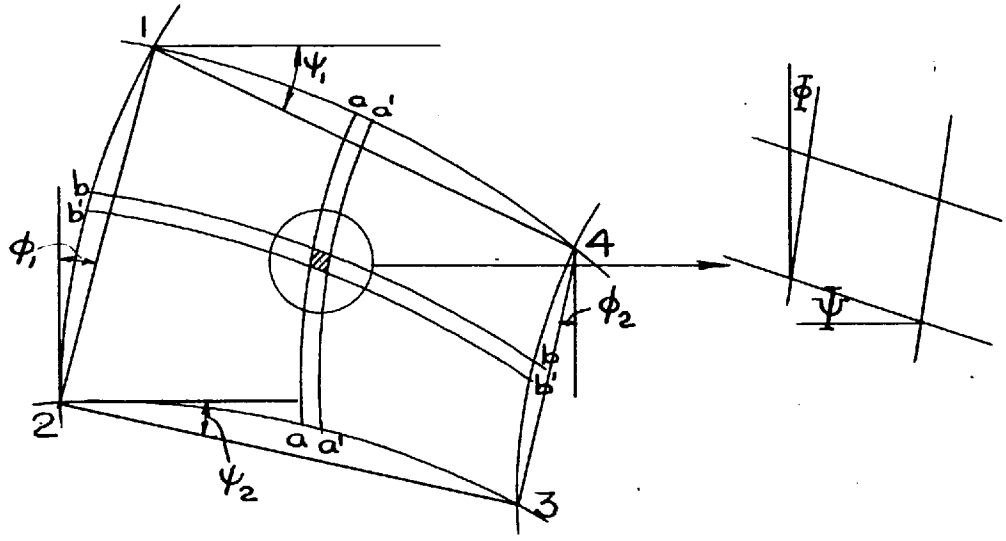
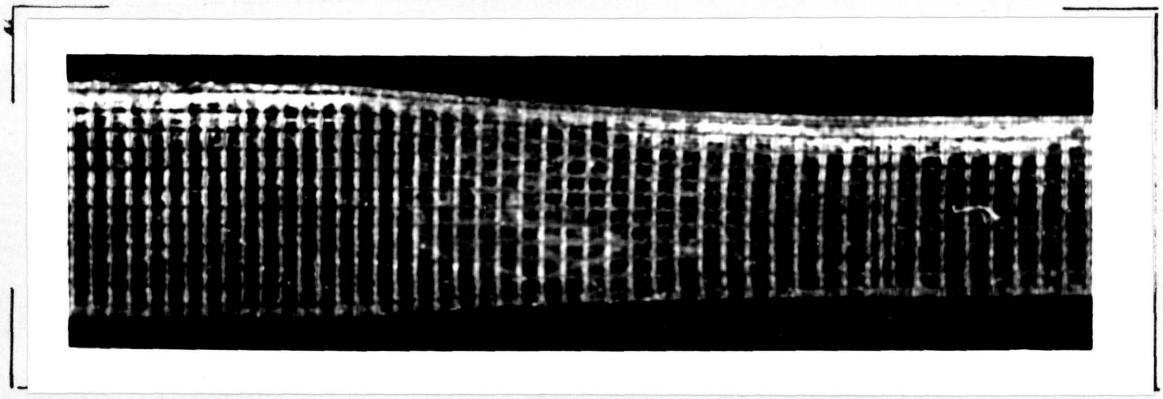
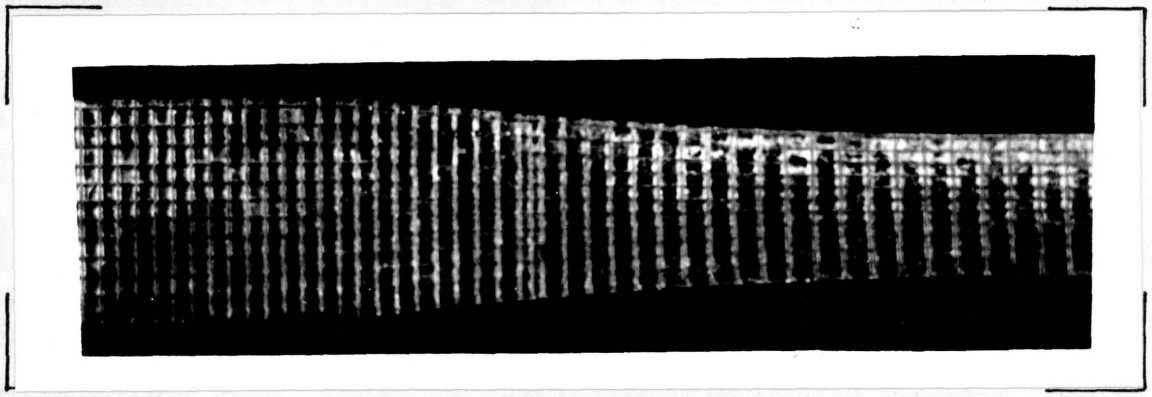


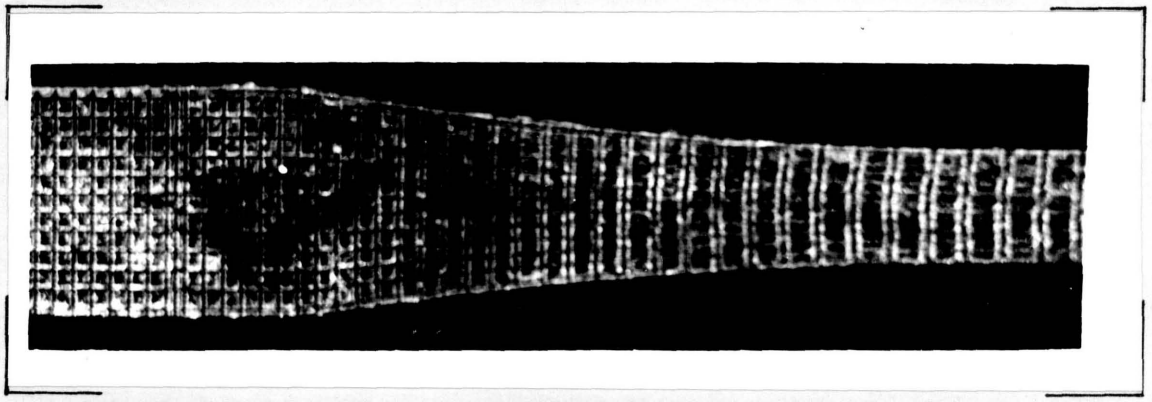
Fig. 37. General Quadrilateral Distortion.



Specimen A. 21.8% reduction.



Specimen B. 35.4% reduction.



Specimen C. 50.2% reduction.

Fig. 38. Photographs of Rolled Specimens. X 10

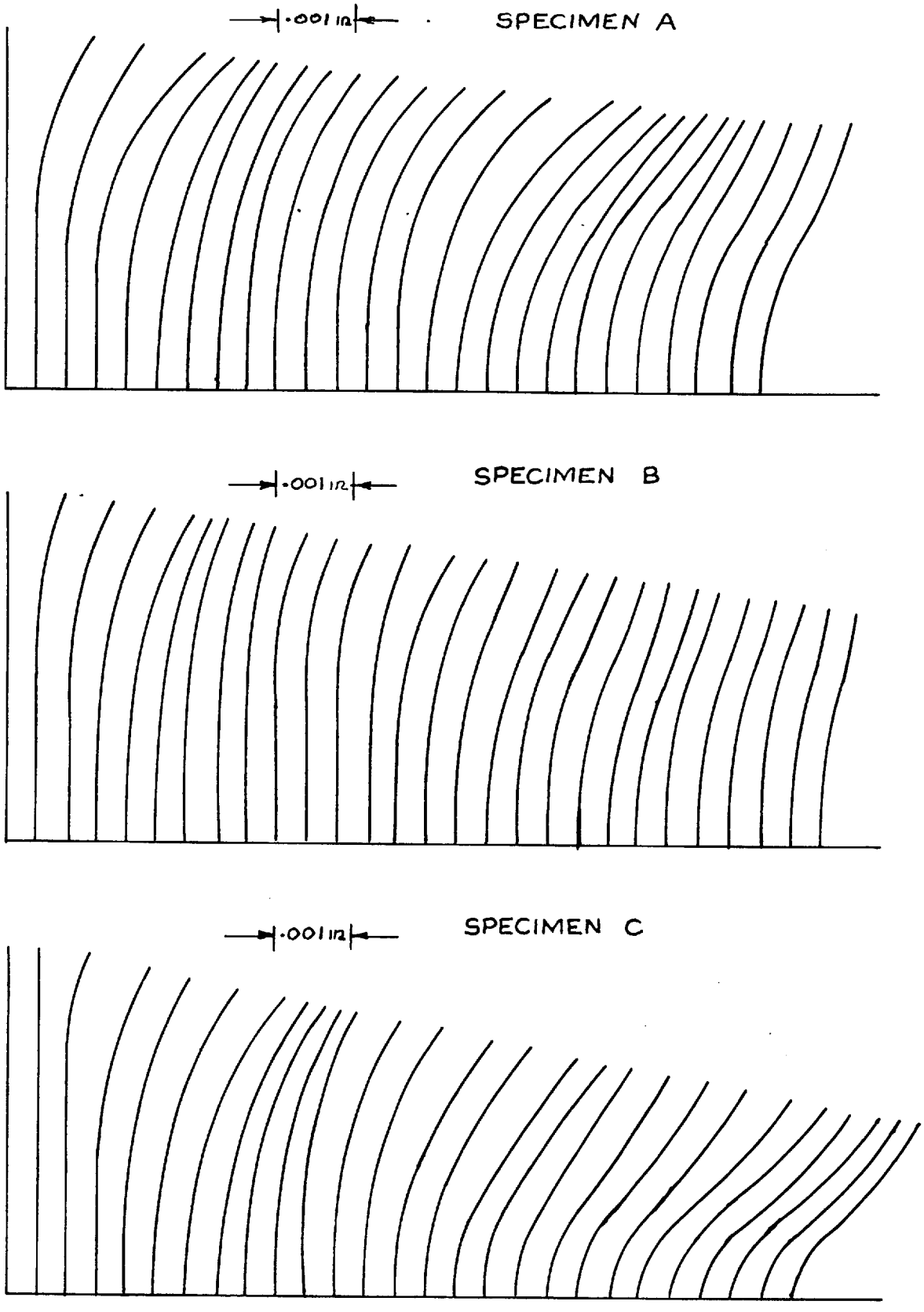


Fig. 39. Pattern of Deformation.

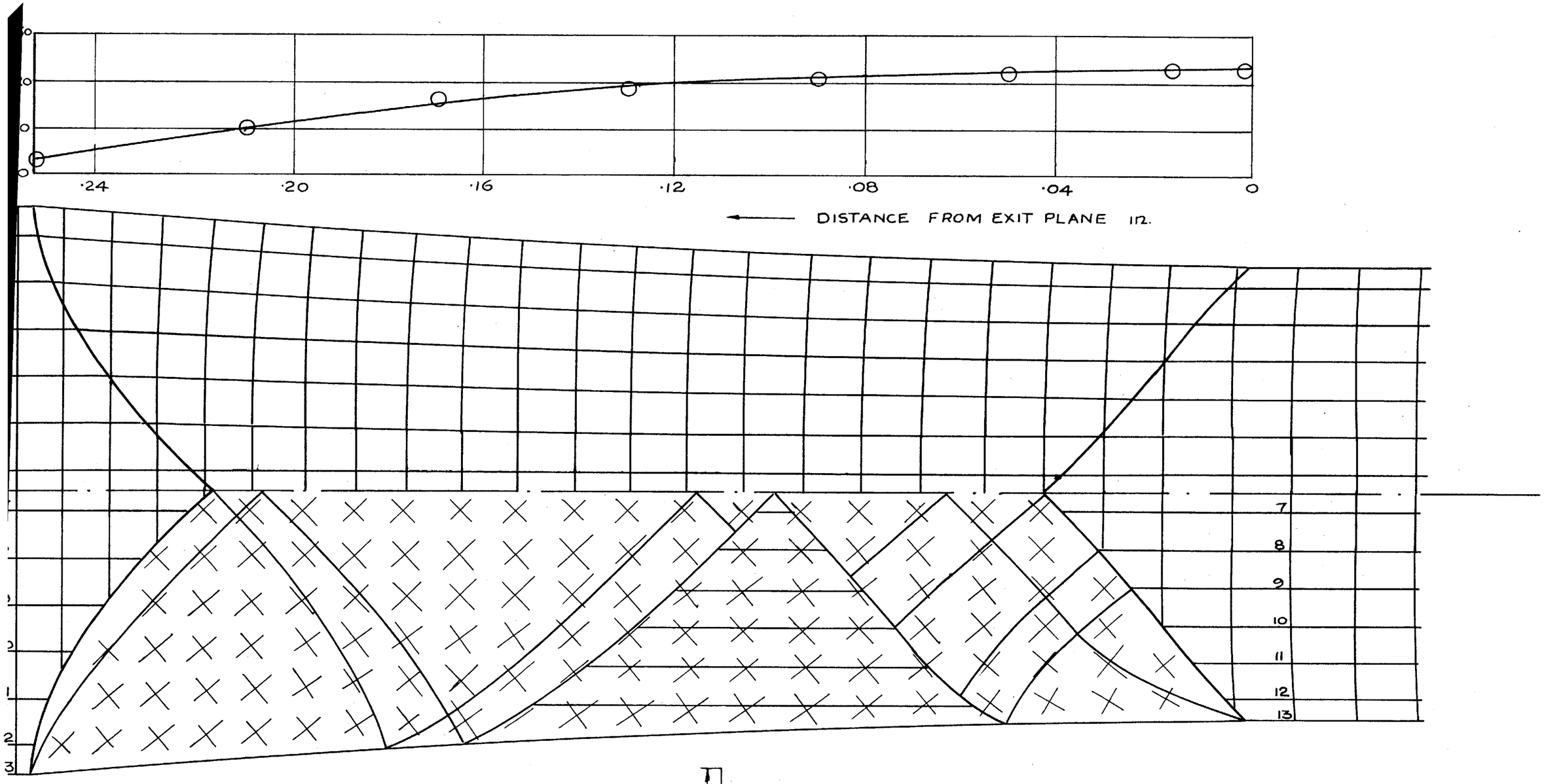
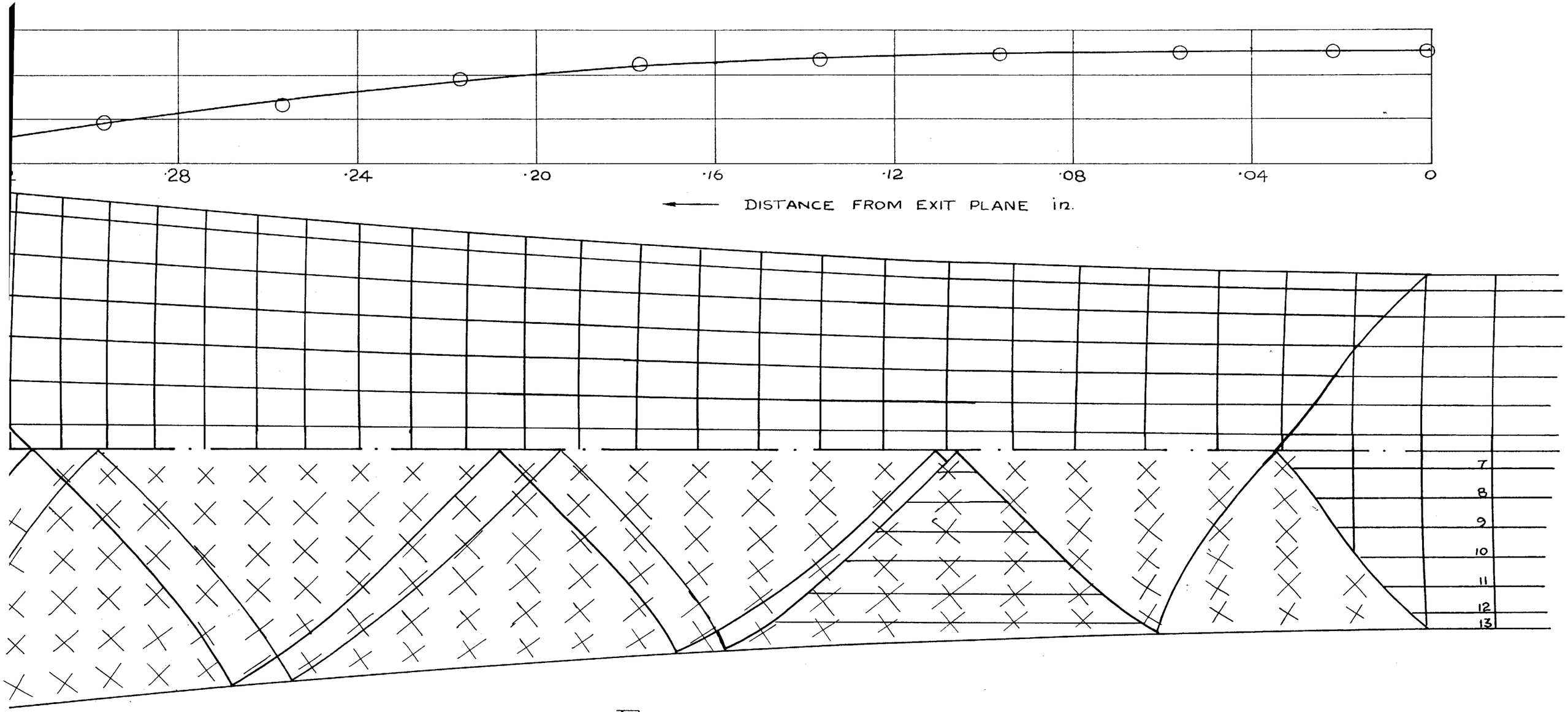


FIG 40 DEFORMED GRID AND SLIP LINE FIELD SPECIMEN A
21·8% RED



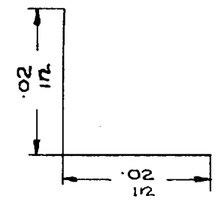


FIG 41 DEFORMED GRID AND SLIP LINE FIELD SPECIMEN B
35·4% RED

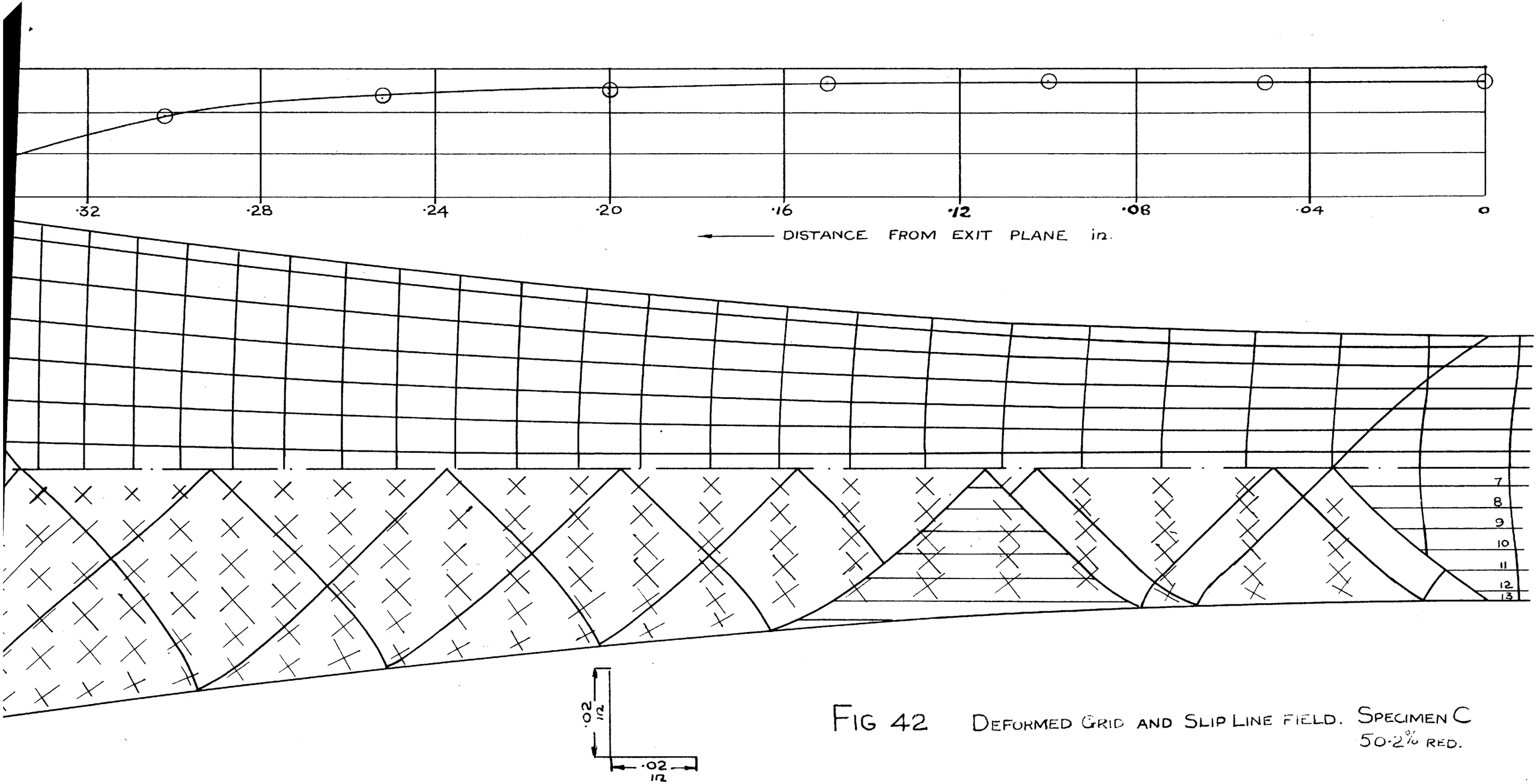


FIG 42 DEFORMED GRID AND SLIP LINE FIELD. SPECIMEN C
50·2% RED.

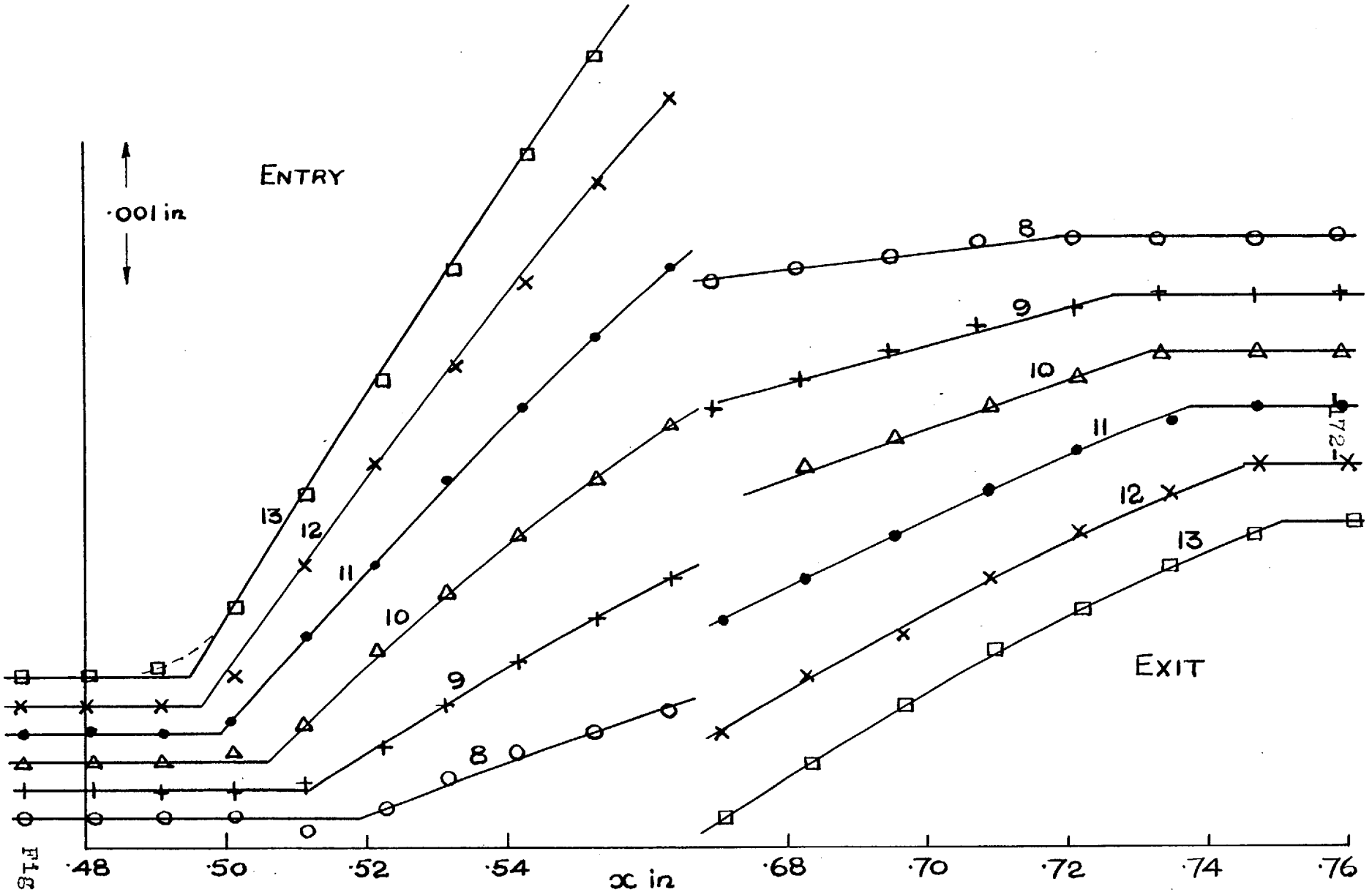


Fig. 43.

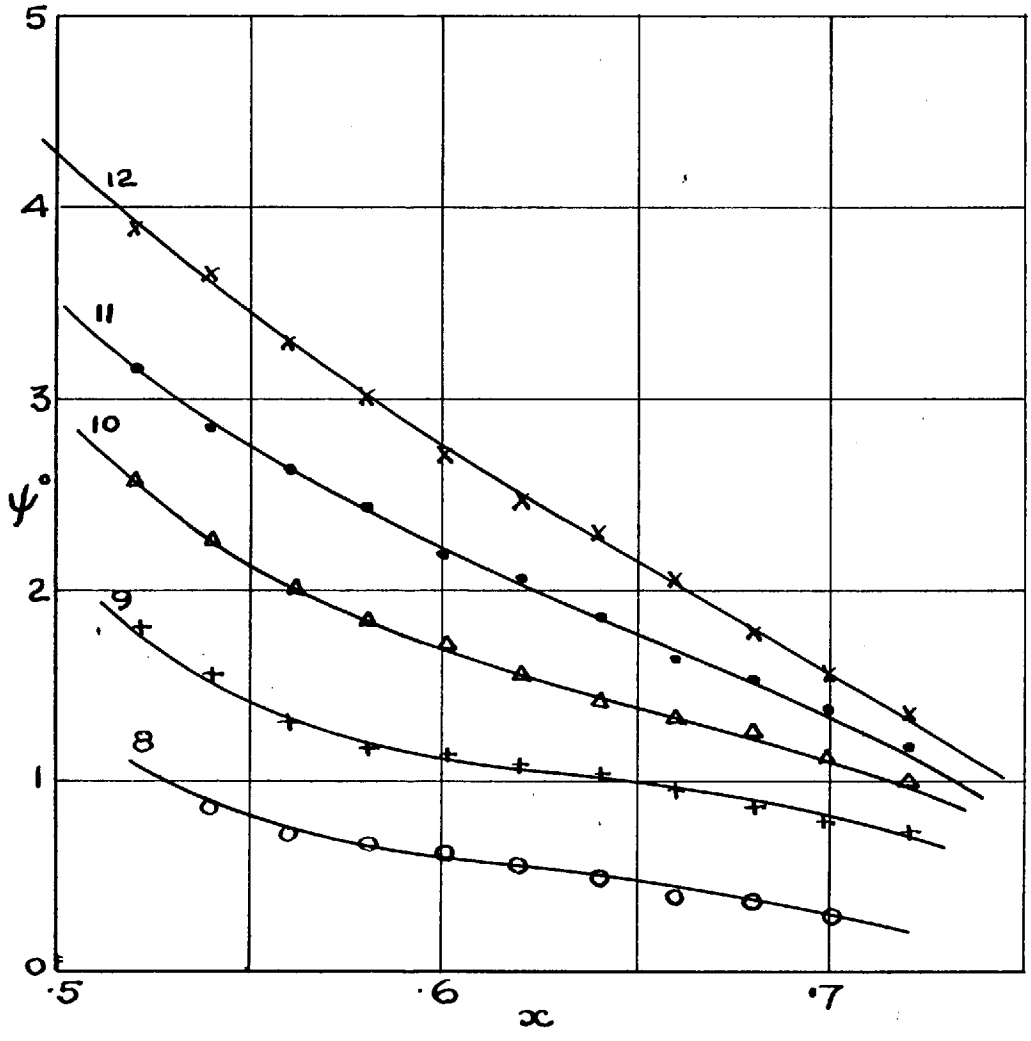


Fig. 44. Specimen A.

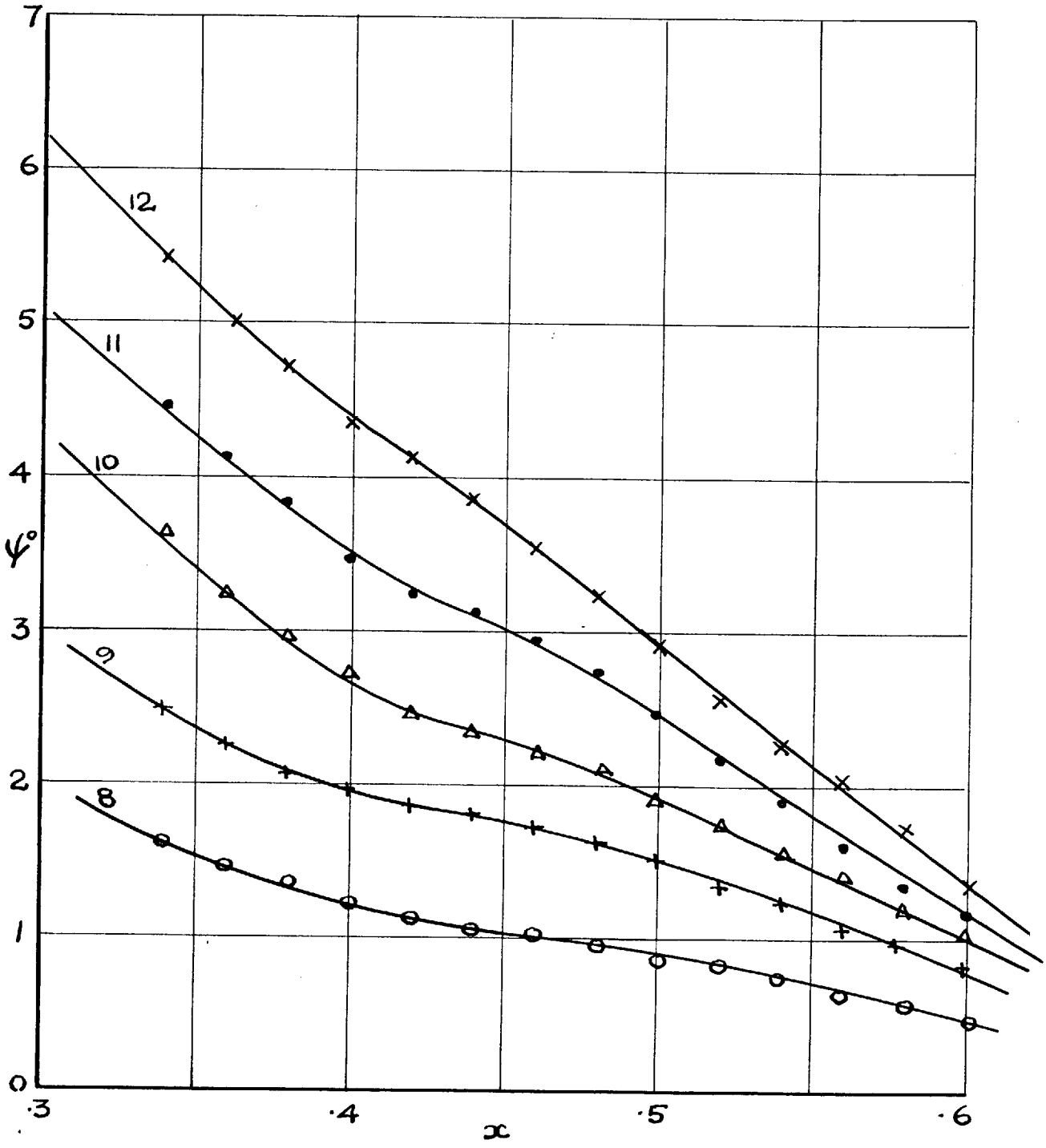


Fig. 45. Specimen B.

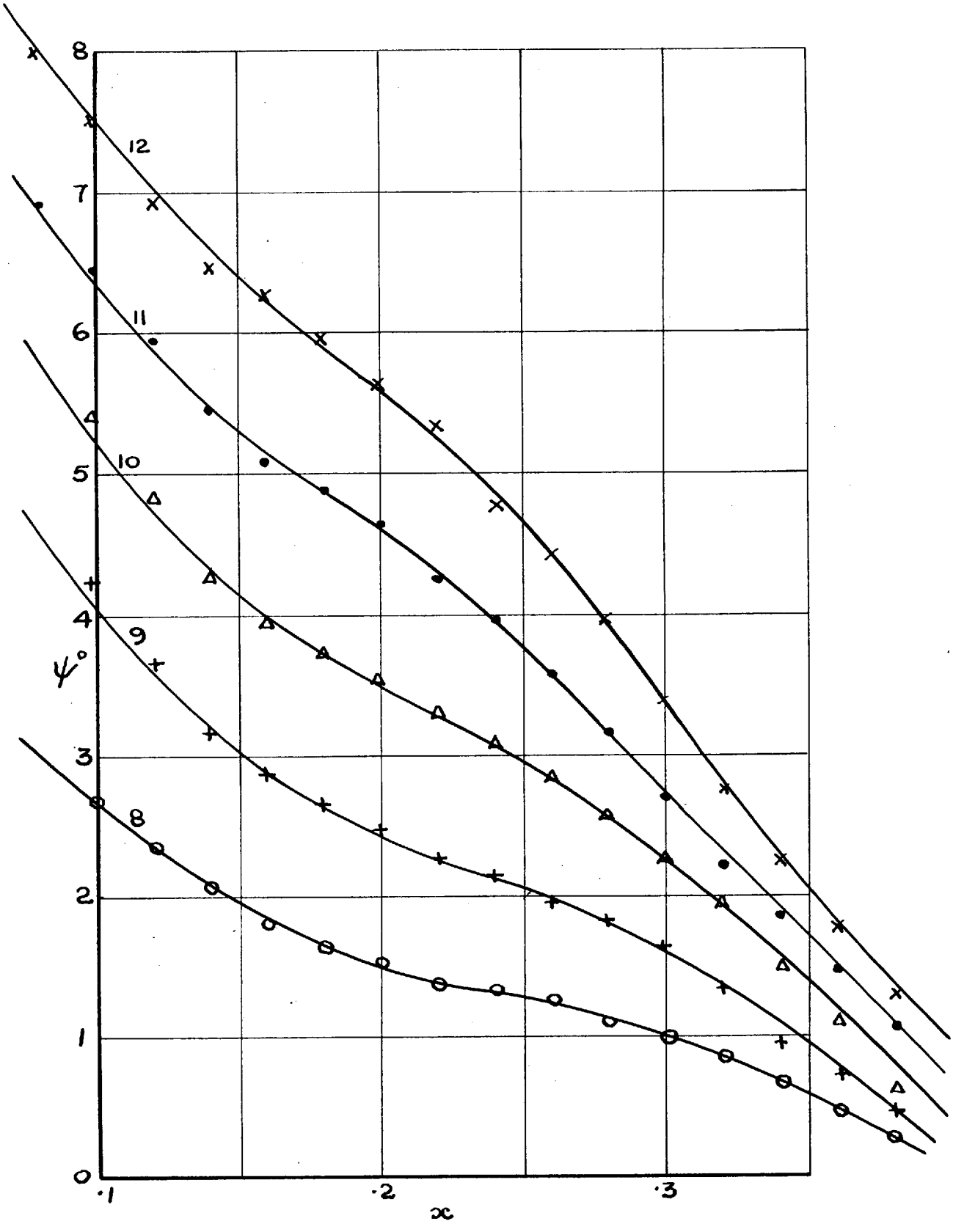


Fig. 46. Specimen C.

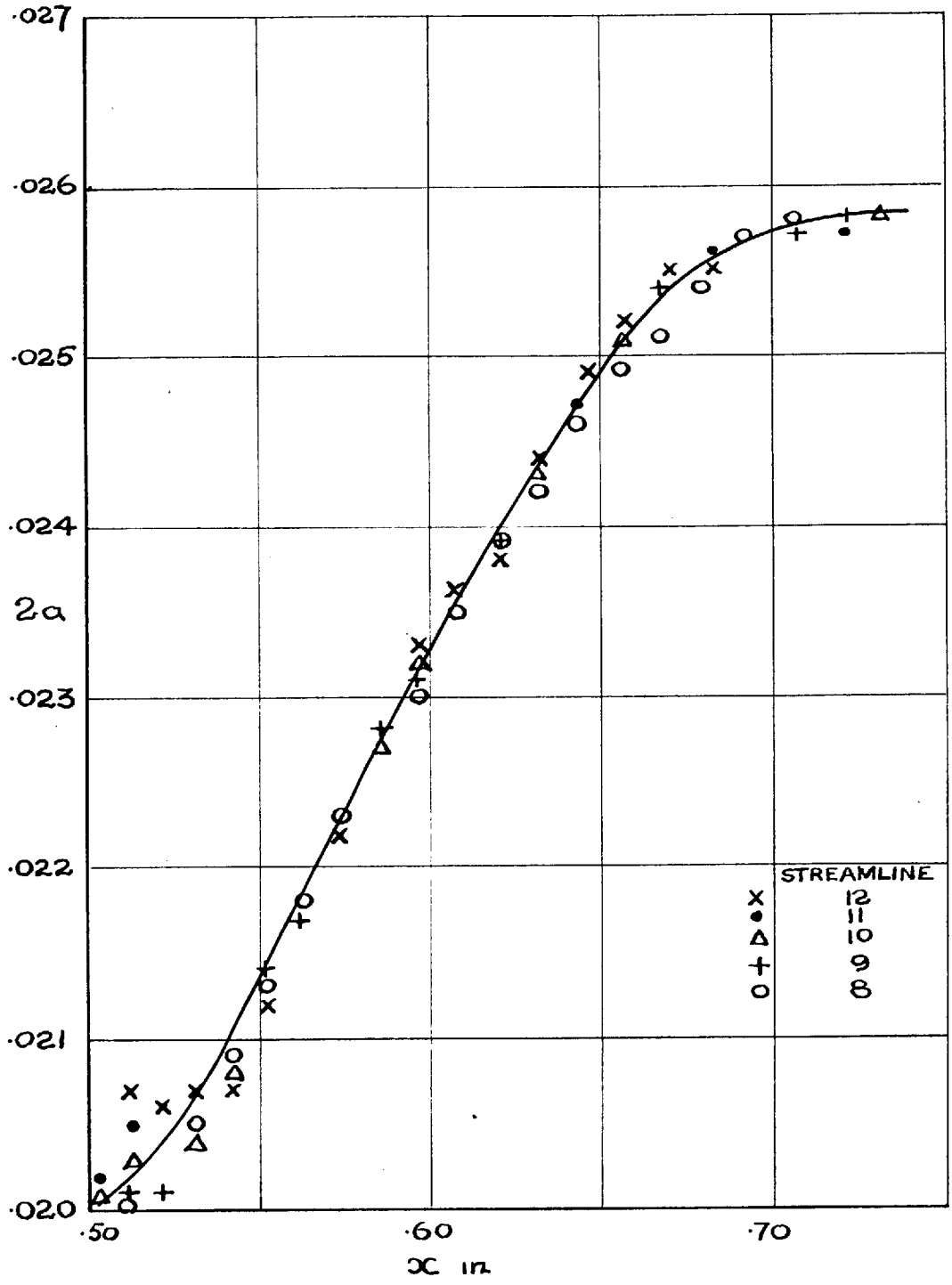


Fig. 47. Specimen A.

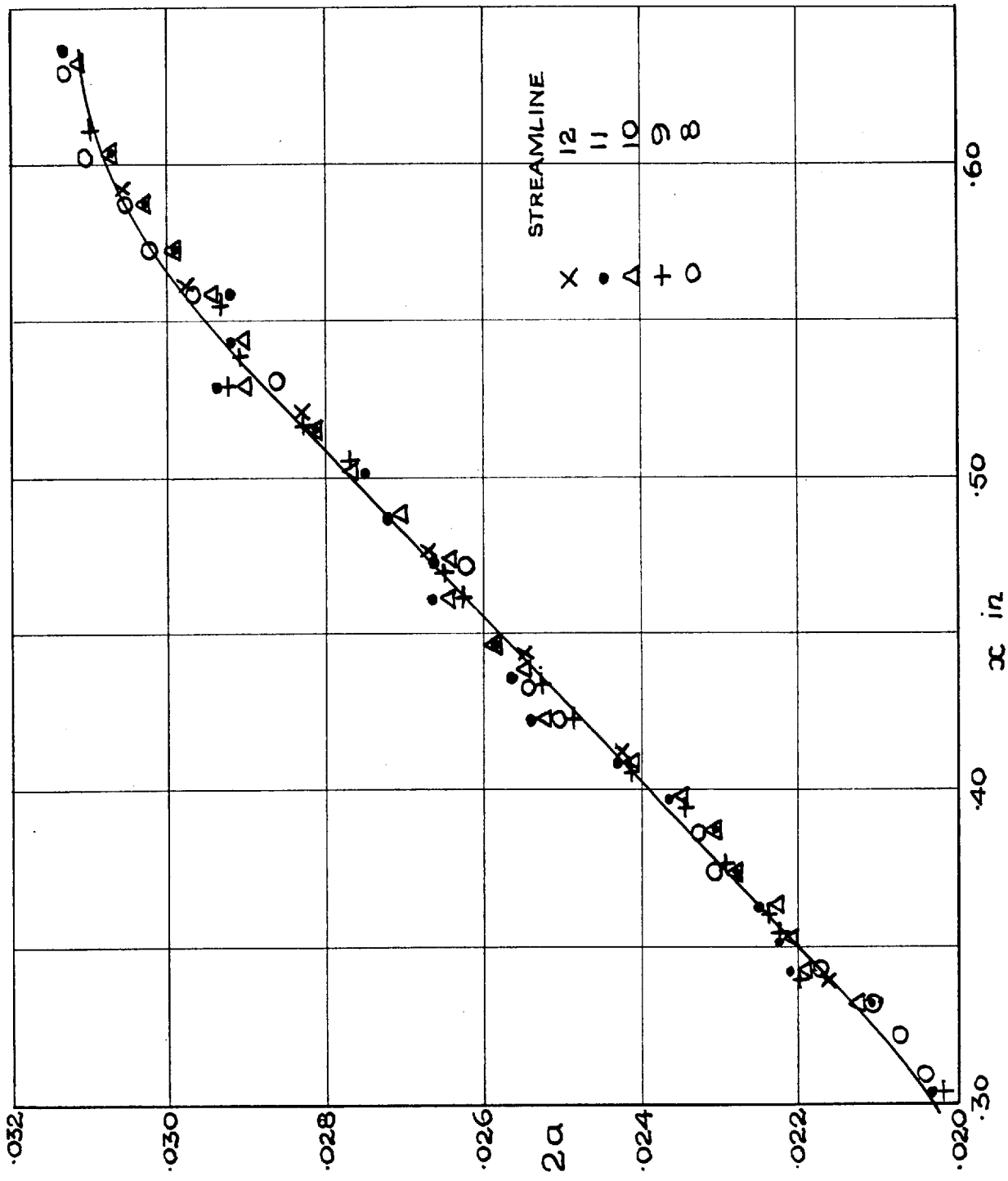


Fig. 48. Specimen B.

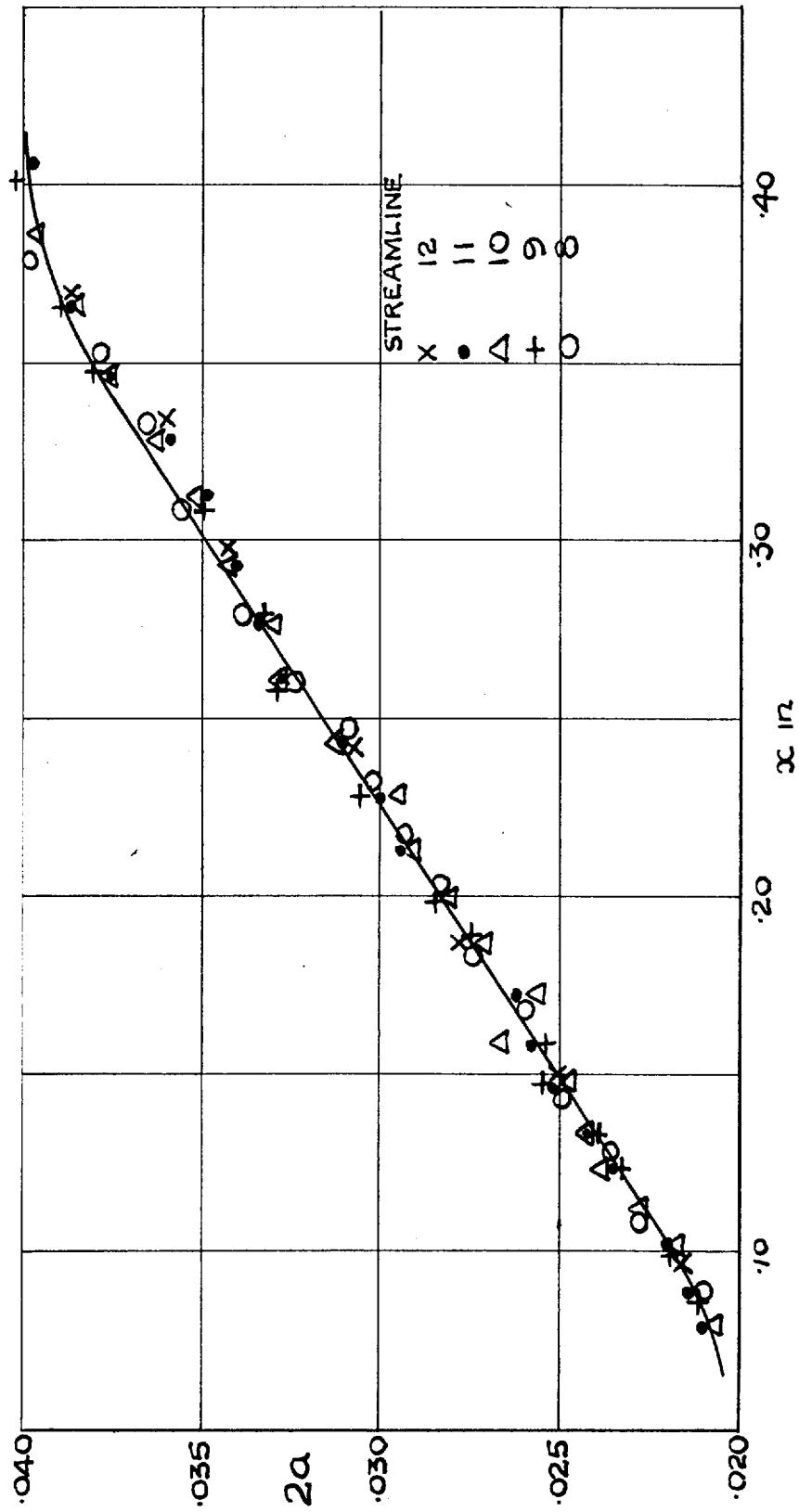


Fig. 49. Specimen C.

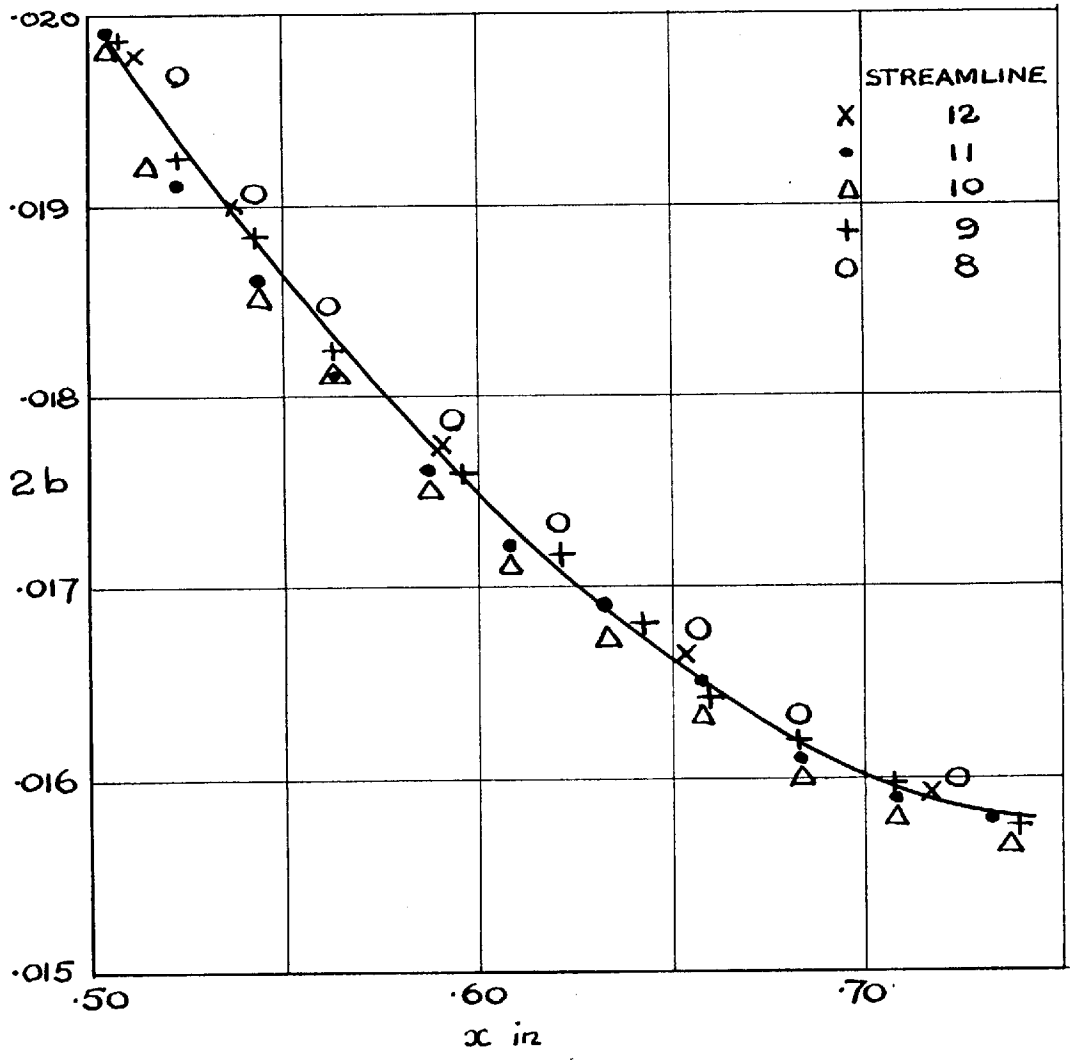


Fig. 50. Specimen A.

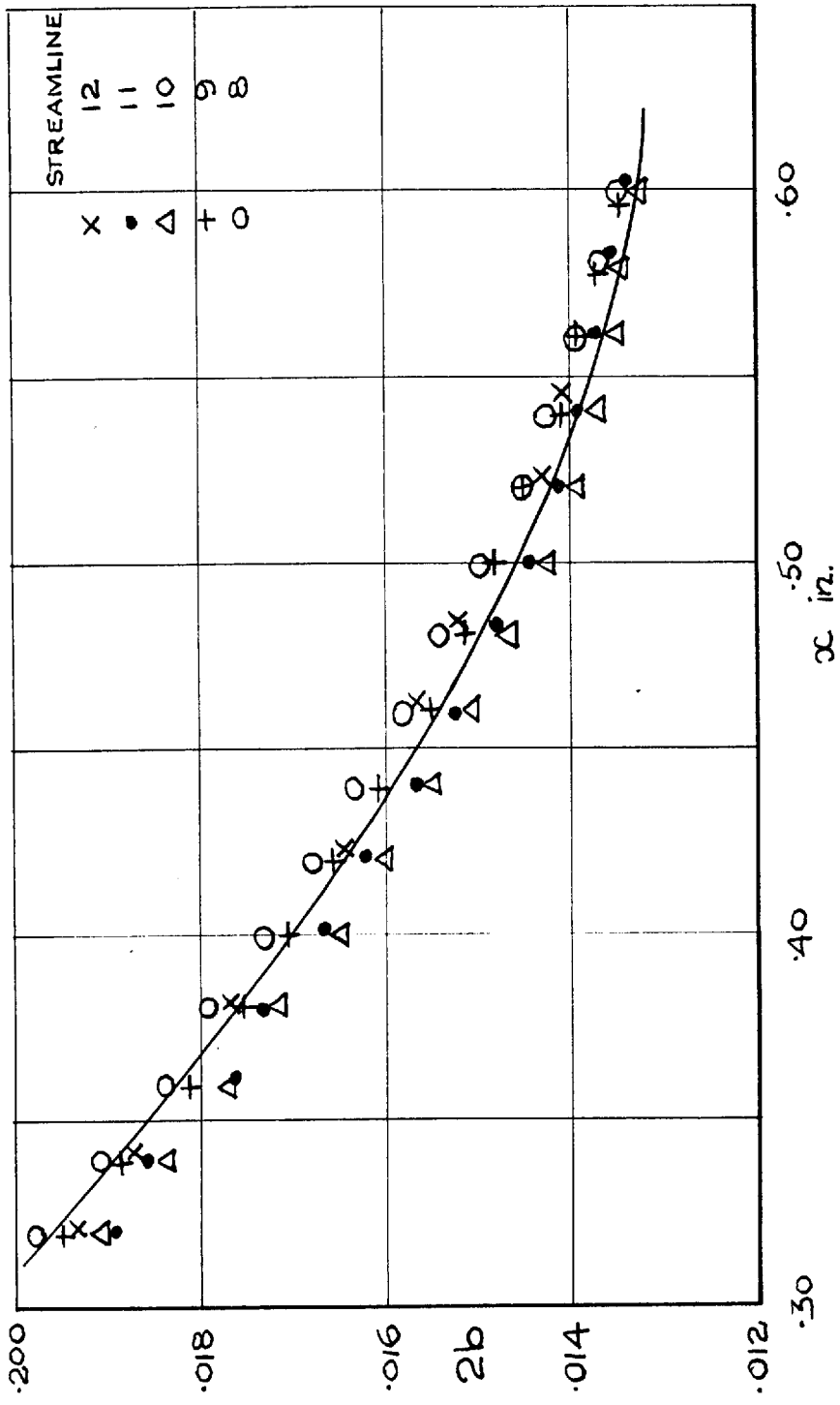


Fig. 51. Specimen B.

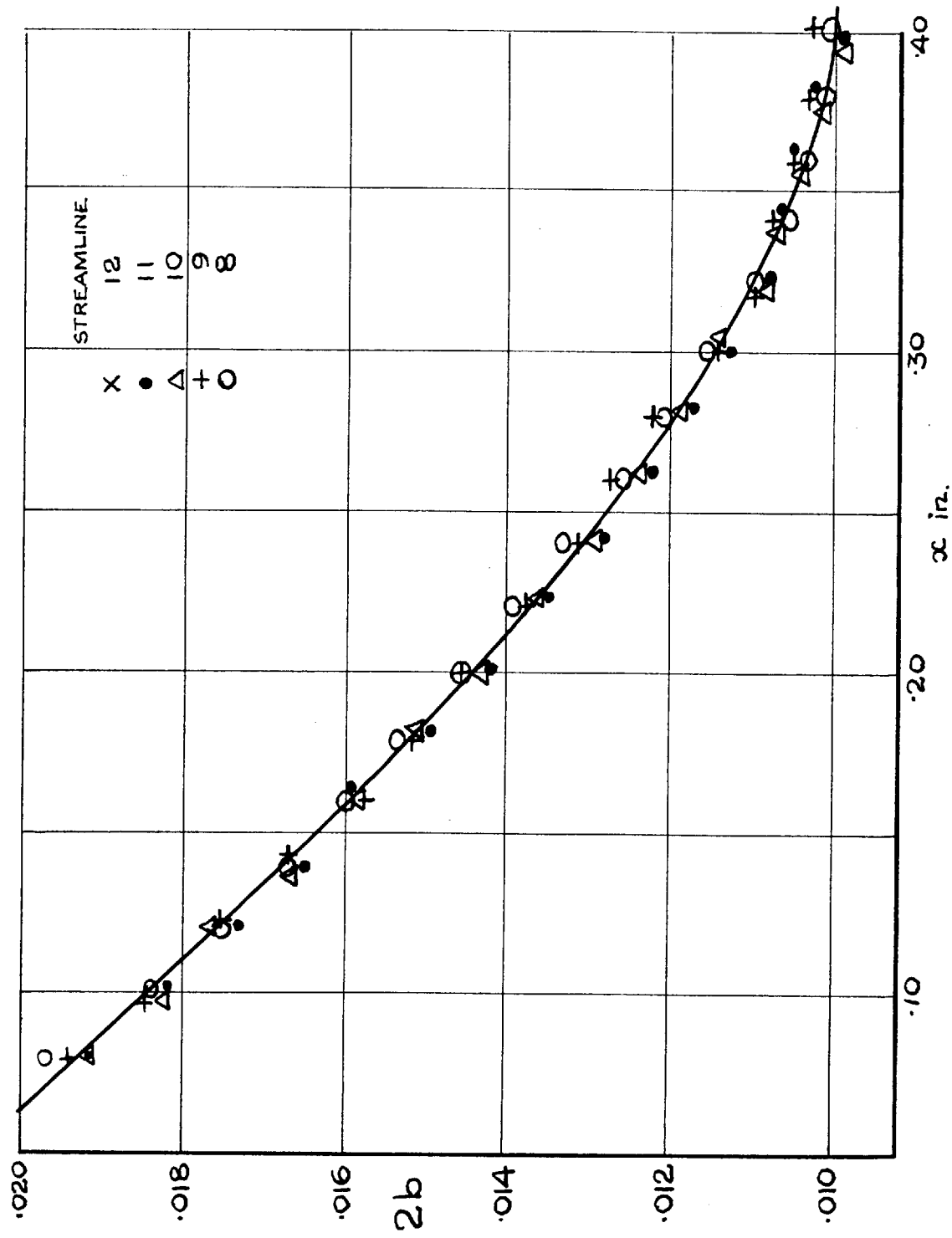


Fig. 52. Specimen C.

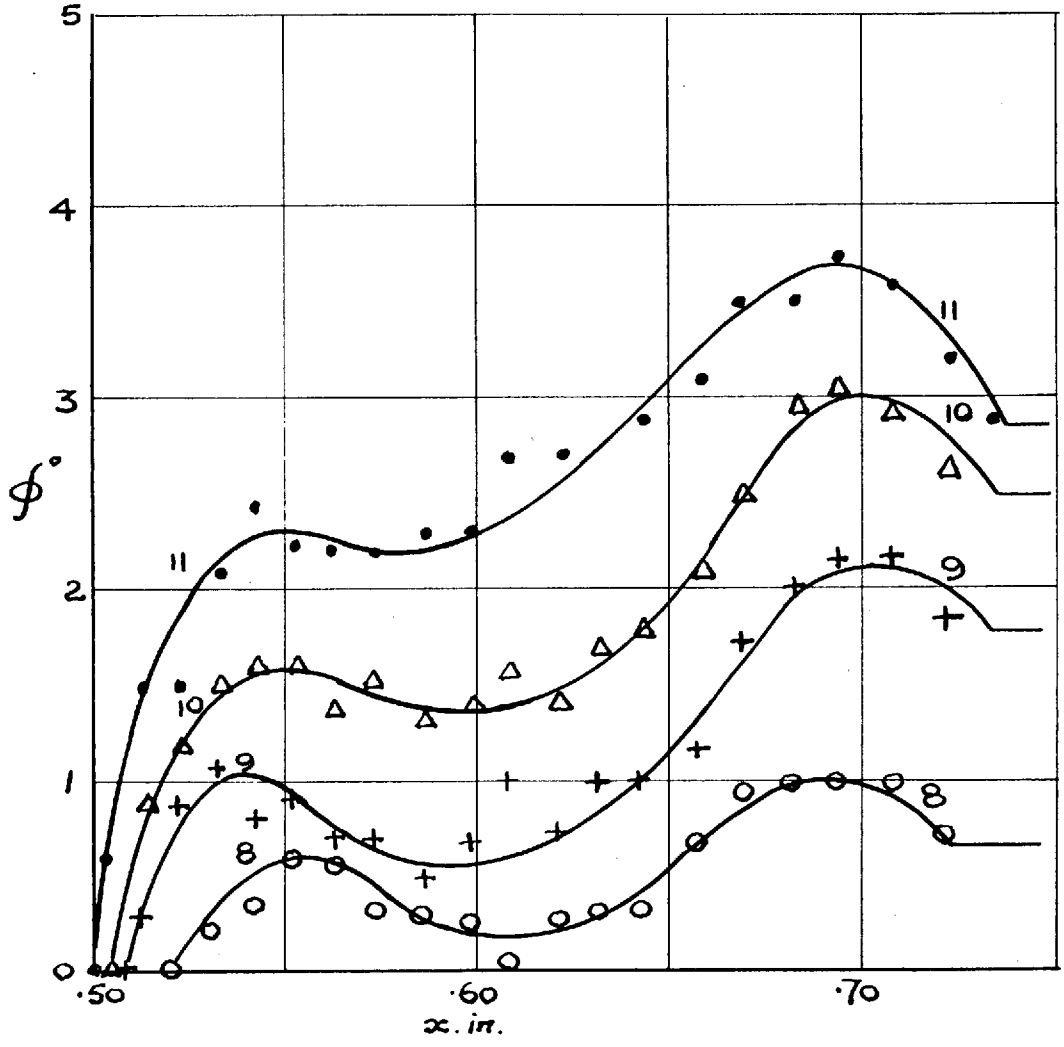


Fig. 53. Specimen A.

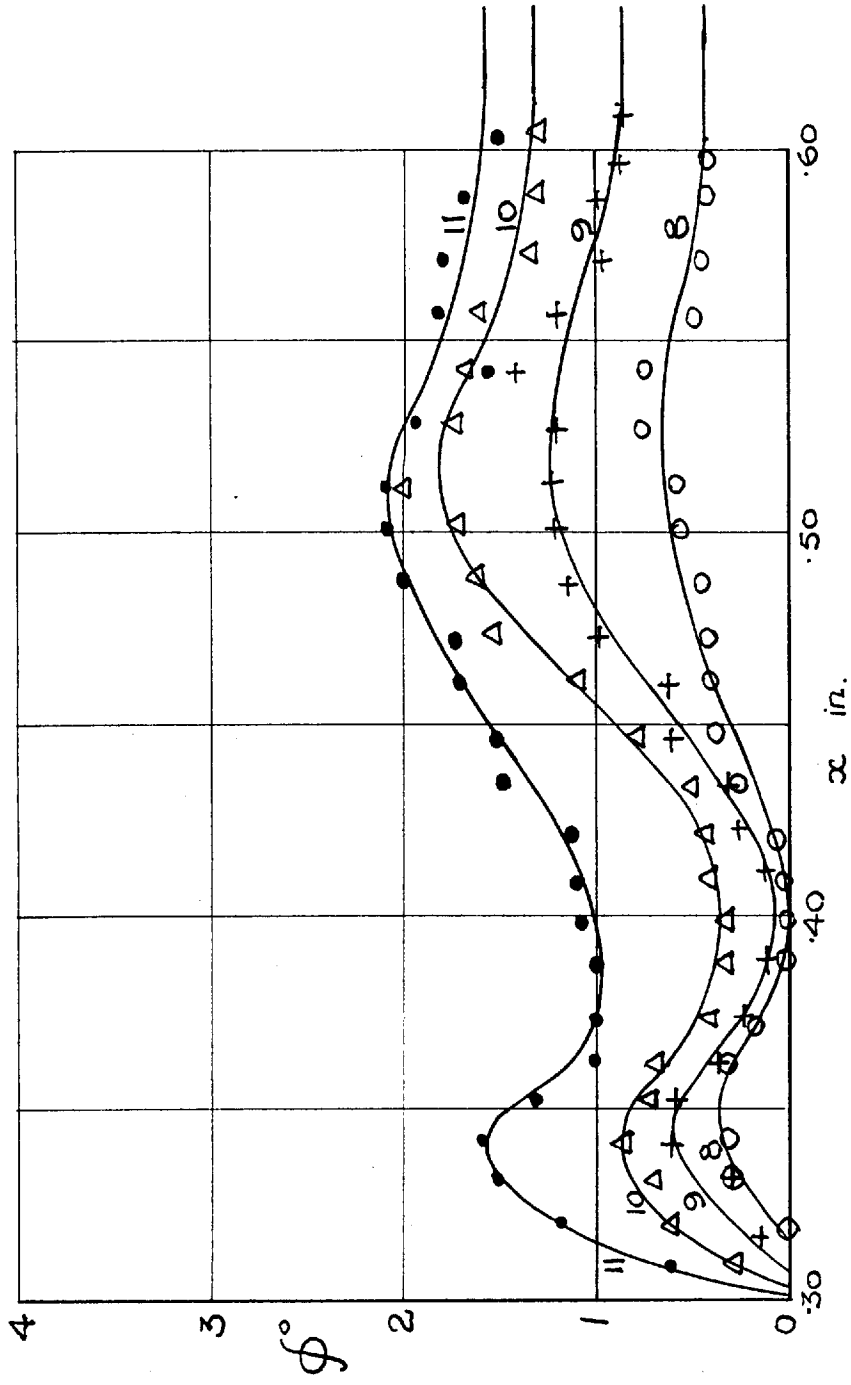


Fig. 54. Specimen B.

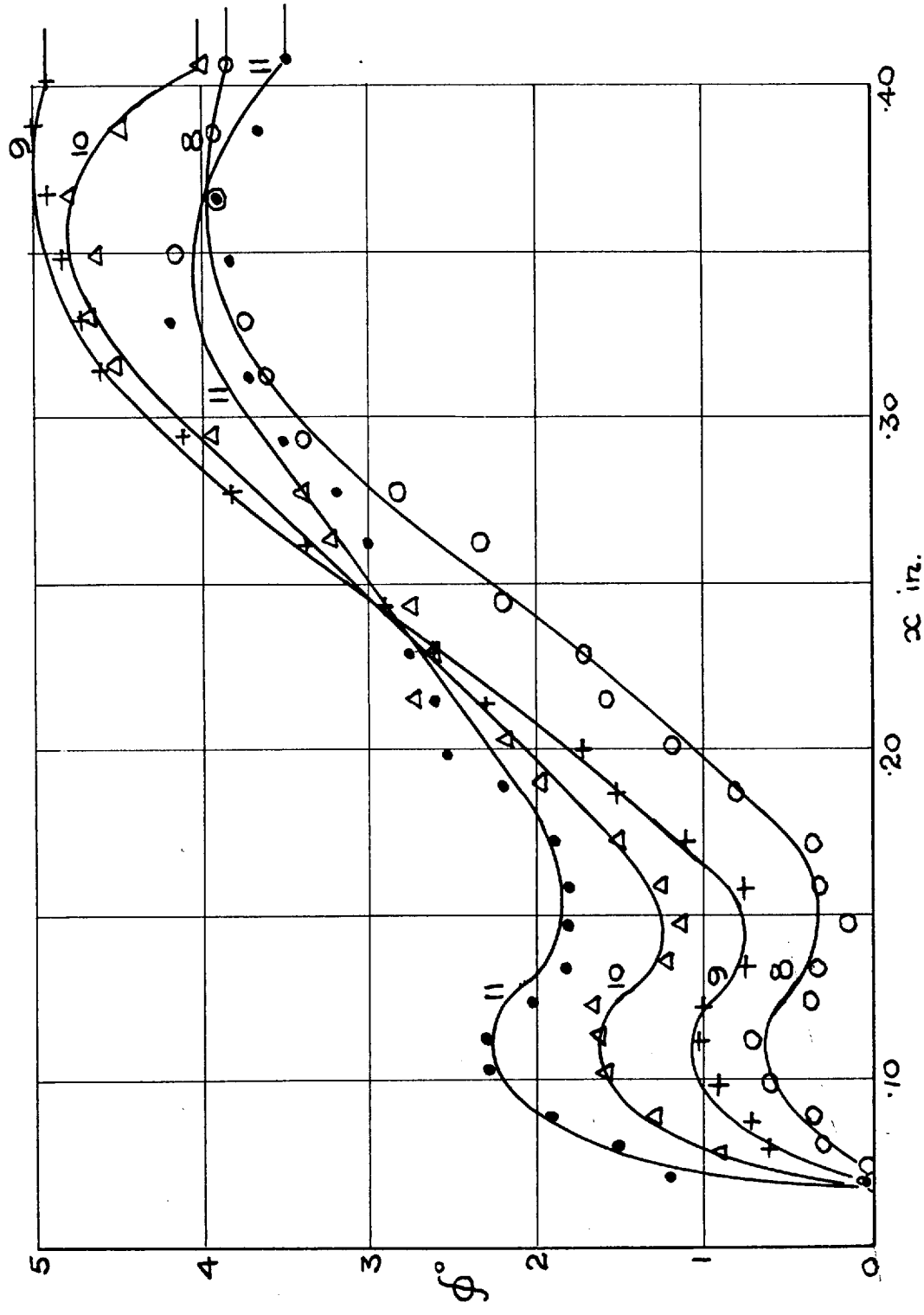
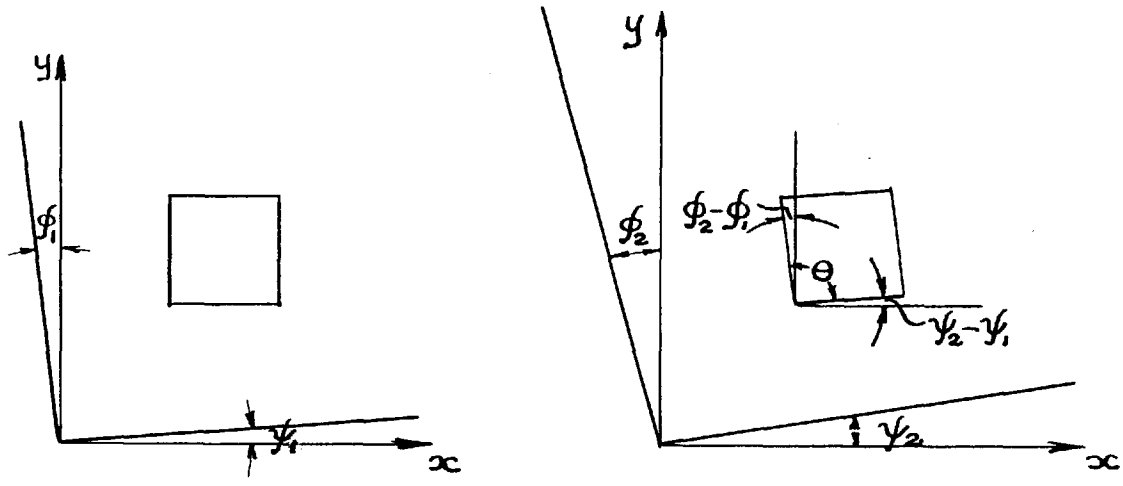


Fig. 55. Specimen C.



1st CONFIGURATION

2nd CONFIGURATION

ANGLES POSITIVE CLOCKWISE

$$\theta = 90+(\phi_2-\phi_1)-(\psi_2-\psi_1)$$

IF $\theta > 90°$ $\quad \alpha_1 = -\{\alpha-(\psi_2-\psi_1)\}$

IF $\theta < 90°$ $\quad \alpha_1 = \alpha+(\psi_2-\psi_1)$

MAXIMUM SHEAR DIRECTIONS

ARE $\alpha_1 \pm \frac{\pi}{4}$

Fig. 56. Sign Convention for Angular Measurements.

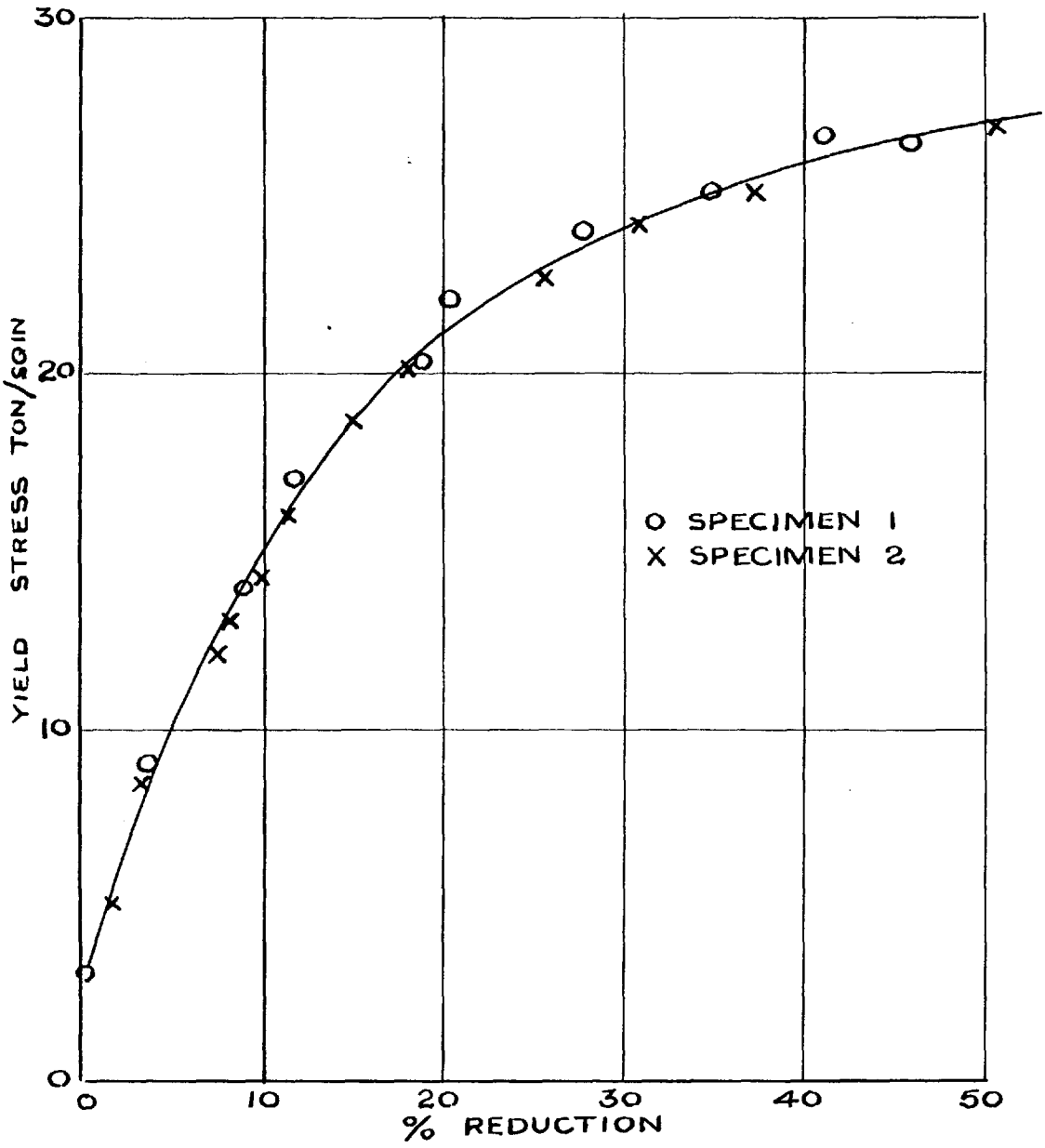


Fig. 57. Yield Stress v% reduction curve.

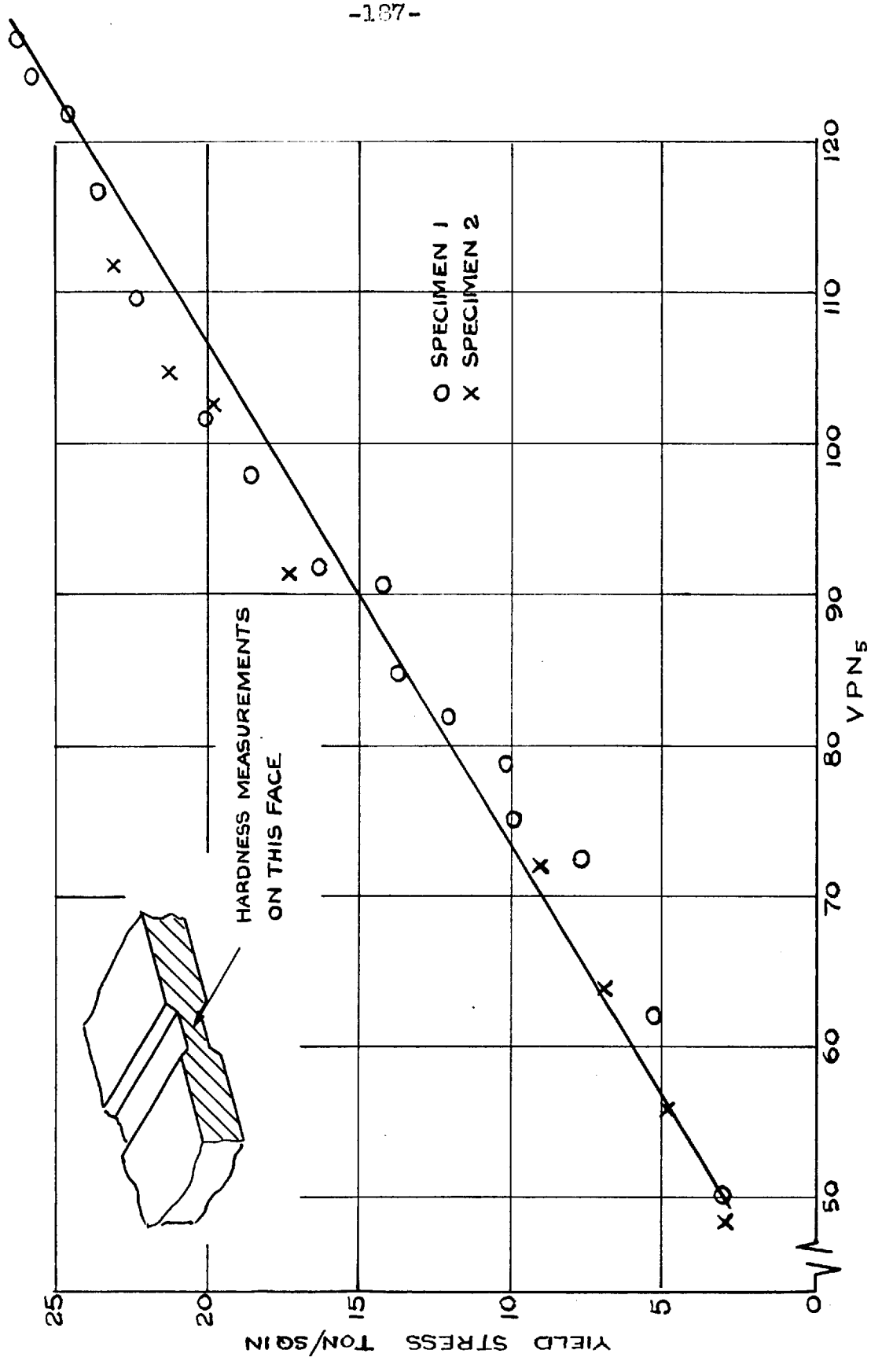


Fig. 58. Yield Stress v Hardness Curve.

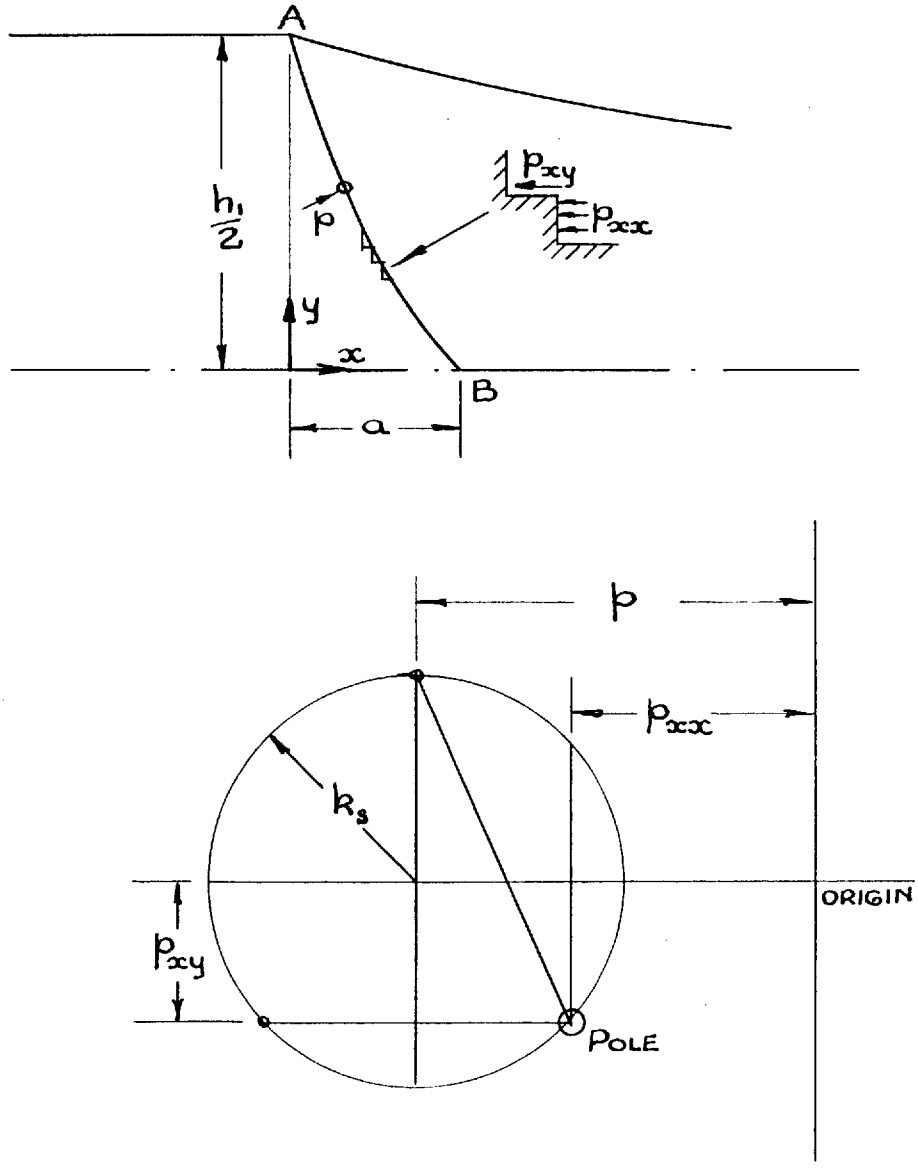


Fig. 59. Determination of Stress along Entry Slip line.

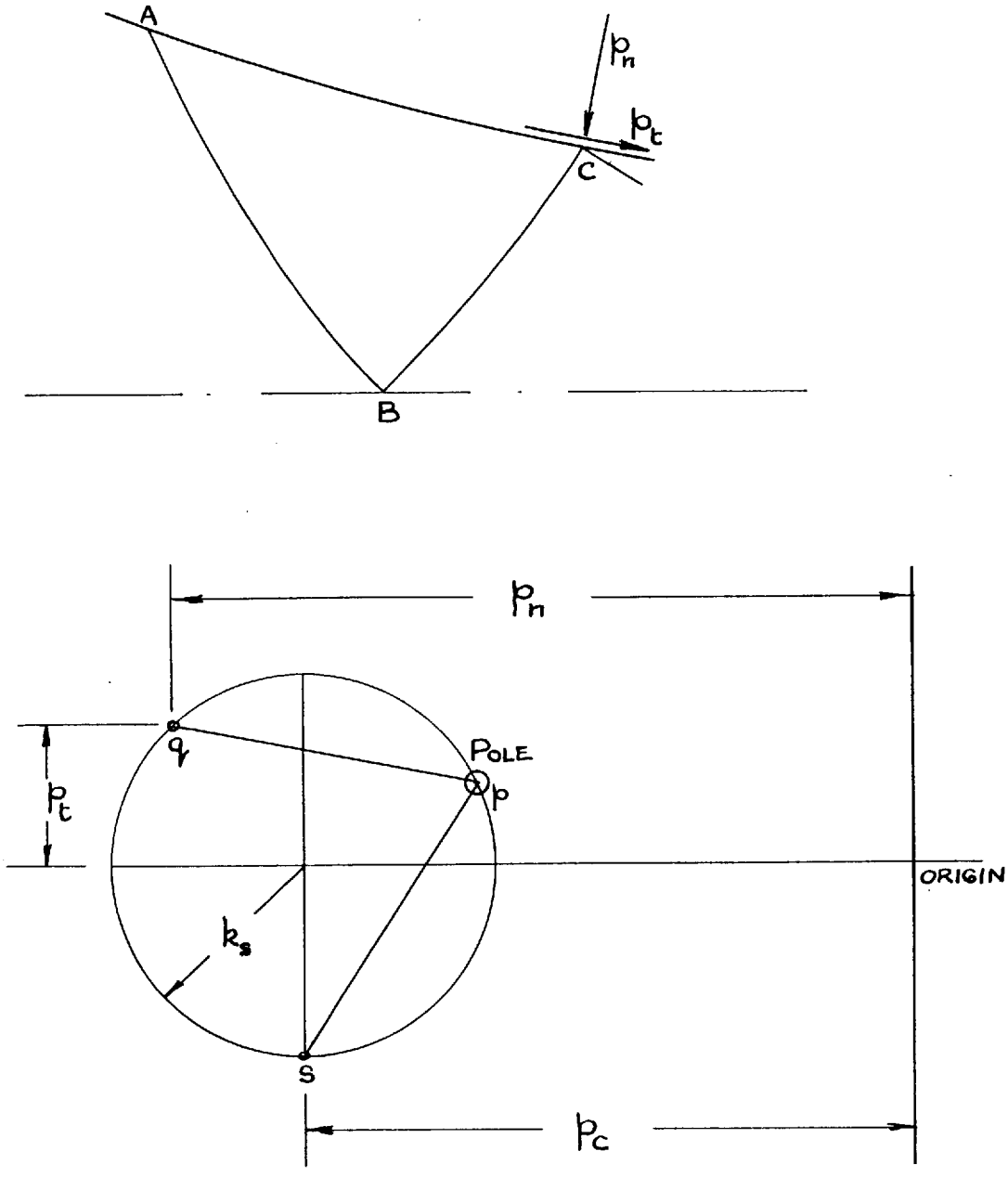


Fig. 60. Calculation of Coefficient of Friction.

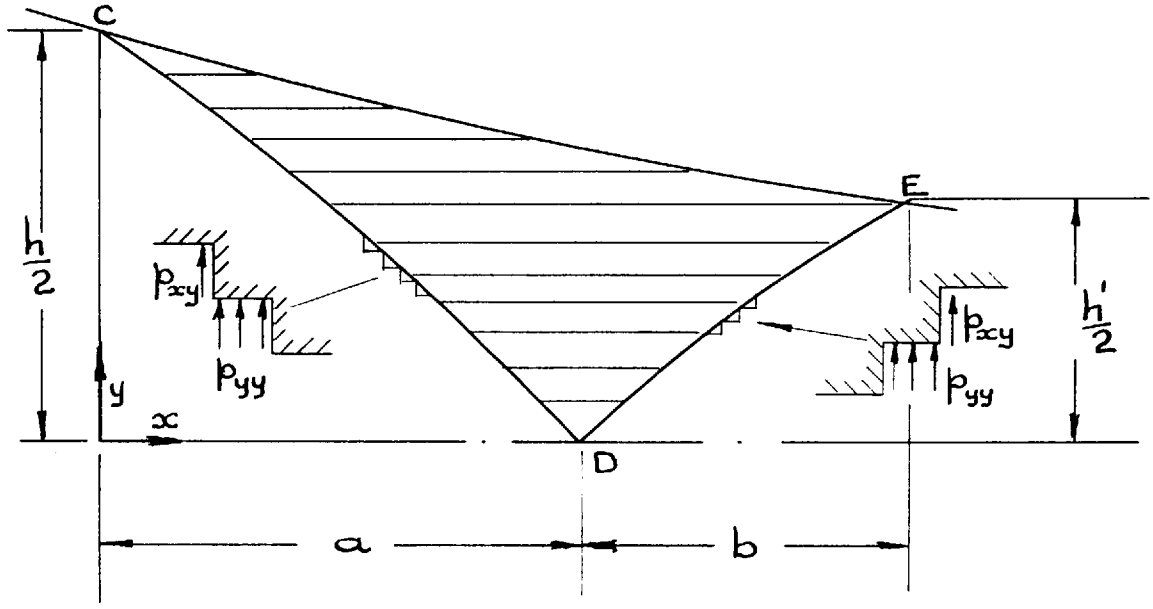


Fig. 61. Stress Conditions in Region of Neutral Zone.

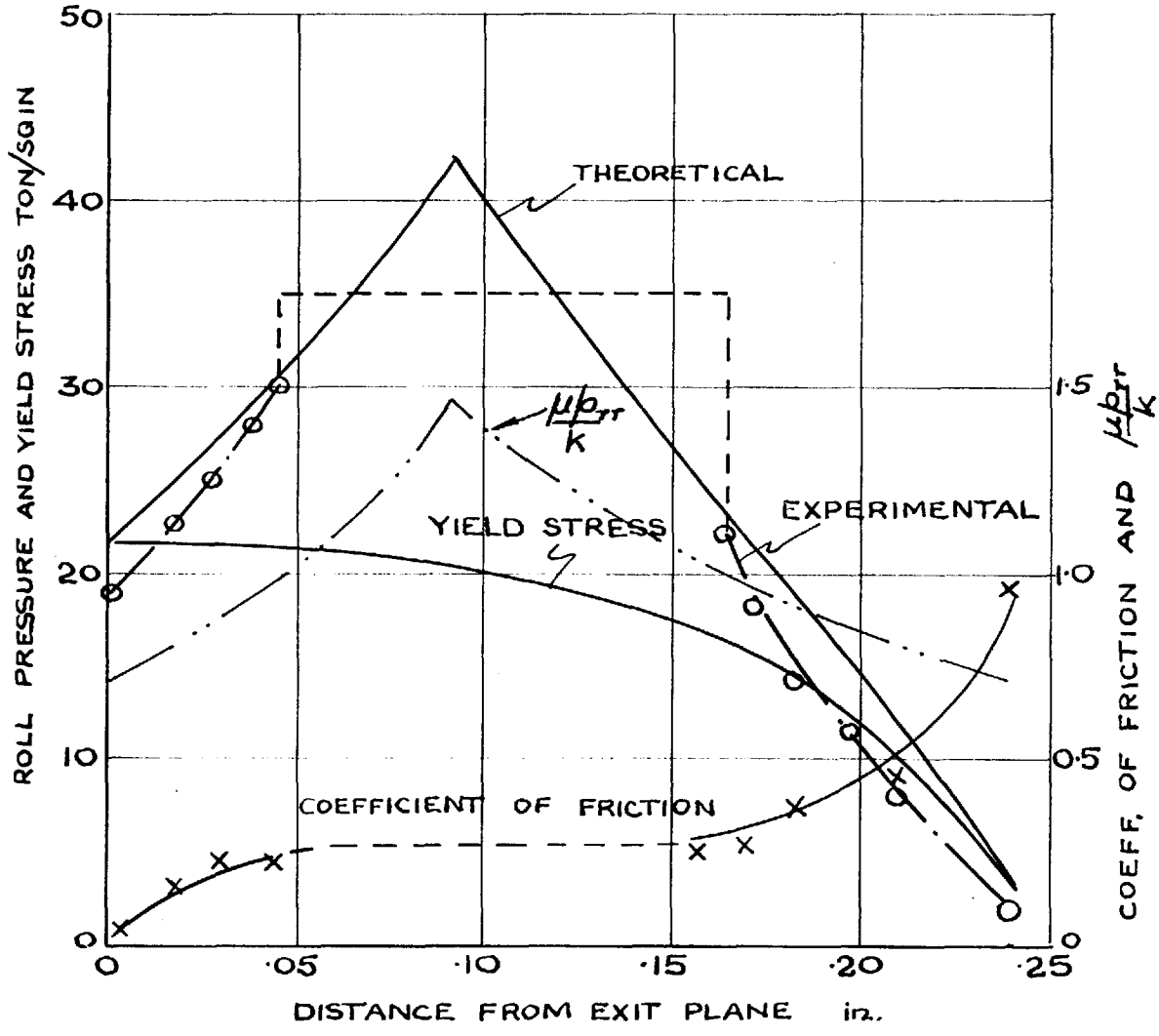


Fig. 62. Roll Pressure Distribution.
Specimen A.

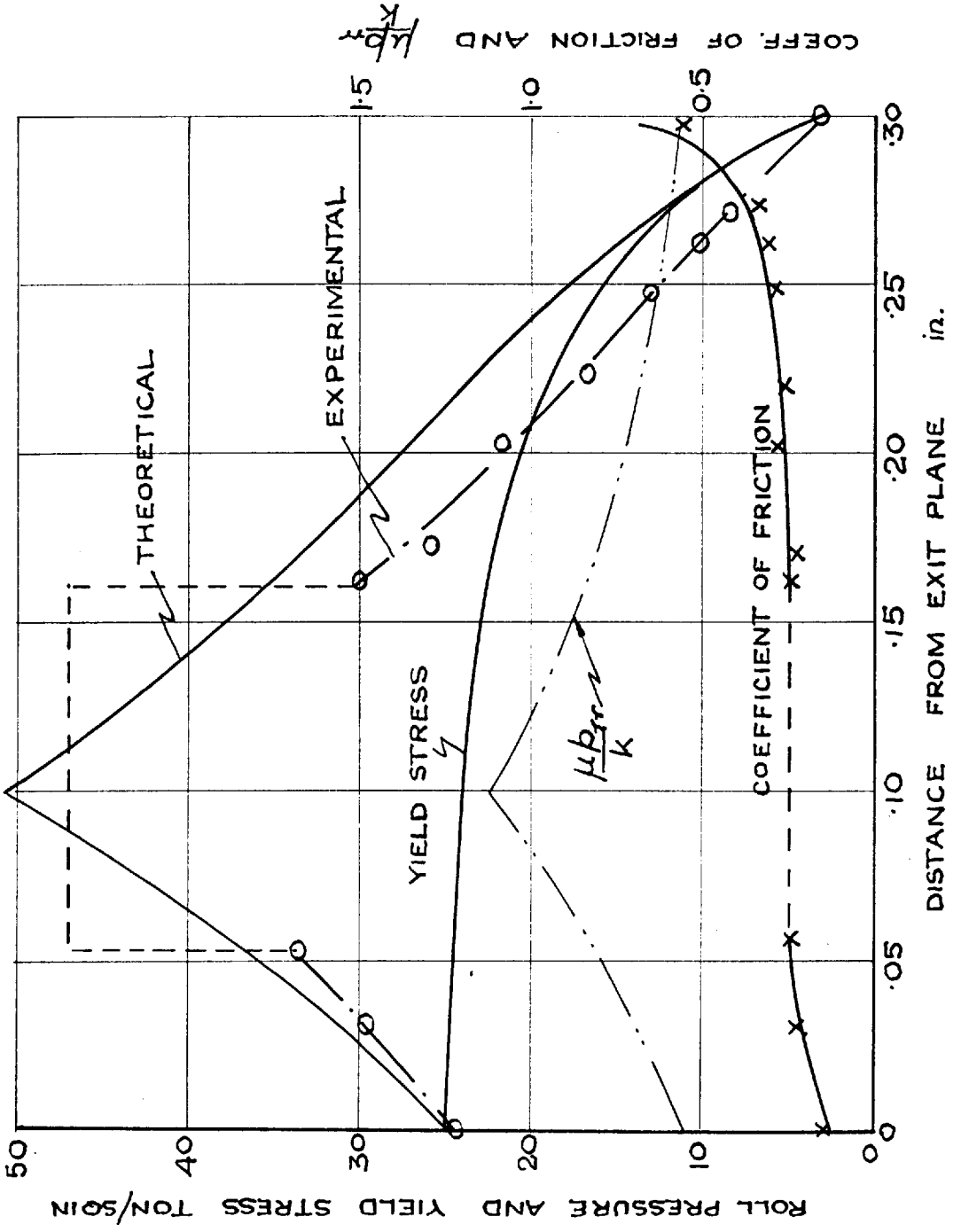


Fig. 63. Roll Pressure Distribution.
Specimen B.

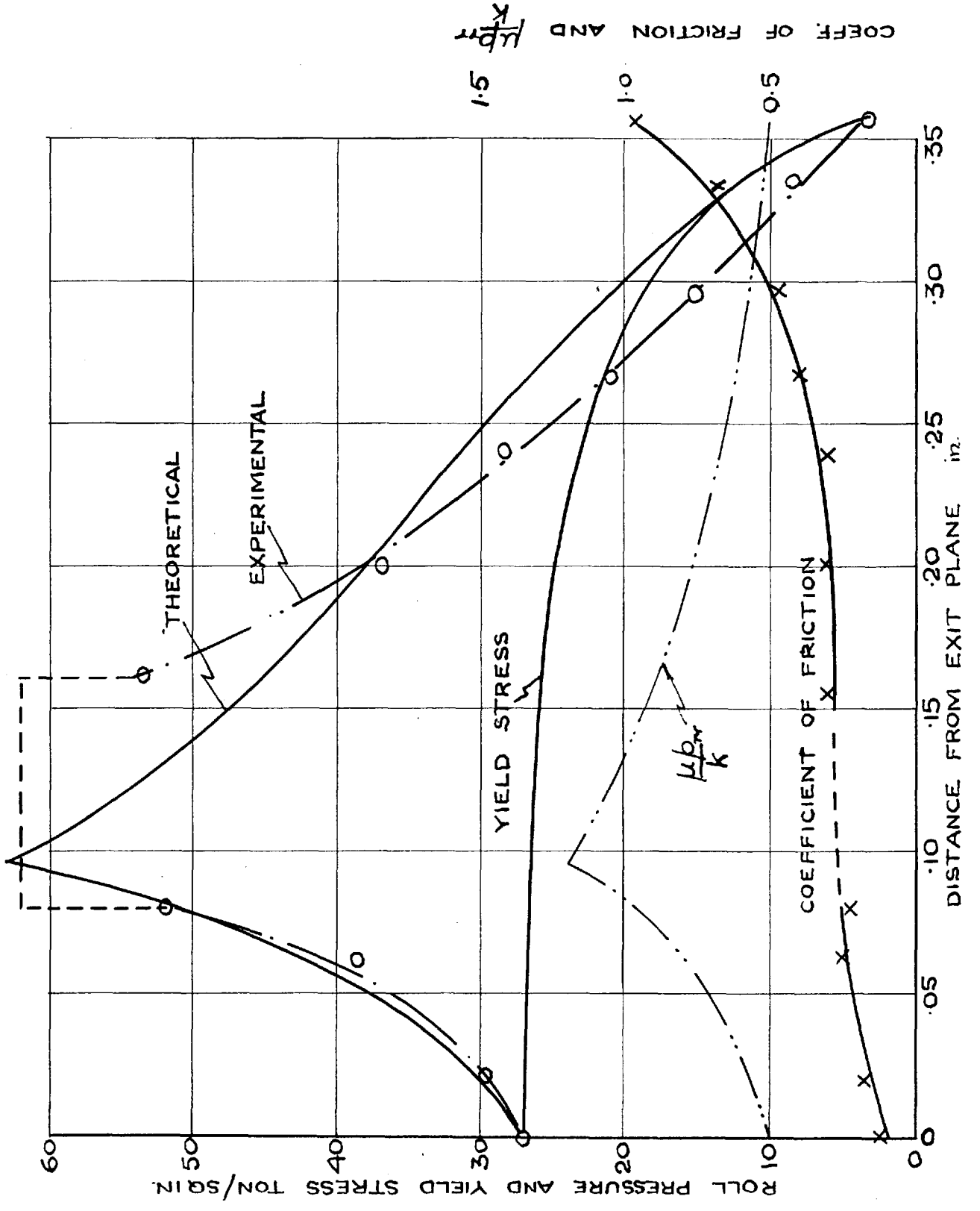


Fig. 64. Roll Pressure Distribution.
Specimen C.

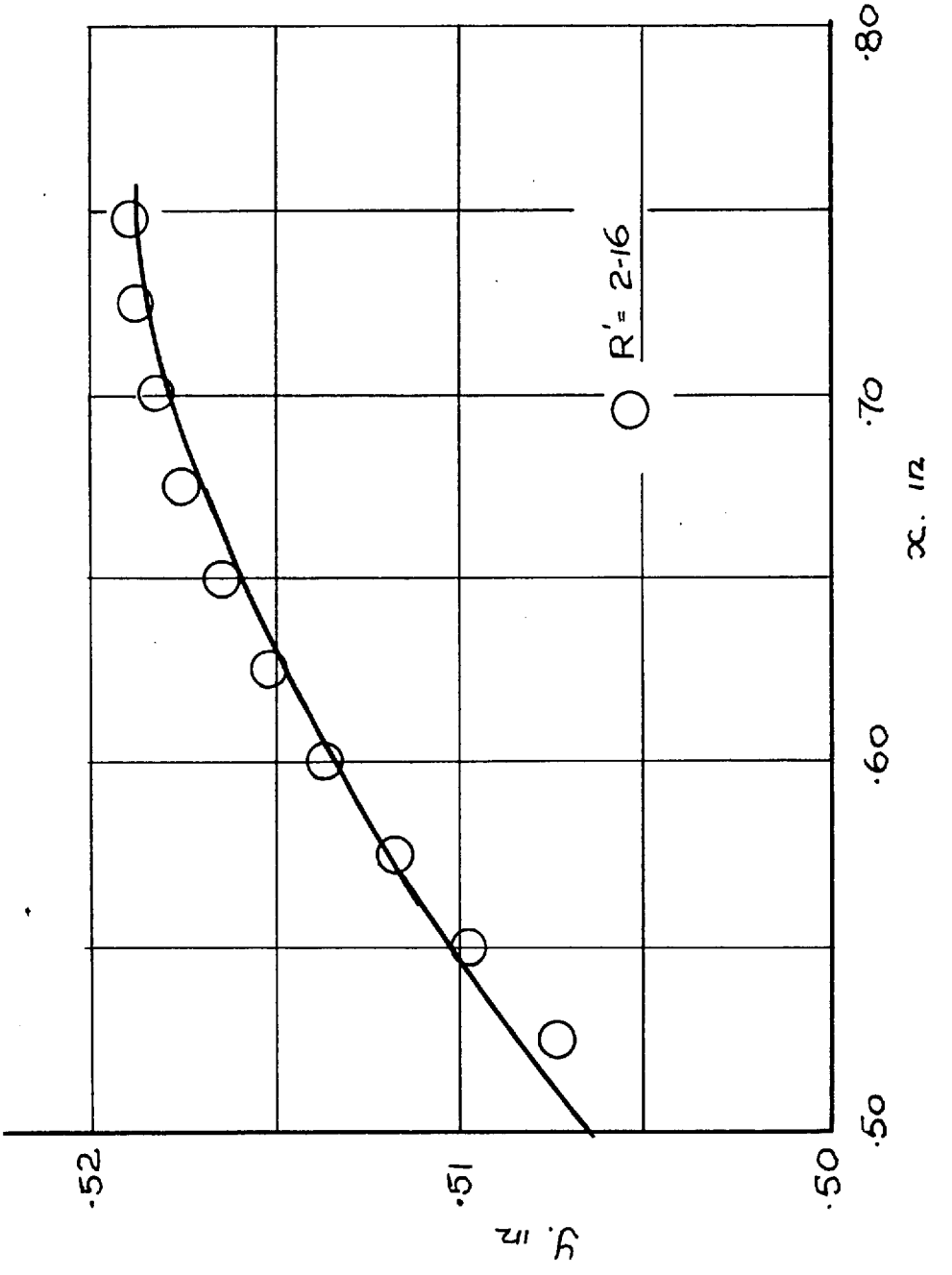


Fig. 65. Deformed Roll Profile.
Specimen A.

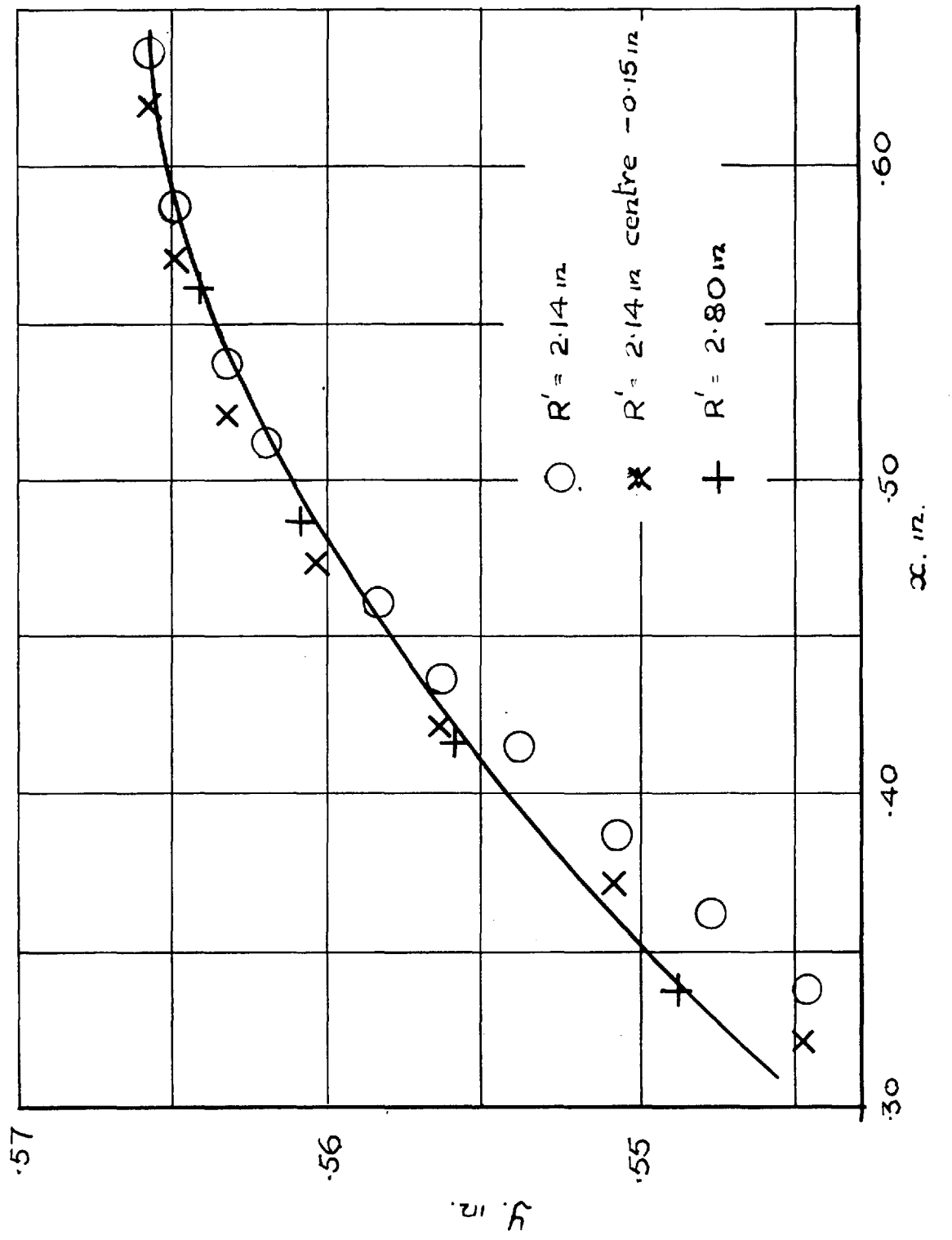


Fig. 66. Deformed Roll Profile.
Specimen B.

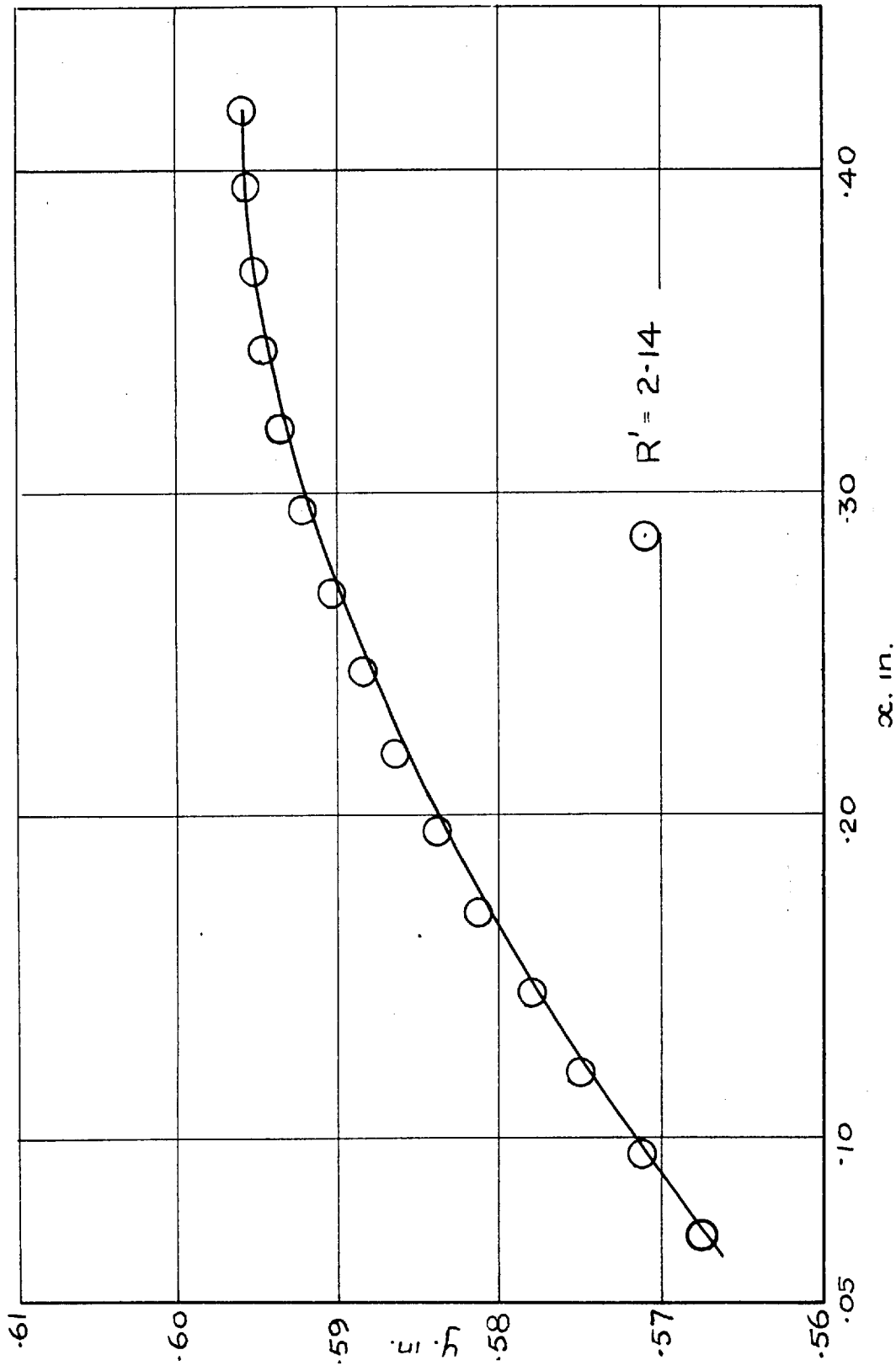


Fig. 67. Deformed Roll Profile.
Specimen C.

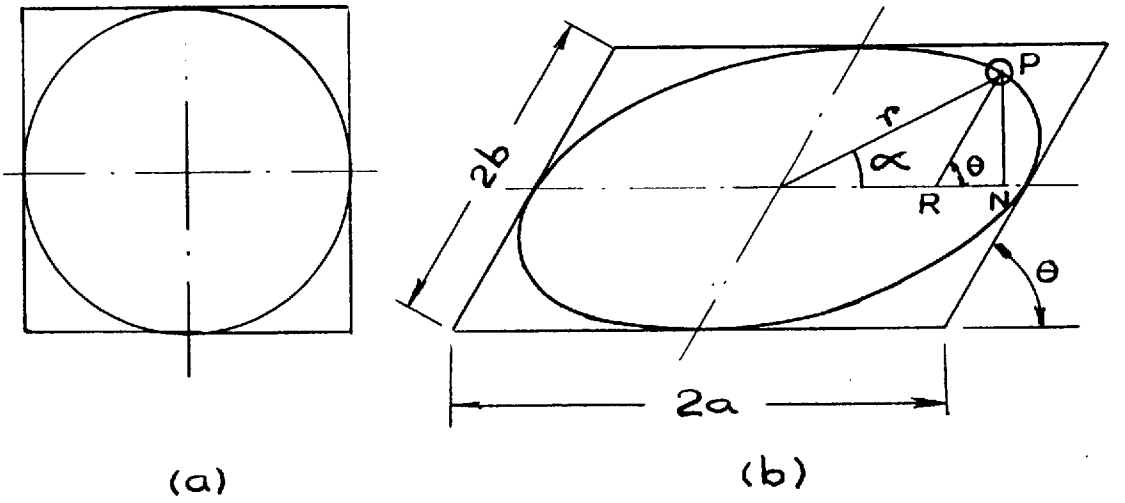
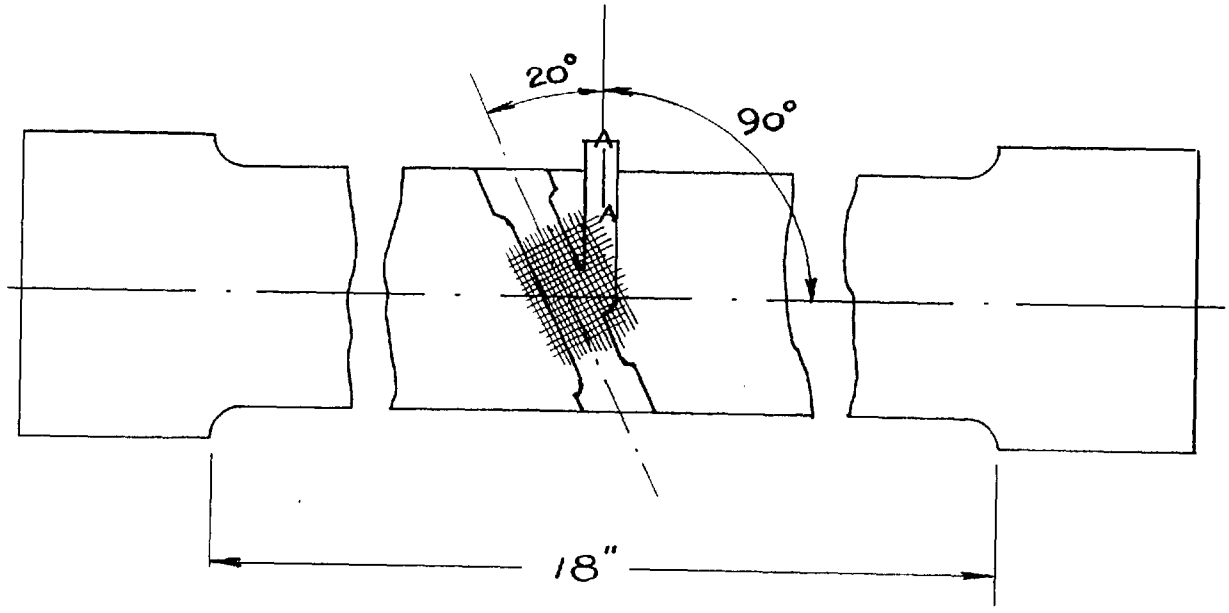


Fig. 68. Figure for Derivation of Strain Formulae App I.



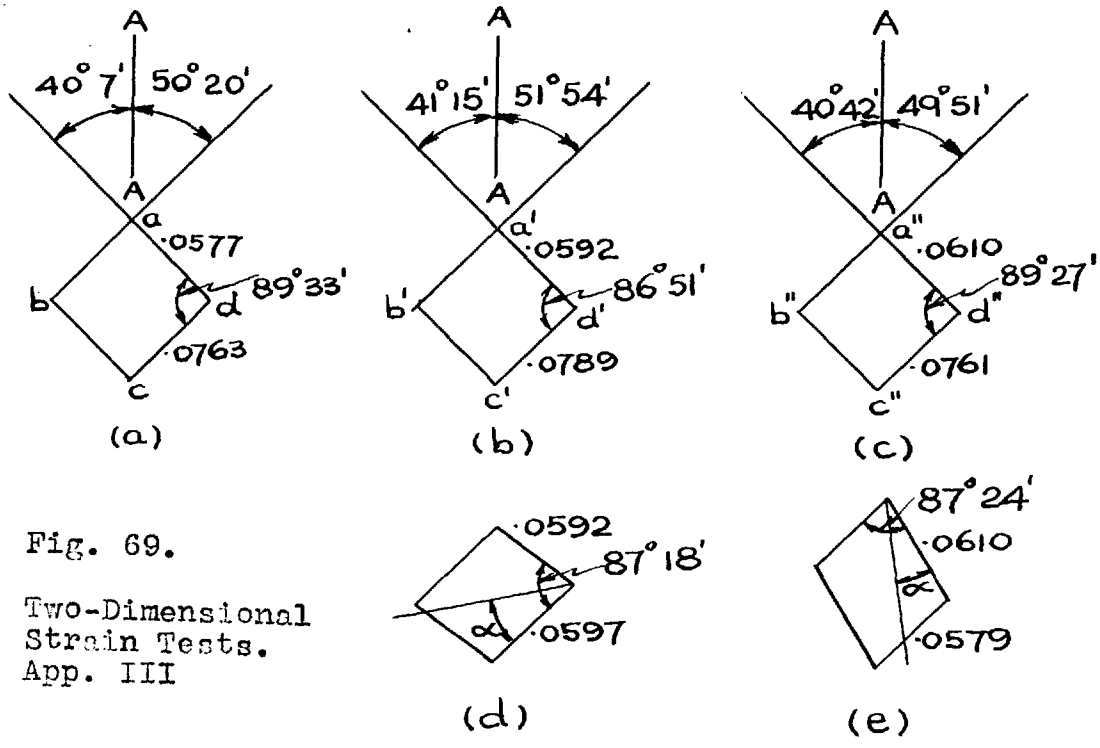


Fig. 69.

Two-Dimensional Strain Tests. App. III

TABLE II(a)

			$(a'/b')^2$					
			1.2		1.4		1.6	
θ	Sin2θ	Cos2θ	tan2α	α	tan2α	α	tan2α	α
90	0	-1.0000	0	0	0	0	0	0
89	.0349	-.9994	.174	5.0	.0873	2.5	.0582	1.7
88	.0698	-.9976	.345	9.5	.174	5.0	.116	3.3
87	.1045	-.9945	.509	13.5	.257	7.2	.173	4.9
86	.1392	-.9903	.666	16.9	.341	9.4	.229	6.5
85	.1737	-.9848	.808	19.5	.417	11.3	.282	7.9
84	.2079	-.9782	.938	21.6	.492	13.2	.334	9.3
82	.2756	-.9613	1.15	24.5	.630	16.1	.431	11.7
80	.3420	-.9397	1.31	26.3	.740	18.3	.516	13.7
75	.5000	-.8660	1.49	28.1	.938	21.6	.631	17.1
70	.6428	-.7660	1.48	28.0	1.012	2[illegible].7	.771	18.8
65	.7660	-.6428	1.37	26.9	1.010	2[illegible].6	.800	19.3

-200-

TABLE II (b)

$(a'/b')^2$	1.001	1.002	1.003	1.004	1.005	1.01	1.02	1.03	1.04	1.05	1.10	1.20	1.40	1.60	1.80	2.0	2.5	3.0	3.5	4.0	6.0	8.0
Θ	α	α	α	α	α	α	α	α	α	α	α	α	α	α	α	α	α	α	α	α	α	α
90	0	0	0	0	0	0	0	0	0	0	0	0	0	0	0	0	0	0	0	0	0	0
89.98	15.11	8.1	5.5	4.2	3.4																	
89.96	27.70	18.1	12.7	10.3	8.1																	
89.94	32.30	22.8	17.1	13.5	11.4																	
89.92	35.58	27.8	22.1	18.1	15.2																	
89.9	36.92	30.0	24.6	20.5	17.4	9.6																
89.8	40.85	36.9	33.3	30.1	27.1	17.5	9.6	6.6	5.0	4.0												
89.7	42.13	39.5	36.9	34.5	32.1	23.0																
89.6	42.75	40.8	38.8	36.8	35.2	27.1	17.5	12.5	9.6	7.8												
89.5	43.11	41.5	39.9	38.3	36.8	29.9																
89.4	43.38	41.98	40.7	39.3	38.3	32.2	23.1	17.5	13.8	11.4												
89.3	43.48	42.3	41.2	40.0																		
89.2	43.58	42.6	41.6	40.5	39.9	35.2	27.1	21.5	17.5	14.6												
89.1	43.65	42.7	41.9	41.0																		
89.0	43.60	42.85	42.1	41.3	40.5	36.6	29.8	24.4	20.3	17.3	9.6	5.0	2.5	1.7	1.3							
88.0					42.0	40.0	36.1	32.6	29.4	26.6	17.2	9.5	5.0	3.3	2.5	2.0	1.3	1.0	0.8	0.65		
87.0					42.2	40.8	38.1	35.6	33.3	31.0	23.4	13.5	7.2	4.9	3.7							
86.0					42.0	41.0	39.0	37.0	35.2	33.4	25.9	16.9	9.4	6.5	4.9	4.0	2.6	2.0	1.6	1.35		
85.0					41.7	40.7	39.3	37.7	36.2	34.7	28.2	19.5	11.3	7.9	6.0							
84.0					41.3	40.6	39.3	38.0	36.7	35.5	29.9	21.6	13.2	9.3	7.1	5.8	3.9	3.0	2.3	2.0		
82.0					40.5	40.0	39.0	38.0	37.0	36.1	31.7	24.5	16.1	11.7	9.1	7.5	5.1	3.8	3.1	2.6		
80.0					39.6	39.2	38.4	37.6	36.8	36.0	32.5	26.3	18.3	13.7	10.8	8.9	6.2	4.7	3.8	3.2	1.95	1.4
75.0					37.2	37.0	36.4	35.9	35.4	34.9	32.5	28.1	21.6	17.1	14.1						2.50	2.0
70.0					34.8	34.6	34.2	33.8	33.4	33.1	31.2	29.0	22.7	18.8	15.9	13.8	10.2	8.0	6.6	5.6	3.50	2.5
65.0					32.3	32.2	31.9	31.6	31.3	31.0	29.6	26.9	22.7	19.3	16.8						4.1	3.0
60.0					29.9	29.8	29.6	29.2	29.0	28.8	27.6	25.6	22.0	19.1	16.8	15.0	11.7	9.6	8.1	7.0	4.5	3.3

TABLE III(a)

$(a'/b')^2$ 1.10

(1)	(2)	(3)	(4)	(5)	(6)	(7)	(8)
θ	α	$\theta-\alpha$	$\sin^2(\theta-\alpha)$	$\sin^2\alpha$	$(a'/b')^2\sin^2\alpha$	$\sqrt{(4)+(6)}$	r/a'
90	0	90.0	1.000	0	0	1.0000	1.0000
89	9.6	79.4	.966	.0278	.0306	.9933	1.0016
88	17.2	70.8	.892	.0874	.0961	.9940	1.0055
87	23.4	64.6	.815	.145	.160	.9877	1.011
86	25.9	60.1	.752	.191	.210	.981	1.018
85	28.2	56.8	.701	.224	.246	.975	1.025
84	29.9	54.1	.656	.248	.273	.964	1.032
82	31.7	50.3	.591	.276	.304	.946	1.047
80	32.5	47.5	.543	.288	.317	.927	1.062
75	32.5	42.5	.457	.288	.317	.880	1.098
70	31.2	38.8	.393	.268	.295	.829	1.133
65	29.6	35.4	.335	.244	.268	.777	1.167
60	27.6	32.4	.287	.214	.236	.723	1.200

TABLE III(b)

$(a'/b')^2$	1.0	1.005	1.01	1.02	1.03	1.04	1.05	1.10	1.20	1.40	1.60	1.80	2.00	2.50	3.00	4.00
θ					r/a'								r/a'			
90.0	1.0000	1.0000	1.0000	1.0000	1.0000	1.0000	1.0000	1.0000	1.0000	1.0000	1.0000	1.0000	1.0000	1.0000	1.0000	1.0000
89.9		1.0003	1.0002													
89.8		1.0008	1.0005	1.0003	1.0002	1.0000	1.0000									
89.7		1.0016														
89.6		1.0024	1.0018	1.0011	1.0008	1.0006	1.0004									
89.5		1.0033		1.0017												
89.4		1.0041	1.0033	1.0022	1.0016	1.0013	1.0010									
89.2		1.0057	1.0049	1.0035	1.0028	1.0022	1.0018									
89.0	1.0085	1.0074	1.0067	1.0050	1.0040	1.0032	1.0027	1.0016	1.0008	1.0004	1.0003	1.0002				
88	1.0172	1.0159	1.0150	1.0130	1.0113	1.0100	1.0088	1.0055	1.0035	1.0015	1.0010	1.0006	1.0006	1.0003	1.0003	1.0002
87	1.0256	1.0246	1.0234	1.021	1.019	1.018	1.0162	1.011	1.0063	1.0035	1.0022	1.0015				
86	1.0343	1.0330	1.0318	1.030	1.028	1.026	1.0238	1.018	1.0107	1.0058	1.0041	1.0030	1.0023	1.0017	1.0013	1.0008
85	1.0424	1.0414	1.040	1.038	1.036	1.034	1.031	1.025	1.0158	1.0089	1.0060	1.0046				
84	1.0509	1.050	1.048		1.044	1.042	1.040	1.032	1.021	1.0129		1.0066	1.0053	1.0037	1.0023	1.0018
82	1.066	1.066	1.065		1.060	1.058	1.056	1.047	1.033	1.021		1.001		1.0061	1.0048	
80	1.082	1.082	1.081	1.079	1.076	1.073	1.071	1.062	1.047	1.030	1.022	1.017	1.0142	1.0096	1.0072	1.0049
75	1.120	1.120	1.119	1.116	1.114	1.111	1.109	1.098	1.081	1.058	1.044	1.037	1.030	1.021	1.016	1.010
70	1.157	1.157	1.156	1.153	1.149	1.147	1.145	1.133	1.112	1.086	1.069	1.057	1.047	1.034	1.027	1.019
65	1.191	1.191	1.190	1.187	1.184	1.181	1.179	1.167	1.145	1.114	1.094	1.078	1.069	1.050	1.039	1.028
60	1.225	1.225	1.221	1.219	1.217	1.213	1.210	1.200	1.175	1.142	1.118	1.100	1.089	1.066	1.053	1.038

TABLE IV

A

α	$B = \frac{2}{\tan 2\alpha}$	$\phi = 1°$	$\phi = 0.1°$
1	57.272	2.000	1.10000
2	28.600		1.0499
3	19.048		1.0332
4	14.286		1.0249
5	11.342	1.198	1.0198
6	9.410	1.164	1.0164
7	8.022	1.140	1.0140
8	6.974	1.122	1.0123
9	6.156	1.107	1.0107
10	5.496	1.096	1.0096
11	4.950	1.087	1.0087
12	4.492	1.078	1.0078
13	4.100	1.072	1.0072
14	3.762	1.066	1.0066
15	3.464	1.061	1.0061
16	3.200	1.056	1.0056
17	2.966	1.052	1.0052
18	2.756	1.048	1.00482
19	2.560	1.045	1.00450
20	2.384	1.042	1.00420
21	2.222	1.039	1.00390
22	2.072	1.036	1.00360
23	1.934	1.033	1.00334
24	1.802	1.031	1.00310
25	1.678	1.029	1.00290
26	1.566	1.027	1.00271
27	1.456	1.025	1.00254
28	1.360	1.023	1.00237
29	1.250	1.022	1.00221
30	1.154	1.020	1.00206
31	1.064	1.019	1.00190
32	.974	1.017	1.00174
33	.890	1.016	1.00158
34	.808	1.014	1.00142
35	.728	1.013	1.00126
36	.650	1.011	1.00110
37	.574	1.010	1.00098
38	.498	1.009	1.00086
39	.426	1.007	1.00073
40	.352	1.006	1.00061
41	.280	1.005	
42	.210	1.004	
43	.139	1.002	
44	.070	1.001	
45	0	1.000	

TABLE V(a)

	Error					
	1%		0.5%		0.1%	
A	ϕ	θ	ϕ	θ	ϕ	θ
1.001	.13	89.87	.09	89.91	.04	89.96
1.002	.18	89.82	.13	89.87	.06	89.94
1.004	.26	89.74	.18	89.82	.08	89.92
1.006	.31	89.69	.22	89.78	.10	89.90
1.008	.36	89.64	.26	89.74	.12	89.88
1.01	.41	89.59	.29	89.71	.13	89.87
1.02	.57	89.43	.41	89.59	.18	89.82
1.03	.70	89.30	.50	89.50	.22	89.78
1.04	.81	89.19	.57	89.43	.26	89.74
1.05	.91	89.09	.64	89.36	.29	89.71
1.06	.99	89.01	.70	89.30	.31	89.69
1.07	1.07	88.93	.76	89.24	.34	89.66
1.08	1.15	88.85	.81	89.19	.36	89.64
1.09	1.21	88.79	.86	89.14	.38	89.62
1.10	1.28	88.72	.91	89.09	.41	89.59

TABLE V(b)

1% Error

α	2α	Cot 2α	Cot $2\alpha(1+e)$	ϕ^c	ϕ°	θ
44	88	.03492	.01955	.01537	.88	89.12
42	84	.10510	.09031	.01479	.85	89.15
40	80	.17633	.16196	.01437	.82	89.18
35	70	.36397	.35019	.01378	.79	89.21
30	60	.57735	.56347	.01388	.80	89.20
25	50	.83910	.82434	.01476	.84	89.16
20	40	1.19175	1.17500	.01675	.96	89.04
15	30	1.73205	1.71129	.02076	1.19	88.81
10	20	2.74748	2.71792	.02956	1.69	88.31
5	10	5.67128	5.61397	.05731	3.28	86.72
7½	15	3.73205	3.69339	.03866	2.17	87.83

TABLE VI

SPECIMEN A

Streamline Number

7		8		9		10		11		12		13	
x	y	x	y	x	y	x	y	x	y	x	y	x	y
·4911	·5627	·4911	·5528	·4911	·5429	·4911	·5328	·4911	·5228	·4911	·5128	·4911	·5061
·5011	·5627	·5011	·5528	·5011	·5427	·5011	·5329	·5011	·5229	·5013	·5130	·5015	·5067
·5112	·5628	·5111	·5527	·5111	·5427	·5112	·5331	·5114	·5235	·5117	·5138	·5119	·5075
·5212	·5627	·5211	·5529	·5212	·5430	·5214	·5336	·5216	·5240	·5219	·5145	·5222	·5083
·5313	·5627	·5312	·5531	·5312	·5433	·5316	·5340	·5317	·5246	·5323	·5152	·5326	·5091
·5415	·5627	·5416	·5533	·5416	·5436	·5418	·5344	·5421	·5251	·5426	·5158	·5429	·5099
·5520	·5627	·5521	·5534	·5522	·5439	·5524	·5348	·5527	·5256	·5530	·5165	·5533	·5106
·5628	·5627	·5629	·5535	·5630	·5442	·5631	·5352	·5634	·5261	·5638	·5171	·5640	·5114
·5738	·5627	·5739	·5537	·5739	·5444	·5741	·5356	·5744	·5266	·5748	·5177	·5750	·5121
·5851	·5627	·5852	·5538	·5852	·5446	·5853	·5359	·5856	·5271	·5860	·5183	·5862	·5127
·5966	·5627	·5966	·5539	·5967	·5448	·5968	·5363	·5971	·5275	·5975	·5189	·5977	·5133
·6083	·5627	·6082	·5540	·6083	·5451	·6085	·5366	·6088	·5280	·6093	·5194	·6095	·5140
·6201	·5627	·6201	·5542	·6202	·5453	·6203	·5370	·6206	·5284	·6211	·5199	·6213	·5146
·6321	·5627	·6321	·5543	·6322	·5455	·6324	·5373	·6327	·5288	·6331	·5204	·6334	·5152
·6443	·5628	·6443	·5544	·6444	·5457	·6446	·5376	·6449	·5292	·6455	·5209	·6457	·5157
·6566	·5627	·6567	·5544	·6568	·5459	·6570	·5379	·6574	·5296	·6580	·5214	·6582	·5162
·6691	·5628	·6692	·5545	·6694	·5461	·6697	·5381	·6701	·5300	·6707	·5219	·6711	·5168
·6817	·5627	·6818	·5546	·6820	·5463	·6824	·5384	·6829	·5303	·6835	·5223	·6837	·5172
·6945	·5628	·6946	·5547	·6948	·5465	·6952	·5387	·6957	·5306	·6962	·5226	·6965	·5176
·7074	·5628	·7075	·5548	·7077	·5467	·7081	·5389	·7085	·5309	·7090	·5230	·7092	·5180
·7203	·5628	·7204	·5548	·7205	·5468	·7209	·5391	·7213	·5312	·7218	·5233	·7220	·5183
·7332	·5628	·7331	·5548	·7334	·5469	·7338	·5394	·7342	·5314	·7346	·5236	·7347	·5186
·7461	·5629	·7462	·5549	·7463	·5469	·7467	·5394	·7470	·5315	·7473	·5238	·7475	·5188
·7590	·5628	·7591	·5548	·7592	·5468	·7596	·5392	·7599	·5315	·7600	·5238	·7602	·5189
·7720	·5627	·7721	·5549	·7722	·5469	·7726	·5395	·7729	·5314	·7730	·5236	·7732	·5189
·7849	·5628	·7850	·5549	·7852	·5469	·7856	·5394	·7858	·5316	·7859	·5238	·7861	·5190

TABLE VII

SPECIMEN 'B

Streamline Number

7		8		9		10		11		12		13	
x	y	x	y	x	y	x	y	x	y	x	y	x	y
·2998	·5994	·2998	·5893	·2998	·5792	·2998	·5692	·2998	·5592	·2998	·5492	·2998	·5446
·3098	·5994	·3098	·5893	·3098	·5793	·3098	·5695	·3099	·5597	·3100	·5501	·3102	·5457
·3198	·5994	·3198	·5896	·3198	·5797	·3198	·5701	·3200	·5606	·3202	·5511	·3204	·5468
·3302	·5995	·3302	·5899	·3303	·5802	·3303	·5708	·3305	·5615	·3308	·5521	·3310	·5479
·3408	·5996	·3408	·5902	·3409	·5807	·3410	·5715	·3412	·5623	·3414	·5532	·3417	·5489
·3517	·5997	·3517	·5905	·3518	·5811	·3519	·5721	·3520	·5631	·3521	·5542	·3524	·5500
·3628	·5998	·3628	·5908	·3628	·5815	·3629	·5727	·3630	·5643	·3632	·5552	·3634	·5509
·3741	·6000	·3741	·5911	·3742	·5819	·3742	·5734	·3743	·5648	·3744	·5562	·3746	·5519
·3856	·6001	·3856	·5913	·3856	·5823	·3856	·5739	·3857	·5655	·3859	·5571	·3860	·5529
·3974	·6002	·3974	·5916	·3974	·5827	·3974	·5745	·3975	·5662	·3977	·5580	·3978	·5539
·4094	·6002	·4094	·5918	·4094	·5831	·4094	·5751	.4095	·5669	.4097	·5589	.4098	·5549
·4216	·6003	·4216	·5921	·4216	·5835	·4216	·5756	·4217	·5677	·4221	·5598	·4221	·5559
·4341	·6004	·4341	·5923	.4342	·5839	·4342	·5762	·4343	·5684	·4347	·5607	.4347	·5568
·4468	·6005	·4468	·5926	·4469	·5843	·4470	·5767	·4471	·5691	·4474	·5616	·4476	·5577
·4598	·6006	·4598	·5928	·4599	·5847	·4600	·5772	.4602	·5698	·4605	·5624	·4606	·5587
·4730	·6007	·4730	·5930	·4731	·5851	·4733	·5777	·4735	·5705	·4738	·5632	·4738	·5595
·4865	·6008	·4865	·5933	·4866	·5855	·4868	·5782	·4870	·5711	·4873	·5640	·4874	·5604
·5002	·6008	·5002	·5935	·5003	·5859	·5005	·5787	·5007	·5717	·5010	·5647	·5011	·5611
·5142	·6009	·5142	·5937	·5143	·5862	·5145	·5791	·5148	·5723	·5150	·5654	·5151	·5618
·5285	·6010	·5286	·5939	·5287	·5866	·5289	·5796	·5291	·5728	·5292	·5660	·5294	·5625
·5430	·6011	·5430	·5941	·5432	·5870	·5434	·5800	·5436	·5734	·5437	·5666	·5438	·5632
·5578	·6011	·5578	·5943	·5579	·5872	·5581	·5804	·5583	·5738	·5584	·5672	·5586	·5637
·5729	·6012	·5729	·5944	·5730	·5874	·5731	·5807	·5732	·5742	·5735	·5677	·5736	·5643
·5883	·6013	·5883	·5946	·5884	·5877	·5885	·5811	·5887	·5745	·5888	·5681	·5890	·5647
·6038	·6013	·6038	·5947	·6039	·5879	·6040	·5814	·6042	·5748	·6043	·5685	·6044	·5651
·6193	·6013	·6193	·5948	·6194	·5881	·6195	·5817	·6196	·5751	·6197	·5688	·6199	·5654
·6348	·6014	·6348	·5948	·6349	·5881	·6350	·5817	·6351	·5753	·6352	·5690	·6353	·5656
·6503	·6013	·6503	·5948	·6504	·5881	·6505	·5817	·6506	·5753	·6507	·5691	·6508	·5656

TABLE VIII

SPECIMEN C

Streamline Number

7		8		9		10		11		12		13	
x	y	x	y	x	y	x	y	x	y	x	y	x	y
·0484	·6208	·0484	·6108	·0484	·6007	·0484	·5909	·0484	·5807	·0484	·5708	·0484	·5665
·0584	·6208	·0584	·6109	·0584	·6008	·0584	·5908	·0584	·5808	·0586	·5707	·0587	·5665
·0684	·6208	·0684	·6108	·0684	·6008	·0686	·5908	·0687	·5809	·0690	·5711	·0691	·5672
·0784	·6208	·0784	·6110	·0785	·6012	·0786	·5916	·0788	·5821	·0791	·5727	·0793	·5688
·0887	·6210	·0888	·6116	·0888	·6021	·0890	·5926	·0892	·5834	·0896	·5741	·0898	·5702
·0994	·6213	·0995	·6121	·0996	·6029	·0998	·5936	·1001	·5847	·1005	·5757	·1007	·5717
·1104	·6215	·1105	·6126	·1106	·6036	·1108	·5947	·1111	·5858	·1115	·5770	·1116	·5731
·1218	·6218	·1219	·6130	·1219	·6044	·1221	·5957	·1224	·5871	·1227	·5785	·1229	·5746
·1336	·6220	·1336	·6135	·1337	·6050	·1338	·5966	·1340	·5882	·1343	·5799	·1345	·5762
·1458	·6222	·1458	·6139	·1458	·6058	·1459	·5975	·1461	·5894	·1464	·5813	·1465	·5777
·1584	·6224	·1584	·6144	·1585	·6064	·1586	·5984	·1588	·5905	·1591	·5826	·1593	·5792
·1713	·6226	·1713	·6148	·1714	·6070	·1716	·5992	·1718	·5916	·1721	·5840	·1723	·5808
·1847	·6228	·1848	·6152	·1849	·6077	·1852	·6001	·1855	·5928	·1858	·5854	·1860	·5823
·1986	·6230	·1987	·6155	·1989	·6083	·1991	·6010	·1995	·5939	·1998	·5868	·2000	·5838
·2130	·6231	·2131	·6159	·2134	·6089	·2137	·6019	·2141	·5951	·2144	·5883	·2146	·5852
·2278	·6232	·2279	·6162	·2282	·6095	·2285	·6028	·2288	·5962	·2292	·5896	·2294	·5867
·2431	·6232	·2433	·6166	·2436	·6101	·2439	·6036	·2441	·5973	·2445	·5910	·2446	·5880
·2589	·6233	·2591	·6170	·2594	·6106	·2598	·6044	·2601	·5984	·2604	·5922	·2605	·5894
·2752	·6234	·2754	·6173	·2758	·6112	·2762	·6052	·2765	·5994	·2768	·5935	·2769	·5907
·2920	·6234	·2923	·6176	·2927	·6118	·2930	·6059	·2934	·6002	·2937	·5946	·2938	·5919
·3094	·6234	·3097	·6179	·3101	·6122	·3106	·6066	·3110	·6010	·3113	·5956	·3114	·5931
·3273	·6234	·3276	·6182	·3280	·6126	·3285	·6072	·3289	·6017	·3293	·5964	·3294	·5940
·3458	·6235	·3461	·6184	·3466	·6130	·3470	·6077	·3474	·6023	·3477	·5972	·3478	·5947
·3650	·6235	·3653	·6186	·3657	·6132	·3662	·6081	·3666	·6028	·3669	·5978	·3670	·5953
·3848	·6235	·3851	·6187	·3855	·6134	·3860	·6084	·3863	·6032	·3866	·5982	·3867	·5958
·4049	·6235	·4052	·6186	·4056	·6135	·4061	·6085	·4063	·6035	·4067	·5987	·4068	·4961
·4250	·6236	·4253	·6186	·4257	·6135	·4262	·6085	·4264	·6035	·4267	·5986	·4268	·5963

TABLE IX

SPECIMEN A

Streamline 12.

x	y	tan ψ	ψ
.50	.5129		
.52	.5143	.0682	3.90
.54	.5156	.0635	3.63
.56	.5169	.0577	3.30
.58	.5180	.0525	3.00
.60	.5190	.0472	2.70
.62	.5198	.0430	2.47
.64	.5207	.0403	2.30
.66	.5215	.0362	2.07
.68	.5221	.0312	1.78
.70	.5227	.0272	1.55
.72	.5232	.0237	1.35
.74	.5237		

Streamline 8.

x	y	tan ψ	ψ
.52	.5529		
.54	.5532	.0147	.85
.56	.5534	.0122	.70
.58	.5537	.0115	.67
.60	.5539	.0107	.62
.62	.5541	.0097	.55
.64	.5543	.0080	.47
.66	.5544	.0085	.50
.68	.5546	.0062	.35
.70	.5547	.0050	.30
.72	.5548		

TABLE X

SPECIMEN A

Streamline 12.

x	y	$x_{n+1}-x_{n-1}$	$y_{n+1}-y_{n-1}$	2a
.4911	.5128			
.5013	.5130	.0206	.0015	.0207
.5117	.5138	.0206	.0014	.0206
.5219	.5145	.0207	.0013	.0207
.5323	.5152	.0207	.0013	.0207
.5426	.5158	.0212	.0013	.0212
.5530	.5165	.0218	.0012	.0218
.5638	.5171	.0222		.0222
.5748	.5177	.0227		.0227
.5860	.5183	.0233		.0233
.5975	.5189	.0236		.0236
.6093	.5194	.0238		.0238
.6211	.5199	.0244		.0244
.6331	.5204	.0249		.0249
.6455	.5209	.0252		.0252
.6580	.5214	.0255		.0255
.6707	.5219	.0255		.0255
.6835	.5223	.0255		.0255
.6962	.5226	.0256		.0256
.7090	.5230	.0256		.0256
.7218	.5233	.0255		.0255
.7346	.5236	.0254		.0254
.7473	.5238	.0257		.0257
.7600	.5238	.0259		.0259
.7730	.5236			
.7859	.5238			

Streamline 8.

x	y	$x_{n+1}-x_{n-1}$	$y_{n+1}-y_{n-1}$	2a
.4911	.5528			
.5011	.5528	.0200		.0200
.5111	.5527	.0200	.0001	.0200
.5211	.5529	.0201	.0004	.0201
.5312	.5531	.0205	.0004	.0205
.5416	.5533	.0209	.0003	.0209
.5521	.5534	.0213	.0002	.0213
.5629	.5535	.0213		.0218
.5739	.5537	.0223		.0223
.5852	.5538	.0227		.0227
.5966	.5539	.0230		.0230
.6082	.5540	.0235		.0235
.6201	.5542	.0239		.0239
.6321	.5543	.0242		.0242
.6443	.5544	.0246		.0246
.6567	.5544	.0249		.0249
.6692	.5545	.0251		.0251
.6818	.5546	.0254		.0254
.6946	.5547	.0257		.0257
.7075	.5548	.0258		.0258
.7204	.5548	.0256		.0256
.7331	.5548	.0258		.0258
.7462	.5548	.0260		.0260
.7591	.5548	.0259		.0259
.7721	.5549	.0259		.0259
.7850	.5549			

TABLE XI

SPECIMEN A

Streamline 11.

x	$2b$ $y_{10}-y_{12}$	$x_{12}-x_{10}$	$\tan\phi$	ϕ
.4911	.0200	0	0	0
.5011	.0199	.0002	.0100	.58
.5114	.0193	.0005	.0259	1.48
.5216	.0191	.0005	.0262	1.50
.5317	.0188	.0007	.0372	2.13
.5421	.0186	.0008	.0430	2.47
.5527	.0183	.0006	.0328	1.88
.5634	.0181	.0007	.0387	2.22
.5744	.0179	.0007	.0392	2.25
.5856	.0176	.0007	.0400	2.28
.5971	.0174	.0007	.0403	2.30
.6088	.0172	.0008	.0465	2.67
.6206	.0171	.0008	.0468	2.68
.6327	.0169	.0007	.0414	2.37
.6449	.0167	.0009	.0540	3.08
.6574	.0165	.0010	.0606	3.47
.6701	.0162	.0010	.0617	3.53
.6829	.0161	.0011	.0685	3.92
.6957	.0161	.0010	.0622	3.57
.7085	.0159	.0009	.0565	3.23
.7213	.0158	.0009	.0570	3.27
.7342	.0158	.0008	.0505	2.88
.7470	.0156	.0006	.0384	2.20
.7599	.0154	.0004	.0260	1.48

Streamline 8.

x	$2b$ y_7-y_9	ϕ
.4911	.0200	0
.5011	.0200	0
.5111	.0200	0
.5211	.0197	0
.5312	.0194	0
.5416	.0191	0.30
.5521	.0188	0.60
.5629	.0185	0.63
.5739	.0183	0.32
.5852	.0181	0.32
.5966	.0179	0.32
.6082	.0176	0
.6201	.0174	0.32
.6321	.0172	0.32
.6443	.0171	0.33
.6567	.0168	0.67
.6692	.0167	1.00
.6818	.0164	1.02
.6946	.0163	1.03
.7075	.0161	1.03
.7204	.0160	0.68
.7331	.0159	0.68
.7462	.0160	0.68

TABLE XII

SPECIMEN A

Streamline 12.

(1) x	(2) y	(3) ϕ	(4) ψ	(5) 2a	(6) 2b	(7) $\phi_2-\phi_1$	(8) $\psi_2-\psi_1$	(9) θ	(10) (a/b)	(11) (a'/b')	(12) $(a'/b')^2$	(13) α°	(14) α_1° (13)+(8)	(15) $\alpha_1^\circ+45^\circ$	(16) $r/a' - 1$
.4950	.5128	0	4.35	.0200	.0200	0	4.35	85.65	1.00						
.5013	.5130	1.00	4.25	.0200	.0198	1.00	-.10	91.10	1.0101	1.010	1.020	32.0	-32.10	12.9	.0058
.5117	.5138	1.70	4.10	.0201	.0194	.70	-.15	90.85	1.036	1.026	1.053	14.8	-14.95	30.05	.0022
.5219	.5145	2.15	3.90	.0203	.0191	.45	-.20	90.65	1.063	1.029	1.059	10.6	-10.80	34.20	.0010
.5323	.5152	2.45	3.75	.0206	.0188	.30	-.15	90.45	1.096	1.030	1.061	7.2	-7.35	37.65	.0004
.5426	.5158	2.70	3.60	.0209	.0185	.25	-.15	90.40	1.1300	1.031	1.063	6.2	-6.35	38.65	.0003
.5530	.5165	2.95	3.45	.0214	.0183	.25	-.15	90.40	1.169	1.032	1.065	6.0	-6.15	38.85	.0003
.5638	.5171	3.10	3.30	.0218	.0181	.15	-.15	90.30	1.204	1.031	1.063	4.8	-4.95	40.05	.0002
.5748	.5177	3.25	3.15	.0223	.0178	.15	-.15	90.30	1.252	1.040	1.082	3.5	-3.65	41.35	.0002
.5860	.5183	3.40	2.95	.0227	.0176	.15	-.20	90.35	1.289	1.029	1.059	5.8	-6.00	39.00	.0002
.5975	.5189	3.60	2.80	.0231	.0174	.20	-.15	90.35	1.328	1.030	1.061	5.8	-5.95	39.05	.0002
.6093	.5194	3.90	2.65	.0235	.0172	.30	-.15	90.45	1.367	1.029	1.059	7.4	-7.55	37.45	.0004
.6211	.5199	4.35	2.50	.0240	.0170	.45	-.15	90.60	1.412	1.034	1.069	8.4	-8.55	36.45	.0008
.6331	.5204	4.70	2.35	.0243	.0168	.35	-.15	90.50	1.445	1.022	1.045	10.6	-10.75	34.25	.0007
.6455	.5209	4.95	2.20	.0247	.0166	.25	-.15	90.40	1.487	1.029	1.059	6.7	-6.85	38.15	.0004
.6580	.5214	5.05	2.05	.0251	.0165	.10	-.15	90.25	1.521	1.025	1.051	5.0	-5.15	39.85	.0002
.6707	.5219	5.00	1.90	.0254	.0163	-.05	-.15	90.10	1.559	1.023	1.047	2.1	-2.25	42.75	0
.6835	.5223	4.95	1.75	.0256	.0161	-.05	-.15	90.10	1.590	1.021	1.043	2.0	-2.45	42.55	0
.6962	.5226	4.60	1.60	.0257	.0160	-.35	-.15	89.80	1.607	1.010	1.020	9.5	9.35	54.35	.0006
.7090	.5230	4.10	1.45	.0258	.0159	-.50	-.15	89.65	1.621	1.010	1.020	16.0	15.85	60.85	.0010
.7218	.5233	3.50	1.30	.0259	.0158	-.60	-.15	89.55	1.639	1.010	1.020	19.0	18.85	63.85	.0015
.7346	.5236	2.90	1.15	.0259	.0158	-.60	-.15	89.55	1.656	1.011	1.022	18.0	17.85	62.85	.0014
.7450	.5238	2.00	1.00	.0260	.0157	-.90	-.15	89.25	1.653	1.00	1.00				

$\Sigma r/a' - 1$

$= .0178$

TABLE XIII

SPECIMEN B

Hardness survey of edge of specimen.
x - coordinate in direction of rolling.
y - coordinate normal to direction of rolling.
x coordinate for plane of entry .159".
All Pyramid Diamond Numbers obtained with a 5 Kgm. load.

x	.0031	.0029	.0029	.0028
y	.3742	.3530	.3320	.3128
Hv	50.2	50.2	46.8	48.0
x	.1595	.1590	.1589	.1586
y	.3700	.3521	.3318	.3122
Hv	49.7	50.9	49.0	47.3
x	.2007	.2008	.2007	.2004
y	.3638	.3444	.3260	.3061
Hv	54.0	50.6	53.6	53.6
x	.2247	.2246	.2246	.2244
y	.3703	.3506	.3318	.3121
Hv	63.2	62.3	62.6	63.2
x		.2464	.2463	.2470
y		.3592	.3392	.3195
Hv		74.9	73.2	75.7
x		.2734	.2731	.2733
y		.3608	.3406	.3223
Hv		84.6	86.7	86.7
x		.2981	.2980	.2980
y		.3547	.3351	.3159
Hv		91.7	91.7	91.1
x		.3236	.3233	.3232
y		.3561	.3368	.3183
Hv		98.4	97.8	97.1

TABLE XIII (continued)

x	.3506	.3504	.3504
y	.3540	.3348	.3157
Hv	102	102	102
x	.3773	.3767	.3769
y	.3655	.3492	.3314
Hv	105	107	107
x	.3998	.3996	.3996
y	.3583	.3423	.3273
Hv	108	110	109
x	.4266	.4267	.4273
y	.3578	.3414	.3265
Hv	108	112	112
x	.4543	.4543	.4543
y	.3535	.3353	.3207
Hv	113	112	110
x	.4773	.4773	.4773
y	.3528	.3348	.3217
Hv	117	117	117
x	.5018	.5015	.5027
y	.3602	.3419	.3284
Hv	118	120	118
x	.7620	.7622	.7630
y	.3600	.3402	.3262
Hv	120	117	118